Master's thesis

NTNU
Norwegian University of Science and Technology
Faculty of Engineering
Department of Geoscience and Petroleum

Lene Margrethe Pallesen

Sediment source-to-sink in a warming Arctic

Thawing moraines, slope processes and river erosion in Longyeardalen, Svalbard

Master's thesis in Geology
Supervisor: Bjørn Frengstad
Co-supervisor: Lena Rubensdotter and Aga Nowak
May 2022

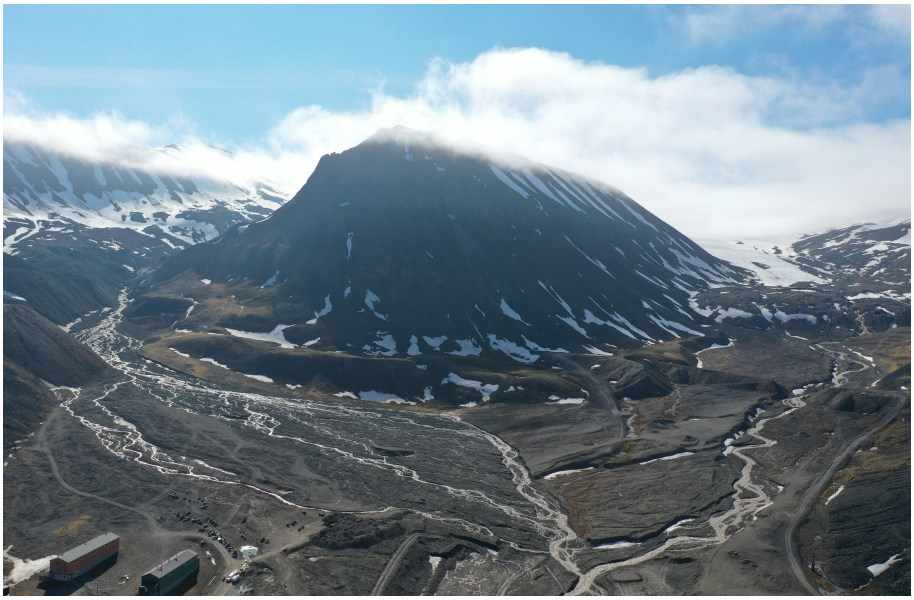

NTNU
Norwegian University of
Science and Technology

Lene Margrethe Pallesen

Sediment source-to-sink in a warming Arctic

Thawing moraines, slope processes and river erosion in Longyeardalen, Svalbard

Master's thesis in Geology
Supervisor: Bjørn Frengstad
Co-supervisor: Lena Rubensdotter and Aga Nowak
May 2022

Norwegian University of Science and Technology
Faculty of Engineering
Department of Geoscience and Petroleum

NTNU
Norwegian University of
Science and Technology

Abstract

The climate change and rapid warming of the Arctic is changing the conditions for source-to-sink sediment transport in Longyearbyen, Svalbard, causing potential problems for infrastructure and human safety. The sediment sources; glaciers, permafrost degradation and gravitational processes are often not well understood, and even less quantified, something this study aims to remedy. The study is part of a long-term monitoring project of Longyearelva (RiS ID 11641) and is completed alongside a twin master study by Ottem (2022). The aims were addressed through detailed mapping of the upper part of Longyeardalen using drone mapping, field observations, sediment volume calculations, and data search of older orthophotos. This was supported by monitoring of discharge, suspended sediment concentration (SSC), and bedload transport.

This study shows that the primary sources of sediment in Longyeardalen are the Larsbreen and Longyearbreen glaciers and ice-cored moraine systems. Secondary sedimentary sources such as snow avalanches and rock glaciers are located along the slopes of the valley and adjacent to active channels. River bank erosion and thaw driven slumps in the moraine systems are important sources of sediment in the late melting season. This is due to active layer thaw destabilising the ground and releasing sediment for erosion.

Daily fluctuations in SSC were most irregular in the middle of the melting season, and largest in the late-season. Sediment transportation increased over the season and correlation of sediment transport with discharge decreased in the late-season. This suggests that active layer thaw is an important control on sediment transport from both primary and secondary sources, with increasing control over the season.

The total volume of sediment that has been removed by slumping in the moraines by 2021 is at least $2.8 \pm 0.6 \times 10^6$ m^3. An acceleration in degradation has occurred over the past 10 years. This is due to retrogressive behaviour of slumps in ice-cored moraines due to exposure to heat and water, and glaciofluvial erosion. It is speculated that acceleration is promoted by an increase in active layer thickness due to warming.

The long-term consequence of warming on sediment transport is difficult to discern. There is some indication that sediment transport in Longyeardalen may increase. This is due to the increasing importance of secondary sediment sources; river erosion and thaw-slumps in moraines. River erosion increases with active layer thaw, which is highly sensitive to warming. Thaw-induced slumping in moraines is an irregular, episodic sediment source with high hydrological connectivity in Longyeardalen. Magnitude and frequency of these sources is expected to increase with warming and rainfall. A shift in sediment source contribution could lead to more irregular, high peaks and increased late-season sediment transport. Thus, the total sediment transport may increase despite the retreat of the glaciers.

Continued monitoring is necessary to further understand the interannual variability and long-term climate change impacts on sediment transport and permafrost degradation in Longyeardalen. It would be beneficial with investigations of active layer thickness in the valley and drone mapping in future years. This study has provided quantified information on sediment sources and transport in 2021, and aids in the understanding of how the Longyeardalen source-to-sink system is responding to a warming climate.

Sammendrag

Klimaendringer i Arktis endrer forutsetningene for sedimenttransport fra kilde til avsetning i Longyearbyen, Svalbard, og skaper potensielle problemer for infrastruktur og menneskesikkerhet. Sedimentkildene; isbreer, destabilisering av permafrost og gravitasjonsprosesser er ofte lite dokumentert, og enda sjeldnere kvantifisert, noe denne studien ønsker å bedre. Studien er del av et langtidsprosjekt for monitorering av Longyearelva (RiS ID 11641) og er gjennomført i samarbeid med et tvillingstudie av Ottem (2022). Målene for oppgaven ble addressert ved bruk av detaljert kartlegging av den øvre delen av Longyeardalen ved bruk av drone, feltobservasjoner, volumutregninger av sediment, og datasøk etter eldre ortofoto. Dette var støttet av monitorering av vannføring, suspendert sedimentkonsentrasjon, og transport av bunnlast.

Denne studien har vist at primærkilder til sediment i Longyeardalen er Larsbreen og Longyearbreen og de tilhørende iskjernemorenene. Sekundærkilder til sediment som snøskred og steinsprang finnes på skråningene i dalen langs aktive elvekanaler. Erosion av elvebredde og slumping i morenene drevet av tining er viktige sedimentkilder mot slutten av smeltesesongen. Dette er grunnet tining av det aktive laget som destabiliserer grunnen og tilgjengeliggjør sediment for erosjon.

Daglige svingninger i suspendert sedimentkonsentrasjon var mest uregelmessige i midten av smeltesesongen, og høyest i sensesongen. Sedimenttransporten økte gjennom sesongen, og korrelasjon mellom sedimenttransport og vannføring avtok mot sensesongen. Dette indikerer at tining av det aktive laget er en viktig kontroll for sedimenttransport for både primær- og sekundærkilder, med økende påvirkning gjennom smeltesesongen.

Det totale volumet av sediment fjernet fra morenene gjennom slumping til og med 2021 var minst $2.8 \pm 0.6 \times 10^6$ m^3. En akselerasjon i destabilisering i morenene ble funnet for de siste 10 årene. Dette er grunnet retrogressiv bevegelse av slumping i iskjernemorenene grunnet eksponering for varme og vann, og glasifluvial erosion. Det spekuleres i om akselerasjonen forsterkes i økt tykkelse av det aktive laget på grunn av klimaendringer.

Langtidsvirkningene av økt globaltemperatur på sedimenttransport er vanskelig å forutse. Det er noen indikasjoner på at sedimenttransporten i Longyeardalen kan øke. Dette begrunnes ved økende viktighet av sekundærkilder til sediment; elveerosjon og tinings-slumping i morenene. Elveerosjon øker ved tining av det aktive laget, noe som kan respondere betydelig til lufttemperaturøkning. Slumping utløst ved tining i morener er en uregelmessig, episodisk sedimentkilde med høy hydrologisk konnektivitet i Longyeardalen. Omfanget og hyppigheten avdisse kildene forventes å øke med temperatur og regn. Et skifte i sentrale sedimentkilder kan føre til mer uregelmessige, høye topper i sedimenttransport og økt transport i sensesongen. Dermed er det mulig at den totale sedimenttransporten kan øke til tross for tilbaketrekning av isbreene.

En fortsettelse av monitorering er nødvendig for å forstå mer om variasjon mellom år og langtidsvirkninger av klimaendringer på sedimenttransport og destabilisering i permafrost i Longyeardalen. Det vil være nyttig med undersøkelser av tykkelse på det aktive laget i dalen og dronekartlegging i kommende år. Denne studien har bidratt med kvantifisert informasjon om sedimentkilder i 2021, og bistår i økt forståelse av hvordan sedimenttransport fra kilde til avsetning i Longyeardalen reagerer på klimaendringer.

Preface

This thesis is submitted as the concluding part of my MSc in Environment and Geotechnology at NTNU Trondheim. Since completing my bachelor's degree in England, I was most confident in writing this thesis in English. This is also in the hopes that it may reach a wider audience, especially considering the internationality of Svalbard. The thesis is intended for digital view and A4 print.

It's difficult to put into words the fulfilment that this project has given me. I am grateful for the opportunity to experience Svalbard, including unique fieldwork and new friends. I would like to express my gratitude towards everyone who has helped throughout the project. To Lena Rubensdotter for her dedication, insight, and knowledge. Her passion for research has given me courage and inspiration to pursue further challenges. To Bjørn Frengstad for his guidance and uplifting feedback. To Aga Nowak for her help in the field and valuable input throughout the project.

This project would not have been the same without my colleague and dear friend Marthe Ottem. I appreciate all her hard efforts and encouragement, and all the joyful moments we have had while working together. A big thank you to Ashton, Sacha, and Louie for their help with fieldwork. In addition, a thank you to Martin Løvaas for advice and transparency to his data. To the UNIS Logistics department for providing field equipment and assistance.

A special thank you to The Arctic Field Grant (AFG) for their financial support that made the stay and fieldwork in Svalbard possible. Gratitude is also given to The Norwegian Water Resources and Energy Directorate (NVE) for their contribution to the project.

I would like to express a big thank you to Asbjørn for always being there and for all our wonderful experiences together, to my mum, dad, and siblings for their continuous support, to my grandma and grandpa for inspiring me to study geology and teaching me to always be grateful, and to my wonderful friends. I am also thankful for the music, dance, and hobbies that have stayed with me and inspired me throughout my studies.

Lene Margrethe Pallesen

Trondheim, 15.05.2022

Cover photo: Upper Longyeardalen and Sarkofagen, July 2021

Contents

List of figures

List of tables

Abbreviations and dictionary

Abbreviation	Definition
DEM	Digital Elevation Model
EC	Electrical Conductivity
ETRS	European Terrestrial Reference System
GIS	Geographical Information System
JPG	Joint Photographic Experts Group
LL	Longyearbyen Lokalstyre
LYR	Layer (file format)
NGU	Geological Survey of Norway
NPI	Norwegian Polar Institute
NTNU	Norwegian University of Science and Technology
NVE	Norwegian Water Resources and Energy Directorate
Q	Discharge
RIS	Research in Svalbard
SfM	Structure from Motion
SOSI	Samordnet Opplegg for Stedfestet Informasjon
SSC	Suspended Sediment Concentration
SSL	Suspended Sediment Load
SSY	Suspended Sediment Yield
TIF	Tagged Image File Format
UNIS	University Centre in Svalbard
UTM	Universal Transverse Mercator
WMTS	Web Map Tile Service
xx-PT	(location) – Passive Tracer

Dictionary	
Norwegian	**English**
Bre	Glacier
By	Town/City
Dal	Valley
Elv	River
Fjell/Berg	Mountain
Lufthavn	Airport
Veg	Road

1 Introduction

1.1 Aims of study

It is generally assumed that the primary origin of sediment transported in Longyeardalen is glacial erosion. It is here hypothesised that warming-related degradation of moraines, slopes, and river banks will be significant sediment sources with different seasonal patterns of sediment release compared to glacier melting. This study aims to check this hypothesis and to accurately define and attempt to quantify the non-glacial sediment sources. Due to the restriction of a master project and one field season, it was chosen to focus mostly on the sediment input from river erosion and rapid processes in the thawing moraines. To define and quantify the sources and transport, the following questions will be addressed:

- What are the important sediment sources in the Longyeardalen source-to-sink system?
- How does sediment input and transport in Longyearelva change on a daily, seasonal, and long-term scale?
- How does warming and active layer thaw influence sediment sources and transport in Longyeardalen?
- How much slumping has occurred in the Larsbreen and Longyearbreen moraine systems in recent years? Is this an important sediment source?

An overview of the potential sediment sources will be achieved by detailed mapping of the Upper Longyeardalen area. Furthermore, the volume of sediment displaced by thaw-induced slumps in Larsbreen and Longyearbreen moraine systems will be calculated for 2009, 2019, and 2021. These objectives will assist in the understanding of the source-to-sink system in Longyeardalen in light of a warming Arctic.

1.1.1 Collaboration and long-term monitoring

This study is part of the long-term project "Hydrology, Sediment transport and erosion in Longyeardalen" (RiS ID 11641). The project was initiated in 2018 at The University Centre in Svalbard (UNIS). The continuation of the project is in collaboration with the Geological Survey of Norway (NGU) and master students from the Norwegian University of Science and Technology (NTNU), with melt-season monitoring in 2019, 2020, and 2021. The project is also in collaboration with Longyearbyen Lokalstyre (LL) and the Norwegian Water and Energy Directorate (NVE).

Most of the fieldwork and data processing was a joint effort with twin study Ottem (2022); "The Longyearelva river-to-ocean system; Monitoring an anthropogenic arctic fluvial system in changing climate over short and long timescales". This approach was chosen with the aim of widening research focuses relating to the long-term monitoring effort. The collaboration increased data quality and quantity, including hydrological monitoring and drone mapping.

1.2 Motivation and relevance

Svalbard is an accessible and thus important location for observing Arctic conditions and climate change consequences. Important topics of interest include permafrost thaw, geohazards, runoff in glacierised catchments, and coastal development. Application of unmanned air vehicles (UAVs) is considered a valuable tool for establishing long-term datasets on Svalbard (Moreno-Ibáñez et al., 2021).

Glaciofluvial systems are a key factor to understand consequences of climate change due to the connection between glaciers and the surrounding environment. It can be assumed that hydrology and sediment transport in High Arctic rivers are closely controlled by meltwater and sediment input from glaciers (Hodgkins et al., 2003). Conditions for a meltwater-dominated system are a cold and dry climate with mild temperatures in the summer season. Climate projections suggest that this may not continue to be the case in the future, and in some cases may already be changing. An increase in air temperature and precipitation could shift the source of runoff and sediments in a catchment. Several factors may influence this change, including permafrost conditions and glacier size (Hanssen-Bauer et al., 2019).

Data coverage in the Arctic is poor spatially and temporally, making it hard to draw conclusions (Killingtveit et al., 2003). Few studies monitor long-term stream discharge and sediment load, as well as bedload transport (French, 2007). Many years of monitoring is required to see trends, interannual variability, and consequences of climate change on hydrology and sediment transport (Hodgkins et al., 2003; Nowak et al., 2020). It is therefore especially important that Longyearelva has been established as a long-term monitoring site, with successful data collection for consecutive years.

A key importance of studies of Longyearelva is its direct influence on Longyearbyen. Building and area plans include already completed and future plans for expansion adjacent to the river (Longyearbyen Lokalstyre, 2017). Continual monitoring of the river and the input factors to runoff and sediment transport is important for safe area plans due to exposure to river bank erosion and potential flooding.

Suspended sediment transport is sensitive to climate change as this is controlled by supply and input. It is therefore important to understand the patterns of sediment storage, erosion, and transport and their interactions (Hodgkins et al., 2003). Sediment erosion in Arctic catchments is controlled by permafrost retention and active layer thaw. Glaciers and moraine systems are considered the most important sediment source for rivers on Svalbard. Future projections of increasing air temperature, glacier melt, and heavy rainfall provide conditions for potential increase in importance of moraine sediment input (Hanssen-Bauer et al., 2019).

1.2.1 Climate challenges

Air temperature rise is especially influential in the Arctic, accompanied by large spatial and temporal variability (AMAP, 2017; Hanssen-Bauer et al., 2019). Thus, consistent data coverage of climate and hydrology data is very valuable. At present, most temperature and precipitation measurement stations are located close to the coast or settlements. This uneven distribution often leads to increased uncertainty in data. Precipitation inferred from stations close to the coast often result in underestimations as precipitation typically increases with elevation (Killingtveit et al., 2003).

Longyearbyen (Svalbard Airport) has from 1971-2000 had a mean annual temperature of -6°C and mean annual precipitation of about 200 mm. Climate projections for Longyearbyen show an increase of mean annual temperature to above 0°C towards the end of the century. Annual precipitation has been projected to increase by 20-40%, varying with different simulations. Heavy rainfall events will also increase in intensity and frequency (Hanssen-Bauer et al., 2019). Trends of increased rainfall and decreased snowfall have already been observed, however a smaller change in Longyearbyen compared to other places on Svalbard

(Nowak et al., 2020). As stated in the Climate in Svalbard 2100 Report, the projected climate changes will likely have the following consequences in the Longyearbyen area:

- Increased river flow and possible increase in flood frequency and magnitude
- Change in seasonal runoff distribution with earlier snowmelt
- Increased glaciofluvial erosion and sediment transport
- Increase landslide and avalanche frequency (Hanssen-Bauer et al., 2019).

An increase in river flow and flooding would cause a higher intensity of sediment erosion and transport intensity. This may initially be limited by permafrost restraining sediment from erosion. However, an increase in active layer temperature or thickness would make more sediment available for erosion. This would promote degradation in the marginal moraines of Larsbreen and Longyearbreen glaciers, thus increasing their importance as sediment sources in the future (Etzelmüller & Frauenfelder, 2009).

1.3 Study area

The study area covers the full extent of Longyeardalen from Larsbreen and Longyearbreen Glaciers to Adventfjorden (Figure 1). The glaciers input meltwater to the two glacial rivers that confluence in the upper part of Longyeardalen and flows through Longyearbyen until the Longyear delta into the fjord. Steep slopes are located along Longyeardalen with mostly flat plateaus surrounding the area. Platåberget is located west of the study area as well as Platåbreen which inputs some meltwater to Longyeardalen (Stenius, 2016).

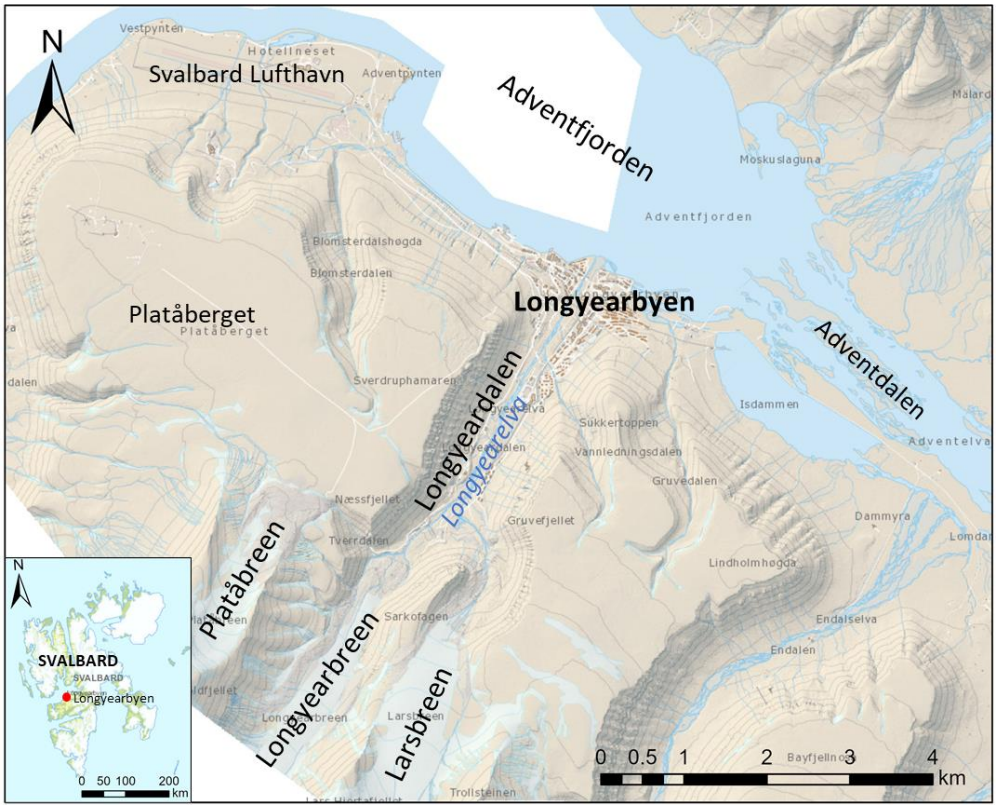

Figure 1 Overview map of the study area Longyeardalen and the surrounding region. Longyearelva runs from Longyearbreen and Larsbreen Glaciers, through Longyearbyen and into Adventfjorden. Adventdalen lies perpendicular to Longyeardalen from the innermost part of the fjord. Svalbard Lufthavn is located northwest of the study area. Platåberget and Platåbreen Glacier lie west of the study area. Scale 1:60000. (NPI, n.d.).

Longyearelva runs through Longyearbyen, the administrative centre of Svalbard. Since the establishment of Longyearbyen as a mining town in the early 1900s, many houses, facilities, and roads have been built. This expansion has been followed by the restriction of the Longyearelva flow path and construction of river banks to secure Longyearbyen from flooding and gain space for further settlement (Longyearbyen Lokalstyre, 2017; NVE, 2017). Further safety constructions and improvements along and in the river have been planned for the next years (NVE, 2020). Before human interference Longyearelva was naturally braided throughout its extent from the moraines until the delta (Hanssen-Bauer et al., 2019).

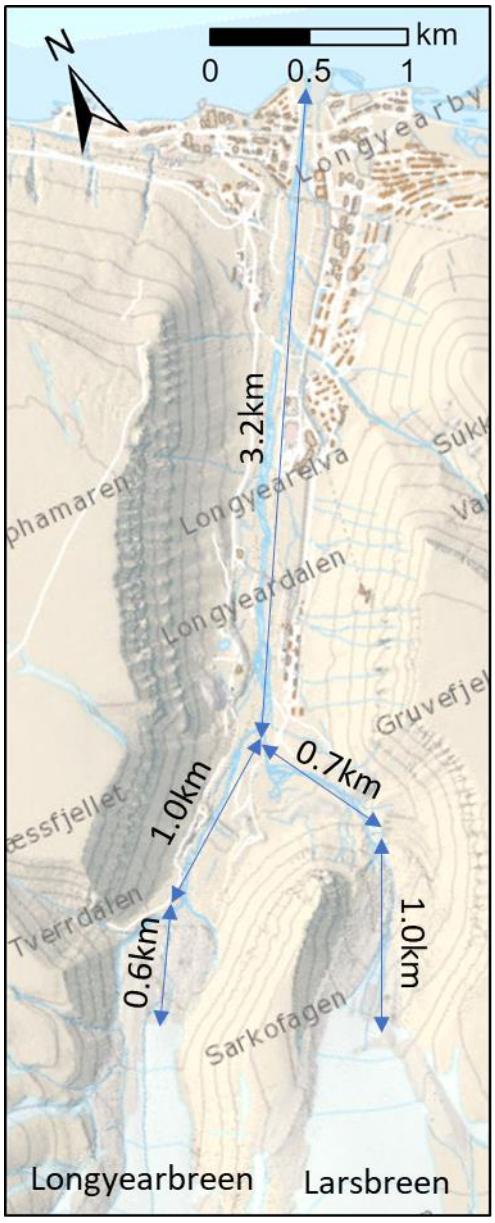

Figure 2 Distances in Longyeardalen along Longyearelva: from glacier fronts to moraine fronts, from moraine fronts to river confluence, and from river confluence to delta front. Total distance from glaciers to sea are 4.8km from Longyearbreen and 4.9km from Larsbreen.

Longyearelva is close to 5km long, including the total stretch from Larsbreen or Longyearbreen Glacier fronts until the sea (Figure 2). The distance from the glaciers until the point of confluence is very similar, where the river from Larsbreen flows the longest distance through the marginal moraine of ~1.0km. The total vertical height difference from the glacier fronts to the sea is approximately 270m and 400m from Longyearbreen and Larsbreen, respectively. Sarkofagen lies between the two glaciers and their marginal moraines.

1.3.1 Geology, permafrost, and glaciers

The geology of the study area is mostly uniform sedimentary bedrock with continuous permafrost. The bedrock is mainly of Tertiary age and consists of shale, sandstone, and siltstone (Etzelmüller et al., 2000). Unconsolidated Quaternary deposits cover more than one-sixth of the broader Adventdalen/Longyeardalen area (Major & Nagy, 1972).

Svalbard lies in a zone of continuous permafrost (Farnsworth et al., 2020; Vatne et al., 1995). The topography is dominated by mountains and valleys, with an extensive coastline. Permafrost on Svalbard typically has a thickness of <100m near coasts, around 100m in major valley bottoms, and >500m in highlands and high mountains (Hanssen-Bauer et al., 2019; Humlum et al., 2003). Warmer permafrost has been found on Svalbard, including Longyearbyen, compared to other Arctic regions such as Siberia and northern Canada (Hanssen-Bauer et al., 2019). As such, permafrost on Svalbard is especially sensitive to changes in temperature (Humlum et al., 2003).

Early studies of Adventdalen found permafrost reaching depths of 200-450 m (Major & Nagy,

1972). The active layer thickness in Adventdalen has increased by 0.6cm/yr in sediments and 1.6cm/yr in bedrock since 2000 (Hanssen-Bauer et al., 2019). Ice-rich permafrost has been found in this area covering about 4m of the top of the permafrost directly beneath the active layer (Gilbert et al., 2019). Ice-rich permafrost has also been observed in Longyeardalen, with the presence of frost-susceptible marine sediments below the marine limit of 62-70masl. These sediments include saline soil, which changes the freezing point, and thus the soil reacts differently to air temperature changes (Gilbert et al., 2019; Hanssen-Bauer et al., 2019; Keating et al., 2018). The upper part of Longyeardalen towards the glaciers lies above the marine limit and thus the soil is not considered saline in these areas.

Longyearbreen and Larsbreen glaciers are both considered cold-based, where some studies indicate the presence of temperate patches and others do not (Etzelmüller & Frauenfelder, 2009; Yde et al., 2008). Supraglacial meltwater drainage is most dominant on both glaciers. Large, ice-cored moraines cover the valleys in front of the glaciers. The till making up the moraines consists of fine matrix with angular gravel to stones, with a higher percentage of fine material found in Larsbreen moraine. The past maximum extent of the glaciers is marked by sharp lines between different colour of the slopes along the sides of the moraines. The majority of meltwater is transported within tunnels in the ice-cored moraine, whilst some water flows on the surface. Runoff through the moraines consists of glacial meltwater, snowmelt, and permafrost melt (Etzelmüller et al., 2000). Thin coal seams and abundant plant fossils are located in the study area. Notably, many fossils have been found in Longyearbreen marginal moraine (Major & Nagy, 1972).

Landslides and avalanches are a common occurrence on the slopes in Longyeardalen. This includes debris flows, snow avalanches, slush flows, and rock falls (Hanssen-Bauer et al., 2019). Snow avalanches often occur as cornice fall avalanches in the area (Eckerstorfer et al., 2013). Snow avalanche deposits have in some cases contributed to the formation of rock glacier, notably in front of the Larsbreen marginal moraine. Some of these rock glaciers have been pushed by the Larsbreen glacier advance during the Little Ice Age (Humlum et al., 2007).

1.4 Previous studies

Previous studies in Longyeardalen and Svalbard are important for understanding long-term changes and interannual variability in the source-to-sink sediment transport system. The project is motivated by a general lack in long-term monitoring and climate change. An advantage to relating observations to climate change in the Longyearbyen area is the availability of weather datasets. Precipitation measurements have been made by the Norwegian Meteorological Institute since 1916 in Longyearbyen, with data gaps until 1957 (Førland et al., 2020).

The Climate in Svalbard 2100 report discusses aspects of climate influence in Longyeardalen, including permafrost, landslides, glaciers, and sediment transport. The report presents hydrological studies of Longyearelva including water balance estimates by Killingtveit et al. (2003), and projected flooding estimates by Stenius (2016) based on data from Bayelva and De Geerdalen (Hanssen-Bauer et al., 2019). Some studies have been done previously of discharge and/or sediment transport in Longyeardalen (Etzelmüller et al., 2000; Grønsten, 1998; Løvaas, 2021; Riger-Kusk, 2006; Stenius, 2016). High suspended sediment

transportation from the glaciers correlated with discharge was found of 1993/1994 by Etzelmüller et al. (2000). Sediment transport increased over the melting season.

A relationship between discharge and SSC has been found in earlier studies on Svalbard. Monitoring in Bayelva found that diurnal SSC peaks slightly preceded diurnal discharge peaks for five successive melting seasons (Repp (1988) in Hodgkins (1997)). Further studies at Bayelva found a gradual seasonal SSC increase, suggesting that the glacier sediment source was dominant and that discontinuous input of sediment due to erosion of a thawed active layer was less significant (Hodson (1994) in Hodgkins (1997)). Gurnell et al. (1994) found that SSC preceded discharge peaks at Austre Brøggerbreen, and that the preceding time gap decreases over the melting season.

Longyeardalen has been photographed by airplanes and satellites sporadically since 1936 with mostly low and variable resolutions (NPI, n.d.). This provides a useful overview of morphological changes in the valley, both anthropogenic and natural. Drone models were produced in 2015 and 2017 of Larsbreen and Longyearbreen glaciers/moraines (Mannerfelt, 2017a, 2017b; Mertes, 2015). Mannerfelt (2017a, 2017b) calculated volume change in the extended moraine systems from July to September 2017 and found that a larger volume of sediment was removed from the moraine system slopes than deposited. Some sediment was redeposited downhill from slumping and glaciofluvial transportation. In September 2019, drone images were collected in Longyeardalen to produce a 3D model from the Larsbreen and Longyearbreen Glaciers to the Longyear delta (Hanna, 2019). Drone mapping was done of Longyearbreen glacier and moraine system in August 2021 (Nowak, 2021).

The long-term monitoring project of Longyearelva was initiated in 2018 (RiS ID 11641). This has started the establishment of a repeated, long-term dataset of hydrology and sediment transport in Longyeardalen. The monitoring effort was supported by a master thesis study in the summer 2020 by Løvaas (2021). This study investigated sediment erosion and transportation in Longyearelva, and the impact and effectiveness of flooding mitigations. Very high sediment transportation was recorded during a flooding event in July 2020.

2 Literature review

2.1 Arctic conditions

The Arctic is defined formally as areas north of the polar circle, i.e. 66.5°N. This is characterized by the occurrence of midnight sun in the summer and polar night in the winter (Serreze & Barry, 2014). More commonly the Arctic is characterized by extreme temperature fluctuations from -40°C to 30°C (Nilsson et al., 2015). Permafrost, extreme winter cold, low humidity, and high winter wind speeds are typical of Arctic locations, however this may also be found south of the Arctic circle (Barchyn & Hugenholtz, 2012; Hanssen-Bauer et al., 2019; Serreze & Barry, 2014).

Glaciers cover a significant part of Arctic land (Serreze & Barry, 2014). This follows large glacial and proglacial deposits covering bedrock (Nilsson et al., 2015). Svalbard is a part of the Arctic with relatively low glacier coverage, particularly along the western coast due to heat from the North Atlantic ocean stream (Sund, 2008).

2.1.1 Climate

Temperature conditions in the Arctic are uniquely low and variable, and highly dependent on land, air, and ocean interactions (Serreze & Barry, 2014). As well as large annual temperature fluctuations, inter-annual variations are often large at high latitudes (Hanssen-Bauer et al., 2019).

The location of the Arctic allows for greater future temperature change than locations closer to the equator. This effect is often referred to as “Arctic amplification” or, more generally, positive feedback (Hanssen-Bauer et al., 2019; Overeem & Syvitski, 2008). This makes the Arctic susceptible to an increase in air temperature, which would also lead to an increase in precipitation (Hanssen-Bauer et al., 2019; Nowak et al., 2020; Serreze & Barry, 2014). Both increase in temperature and precipitation have already been observed generally in the Arctic, however with large spatial variability (Førland et al., 2020).

Along with increased precipitation, it is expected that in the future a larger percentage of precipitation will be rain instead of snow in the Arctic (Hanssen-Bauer et al., 2019). Simulations of future rainfall have been made based on observations from Svalbard Airport and other Svalbard meteorological stations. These showed a ~10% increase in rainfall from 1961-1990 to 2071-2100, with a >20% increase in rainfall in autumn and winter (Førland et al., 2011).

2.1.2 Permafrost and active layer

Permafrost is defined as ground with a temperature below 0°C over a period of at least two years (Christiansen et al., 2020; French, 2007; Matveev, 2019; Rogger et al., 2017; Woo, 2012). The distribution of permafrost may be continuous, discontinuous, sporadic, or isolated, where continuous permafrost is most common in the High Arctic (French, 2007; Serreze & Barry, 2014).

The thickness and distribution of permafrost depends on air temperature, topography, snow cover, distance to the ocean, and more. Permafrost is typically thicker at high altitudes due to lower air temperature. This may also be the case in valleys if shadows are cast for long periods of the day (Humlum et al., 2003). Permafrost is usually thin or even absent below glaciers or very thick snow covers. This is because the ice/snow cover intervenes with the

energy exchange between the air and ground (Christiansen et al., 2020). The distance to the sea is important as the sea is a major heat source, resulting in thinner permafrost (Humlum et al., 2003).

The distribution of permafrost with depth is illustrated in Figure 3. The top layer of permafrost is referred to as the active layer, defined as seasonally-frozen ground. This layer thaws in the summer and freezes in the winter (French, 2007; Rowland et al., 2010; Woo, 2012). Active layer thickness is controlled mainly by thermal conductivity, where heat penetrates frozen ground more easily than non-frozen ground (French, 2007). Permafrost is underlain by non-frozen ground (Matveev, 2019).

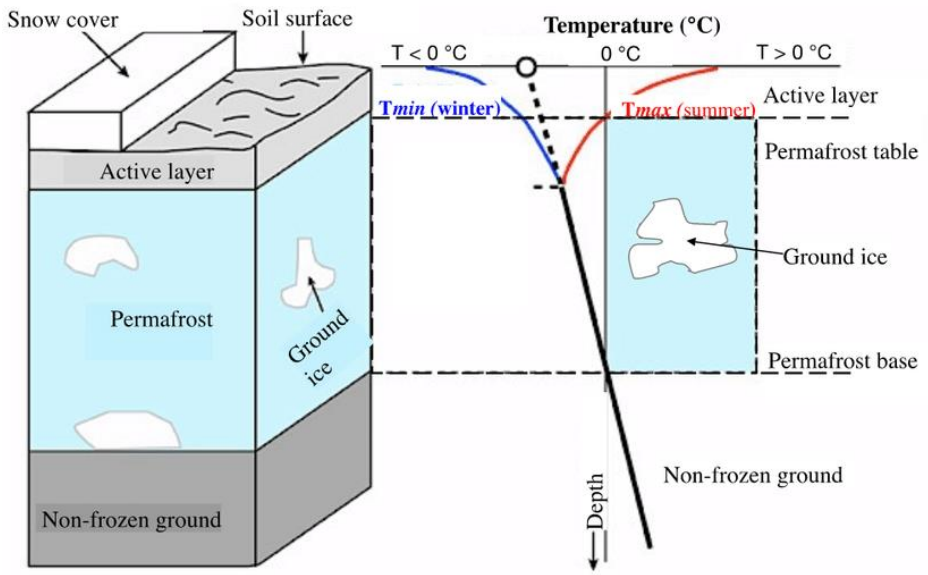

Figure 3 Illustration of permafrost distribution with depth. The active layer freezes during the winter and thaws during the summer. Permafrost may have pockets of ground ice within. Non-frozen ground is located below the permafrost base. The annual ground isotherm is positive with depth (black line), with seasonal non-linear isotherms in the active layer and the top of the permafrost layer (blue and red). From Matveev (2019).

As illustrated in Figure 3, permafrost and active layer conditions fluctuate yearly. Interannual variations may also affect permafrost thickness depending on the temperature and precipitation each year. A dry and cold autumn amplifies cooling and refreezing of the active layer after the summer. Large amounts of snowfall in the late winter protects ground from early summer thaw. This would delay or possibly limit the thaw of the active layer (Humlum et al., 2003).

2.2 Hydrology and sediment transport

Rivers are important landscape features responsible for erosion, transportation, and deposition of sediments (Nichols, 2009). Runoff in a river depends on the available water within the topography leading to river channels, i.e. in a catchment. Measurements of river discharge provides an inferred representation of volume of water in the catchment (Dingman, 2015). Runoff is usually a result of varying degrees of snowmelt and rainfall. The hydrology in a catchment is influenced by the dominant type, timing, and magnitude (Lafrenière & Lamoureux, 2019).

2.2.1 Sediment transport

Sediment transport in rivers occurs as suspension of fine grains and as bedload transport of coarse grains (Figure 4). Bedload transport occurs through sliding, rolling, or saltation on the riverbed. Sediments are eroded, transported, and deposited in fluvial systems.

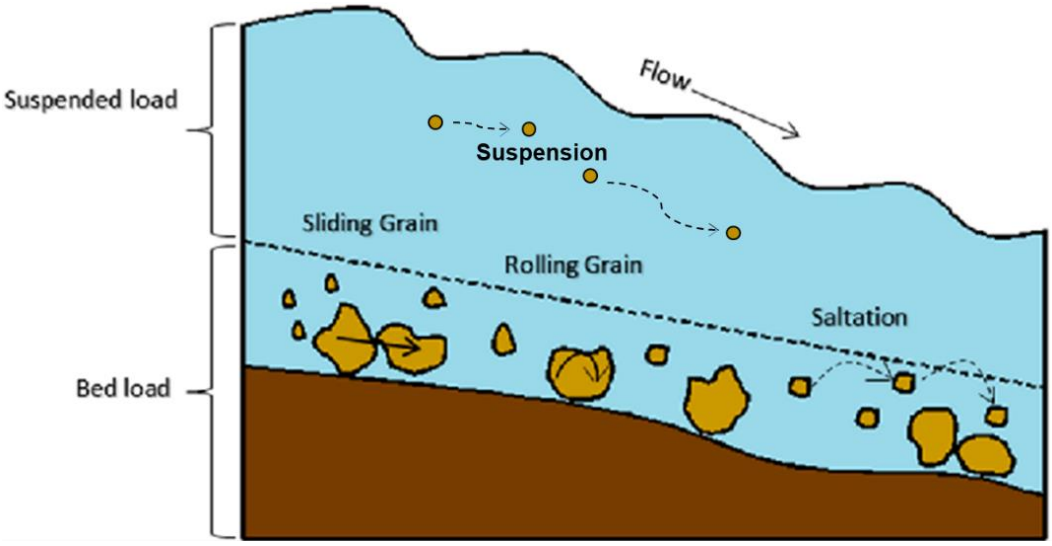

Figure 4 Grains in suspended load and bedload transport in a river. Suspended load is transported by suspension. Bedload is transported by sliding, rolling or saltation. Flow direction is to the right. Modified from Awang Ali et al. (2017).

Sediment transport as suspension is mainly controlled by sediment input, such that suspended sediment concentration (SSC) may be used as a simplified direct measure of input. Bedload transport is mainly controlled hydraulically, i.e. by the water flow. The real transport of sediments in these forms will vary and respond differently to external influence such as temperature increase (Hodgkins et al., 2003).

Sediment load and yield may be obtained using SSC and discharge measurements (Bogen, 1996). Sediment load (tonne/yr) describes the total transport of suspended sediment with observed discharge over the year. Sediment yield (tonne/km^2/yr) describes the sediment load per area in a catchment (Bogen & Bønsnes, 2003).

Flow and friction are the main controls on degree of erosion and deposition. The competence of a river is the maximum particle size that may be transported. This is directly related to the flow velocity, i.e. the competence increases with velocity. A rivers capacity is the maximum number of particles that can be transported (Brattli, 2019).

River erosion is limited by a critical velocity (v_c). If the flow velocity reaches this value, erosion of river bottom particles of a certain size may occur. This is expressed with the following equation:

$$v_c = kW^{\frac{1}{6}}$$

Where v_c = critical velocity, k = empirical constant, and W = weight of particle (Brattli, 2019). Hjulströms diagram visualises the equation above to show the response of different grainsizes to flow velocities (Figure 5).

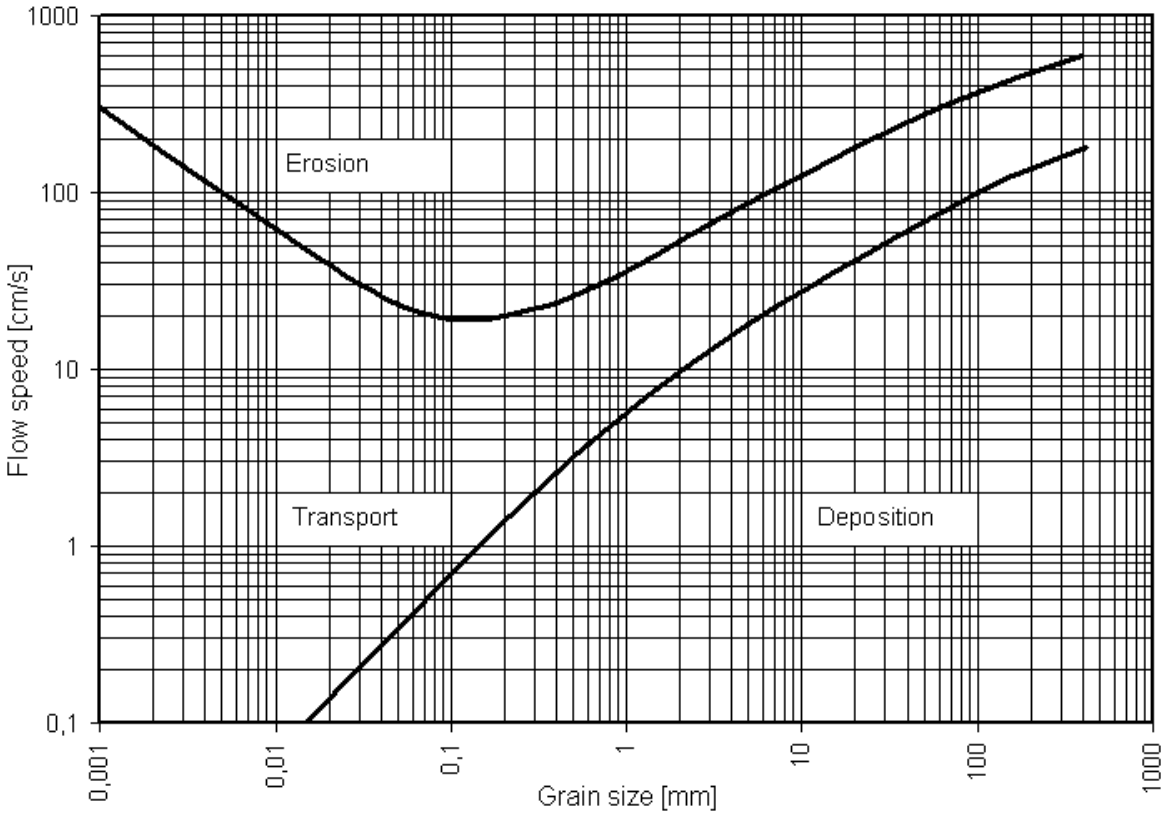

Figure 5 Hjulströms diagram: The relationship between grainsize (mm) and flow velocity (cm/s) in a river. Displays the critical values of erosion, transport and deposition of grains. From Hjulström (1935).

2.2.2 Braided rivers

A braided river is characterized by the presence of several alternating channels that shift paths over time due to erosion (Figure 6). Channel bars are typically formed in the middle of channels from deposition. As channels shift, they may become inactive for short or very long periods of time, and sometimes completely abandoned. Near vertical erosion banks often form on river banks as material is eroded by the river (Nichols, 2009). The morphology of a braided river system depends on frequency of channel shifts, sediment supply, discharge, and bed slope (Ashworth et al., 2004).

Sediment transport in braided rivers is controlled by the intensity of braiding. Increased number of channels reduces the flow velocity in each channel, decreasing the bedload transport rate (Ashmore et al., 2011). Intensity may change over time, resulting in temporary storage of larger bedload rocks during low flow periods and high erosion rates during high flow periods. Changes in discharge on an hourly, daily, and yearly scale promote adjustments in channel braids (Peirce et al., 2018).

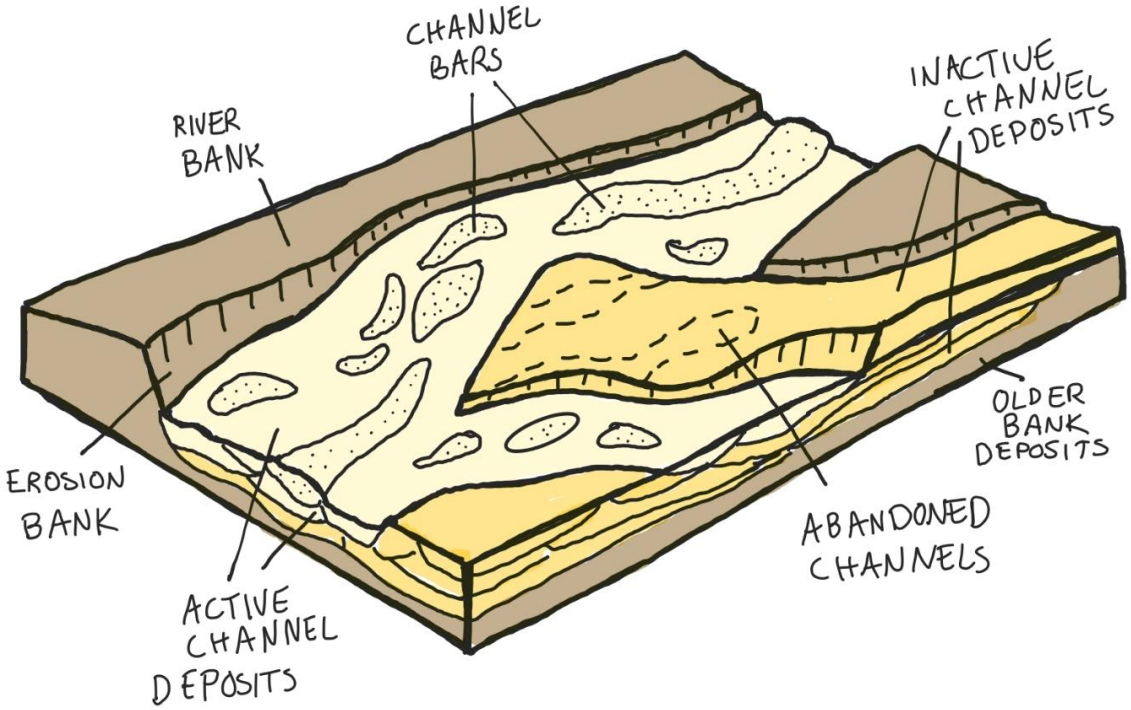

Figure 6 Illustration of a braided river. Pale yellow: active channels with channel bars. Dark yellow: inactive channels. Brown: unspecified/floodplain deposits. River banks with erosion banks are formed by active and inactive channel erosion. Abandoned channels are present in some inactive channel deposits. Modified from Mount (1995).

2.2.3 Roundness of rocks

The roundness of a rock describes the visual appearance of its surface, edges, and corners. Figure 7 shows a commonly used classification of a scale of six degrees of roundness; well rounded, rounded, subrounded, subangular, angular, and very angular (Nichols, 2009).

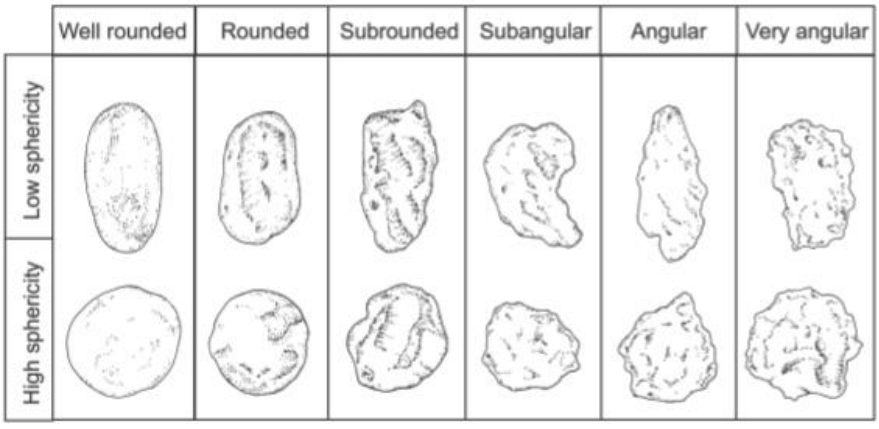

Figure 7 Classification of six degrees of roundness of rocks for low and high sphericity grains. These are: well-rounded, rounded, subrounded, subangular, angular, and very angular. From Nichols (2009).

When grains are transported, they collide with other grains. Sharp corners and edges are exposed and may be broken off or blunted by this. During transport, a grain will continuously be smoothed, thus increasing its degree of roundness. Grains transported a very short distance are likely to be very angular, e.g. snow avalanche or rock fall deposits. Grains that are

transported far and/or that are in environments with a lot of potential friction and movement are likely to be well rounded, e.g. fluvial or beach deposits (Nichols, 2009).

Roundness is distinguished from sphericity as a spherical grain is not necessarily rounded, and a well-rounded grain is not necessarily a sphere. The main determining factor of roundness is typically the sharpness of edges and corners on the grain (Wadell, 1932). This is usually estimated visually, but may also be calculated using the shape of cross-sections (Nichols, 2009). Roundness has a relationship to size, meaning that through contact and transportation grains will break and decrease in size as well as become more rounded. This means that at a certain location, grains of the same source may display increased roundness with decreased size (Burki et al., 2010).

2.3 Arctic hydrology and sediment transport

Arctic hydrology is unique due to only a few months in the summer with running water in channels when air temperature is above freezing (French, 2007). The melting season is typically from May to October, where river runoff occurs within this period (Killingtveit et al., 2003; Nowak et al., 2020). Unique conditions such as permafrost result in large seasonal variability in discharge and sediment transport in the Arctic. In glacial catchments it is common that sediment transport occurs in larger, discontinuous events (French, 2007; Overeem & Syvitski, 2008).

Channels in continuous permafrost areas consist of almost entirely surface runoff. With discontinuous permafrost, typical in sub-arctic areas, channels are fed by both surface runoff and groundwater. Periods of flow is influenced by air temperature and amount of snow, as this may delay or accelerate break-up and freeze-up of channels (French, 2007).

Groundwater runoff is often assumed non-significant in studies of Arctic catchments. This is because groundwater flow in permafrost ground usually only occurs in the active layer. Infiltration may occur in this top 1-2m layer with precipitation or meltwater moving from the surface and down into the ground (Killingtveit et al., 2003). Rainfall infiltrated to the active layer may be stored for up to two hydrological years (Nowak et al., 2020).

2.3.1 Sediment sources and transport

Sediment sources in the Arctic can be divided into three main groups; glacial, colluvial (landslide soil), and fluvial (Orwin et al., 2010). Fine particles may come from weathering or aeolian transport, whereas coarse sediment sources are typically glacial sediment and mass-wasting processes (French, 2007). In a source-to-sink system, these sources may be divided into primary, secondary, and transportation sources (Figure 8). Primary sources can be defined as sediment added directly to active channels. Secondary and transportation sources of sediment may be added to channels indirectly after initial deposition. These may all input sediment that are transported to the sink. The sink comprises deposition of sediment and transport out of the system e.g. into a marine system.

Figure 8 Flow chart of a source-to-sink system, with three categories of sources.

Sediment in arctic rivers can be transported as solution, suspension, or bedload transport. Some studies suggest that bedload transport is most prominent (French, 2007). One example from Canada found around three times as much bedload transport compared to suspended load over a 12-day period during peak discharge (Priesnitz & Schunke, 2002). This differs from a long-term study in an Alpine catchment that found that 76% of total sediment transport was suspended load, where most of this occurred during flood events (Lenzi et al., 2003). This relative transport of suspended and bedload sediment will vary based on glacier characteristics, from 40% to > 90% suspended load of the total transported sediment (Bennett & Glasser, 2011).

Suspended sediment input strongly depends on the stability of the coarse surface of the river bed. Fine sediment may be locked below the surface, then become available with increased bed instability, typically due to seasonal thaw and discharge (Lenzi et al., 2003). The potential maximum suspended sediment concentration (SSC) in glacial rivers is higher than most non-glacial rivers (French, 2007). Studies from Alaska found that SSC in a glacial stream was 36 times higher than in a non-glacial stream, with a 15 times higher runoff rate (Wada et al., 2018). High SSC may influence the water quality as well as channel morphology and erosion (Lenzi et al., 2003).

2.3.2 Permafrost influence on hydrological systems

The presence of permafrost influences the seasonal development of hydrological systems and sediment availability and transport (Hodgkins, 1997). A visual representation of the seasonal effects of permafrost and ice on a proglacial system is shown in Figure 9. In the early melting season runoff increases abruptly when snow and glacial melt starts, but ice still blocks the river channel (Killingtveit et al., 2003). This causes water to flow outside the channel over frozen permafrost ground, where erosion is limited to fine, loose sediments. Throughout the season meltwater may flow in the channel and the active layer thaws. Seasonal thaw decreases the stability of river banks, allowing bank erosion. Discharge increases with sediment availability, giving potentially very high erosion and sediment transport rates (Figure 9).

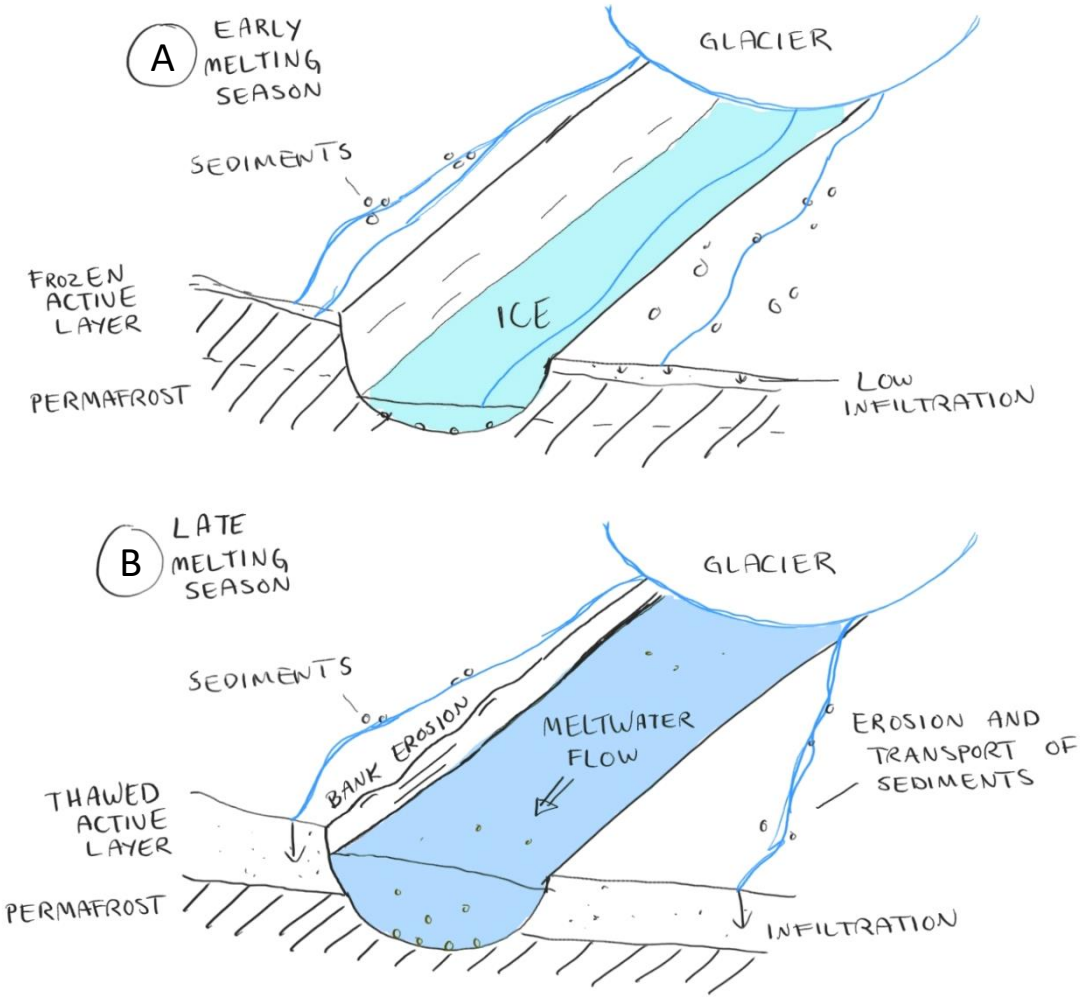

Figure 9 Illustration of a proglacial channel in a continuous permafrost area during A) early melting season: Ice blocks meltwater from flowing in the channel, and very little infiltration and sediment erosion occurs due to frozen ground. B) late melting season: meltwater flows freely in the channel and active layer is thawed, such that more sediment is available for erosion and transportation in and around the channel.

The relationship between suspended sediment concentrations (SSC) and discharge in the Arctic is unique. Low SSC in the early melting season can be explained by the retention of sediment in frozen ground. Throughout the melting season, increased SSC has been observed without an exhaustion of sediment supply as more becomes available over the summer. This differs from Alpine catchments, where highest SSC has been observed early in the season with a gradual decrease indicating exhaustion of the sediment supply (Gurnell et al., 1994). This difference in seasonal development of sediment transport highlights the significance of permafrost for suspended sediment transportation.

Permafrost may reduce subsurface storage and infiltration of runoff, thereby giving a more rapid runoff response and potential flooding (McNamara et al., 1998). Disappearance of permafrost, on the other hand, may increase runoff due to the increased infiltration and deeper flow channels. Furthermore, this may decrease the seasonal variability in runoff. Simulations from Austria of permafrost disappearance found that the peak runoff in July decreased, but the baseline runoff in the early and late season was higher (Rogger et al., 2017).

2.3.3 Daily and seasonal cycles

Daily and seasonal variability in discharge and sediment transport is prominent in arctic rivers. Daily discharge fluctuations are a common effect of air temperature increasing during the day, thus increasing ablation of glaciers. A typical cycle includes low discharge in the morning, higher discharge in the afternoon and evening, and decreasing discharge in the night. Daily fluctuations are most prominent in the summer, increasing towards the mid-late season when ablation reaches its peak (Bennett & Glasser, 2011; Hodgkins et al., 2003).

Seasonal variability in discharge and suspended sediment concentration (SSC) may be influenced by several factors. This could be changes in sediment input from subglacial channels (Østrem, 1975). In a glacially controlled system, SSC typically peaks early- to mid-season due to a rapid emptying of the fluvial system within the glacier (Bennett & Glasser, 2011). The variability in SSC is mainly controlled by runoff (Vatne et al., 1995).

Daily fluctuations in discharge and SSC may shift over the melting season, resulting in peaks at different times in June, July and August (Hasnain, 1999). This has also been observed outside of the Arctic, where the cause is e.g. monsoons in the Himalaya area (Hasnain, 1999). Correlation between discharge and sediment may be present in catchments in the Arctic. This presumes that sediment availability for erosion is sufficient at the time of increased discharge. As such, correlation in discharge and SSC may vary seasonally, or appear or disappear depending on sediment availability and ground thaw (Bogen & Bønsnes, 2003).

2.4 Glaciers

Glaciers and ice-caps cover more than 50% part of Svalbard (Farnsworth et al., 2020). The islands were glaciated several times in the late Quaternary, where the last occurrence was during the Last Glacial Maximum of ~20ka (Gilbert et al., 2019).

Glaciers may be classified based on thermal conditions and size. Processes in the base and beneath a glacier relies highly on the temperature of basal ice. This depends on how much heat is generated at the base and the temperature gradient of the ice. Commonly used classifications are cold-based, warm-based, and polythermal glaciers. Cold-based glaciers are frozen to the ground below, and thus no meltwater flows below the glacier. This is typical of thin, slow moving glaciers with significant cooling in the winter and limited melting in the summer. Warm-based glaciers have higher temperatures at the base, causing some melting in the boundary between ice and ground. This is common for thick, fast moving glaciers with considerable summer melting (Bennett & Glasser, 2011). In literature, the term temperate is often used interchangeably with warm-based (Hodgkins, 1997).

The thermal condition of a glacier may vary spatially within a glacier, and also through time (Bennett & Glasser, 2011). The term polythermal is often used to describe glaciers with variable temperature, displaying traits of both cold- and warm-based glaciers. Cold-based glaciers may still have some temperate patches or layers distributed within the glacier base. Cold-based glaciers typically have lower basal erosion potential (Etzelmüller et al., 2000).

Glacier size is mainly determined by climate. Thus, changes in climate can cause a glacier to advance or retreat on an annual or long-term basis (Bennett & Glasser, 2011). Glacier development due to climate has important impacts on the wider environment in the Arctic. After the Holocene, glacioisostatic rebound has dominated regions previously covered by glaciers. Arctic areas, including Svalbard, have experienced uneven post-glacial uplift due to

variable ice-cover, duration, and more. Uplift lead to a lowered relative sea level, resulting in a increased elevation difference between many current glaciers and sea level (Farnsworth et al., 2020). More recently, glaciers on Svalbard are retreating, reducing the area coverage of glaciers of -0.2% per year, with spatial variability (Hanssen-Bauer et al., 2019).

2.4.1 The Little Ice Age

The Little Ice Age is typically referred to as the "glacial advance of the last few centuries" (Grove, 1988), of which the period varied globally and is not exactly agreed upon. Recent definitions include "a slightly cooler period in the Holocene, lasting from about 1300 to 1850" (Paul & Bolch, 2019). Other suggestions include 1550-1800 (Lamb, 1977), 1350-1850 (Wanner et al., 2008), and 1250-1920 (Farnsworth et al., 2020). The period marks the most recent maximum extent of glaciers in most regions of the world (Paul & Bolch, 2019).

Important occurrences during the Little Ice Age are a lot of lateral accumulation of rock and debris, marginal moraine formation, and considerable changes within the glacial forefield. The boundary of marginal moraines typically stayed consistent through the period. Therefore, it is often possible to reconstruct the maximum extent of the glacier during the Little Ice Age in the field (Paul & Bolch, 2019).

2.4.2 Glaciofluvial sediment transport

Glaciers have a significantly large influence on catchments by shifting the typical seasonal meteorological response and increasing runoff considerably during the melting season (Hodgkins, 1997). This, in turn, gives different conditions for sediment transport compared to non-glacierized catchments. The distribution of suspended sediment transport, which is typically controlled by runoff, will vary depending on the glacier characteristics. For cold-based glaciers the sediment availability for glaciofluvial transport is typically controlled by ground thaw, compared to subglacial erosion for warm-based glaciers (Hodson et al., 2016).

Glacial sediment is transported and deposited at varying distances from the glacier. Proximal sediment deposition is controlled by rate of supply and meltout till availability. This may act as a temporary depositional location with buildup and erosion of sediments during low and high periods of meltwater, respectively. Beyond the initial front, a braided river pattern is typical, with consistent glacial influence on discharge and sediment transport. Fine sediment proportion increases with distance from the glacier, and distal glaciofluvial channels have decreased glacial influence. Typically, with longer transport distance, glacial rivers act more similar to non-glacial rivers (Bennett & Glasser, 2011).

2.4.3 Rock glaciers

Rock glaciers are lobate forms of ice and frozen debris that move due to gravity and deformation of internal ice (French, 2007). Rock glaciers are found in permafrost regions, typically where there is steep topography (Humlum et al., 2003). They consist of very coarse-grained surface material, often with a large amount of talus, underlain by fine-grained material. Some rock glaciers contain lenses of massive ice (Rogger et al., 2017). The material often accumulates from snow avalanche deposits, consisting of mixed rock fragments and ice (Humlum et al., 2003).

There are two main types of rock glaciers: active and fossil rock glaciers. Active rock glaciers contain permafrost and are moving. Fossil rock glaciers do not contain permafrost and are not moving (Rogger et al., 2017). Active rock glaciers are typically 20-100m thick and 200-800m

long in the movement direction. Their movement speed is typically 0.1-1m/yr, which is slower than ice glaciers (Humlum et al., 2003).

2.4.4 Moraines

Moraines are large forms of accumulated glacial till deposits located along the margins of glaciers. Typical deposits are poorly sorted and display highly variable degrees of grain rounding. Morphological features, including ridges, eskers, and drumlins, may form in moraine systems due to a range of glacial depositional processes (Nichols, 2009).

In permafrost landscapes such as Svalbard, many glaciers are associated with large ice-cored moraines and ablation moraines (Etzelmüller et al., 1996; Etzelmüller et al., 2000; Hanssen-Bauer et al., 2019). Ablation moraines are formed by supraglacially transported debris deposited at the glacier margin. With increasing thickness of such debris, parts of the glacier may become separate from the main glacier and thus stagnant, which can then become an ice-cored moraine (Bennett & Glasser, 2011; Østrem, 1964). Ice-cored moraines are formed based on the thermal regime and dynamics of the associated glacier. Conditions favouring ice-cored moraine formation are cold-based glaciers and the presence of permafrost. They are often large, up to 50m high. Englacial melt-out material is often deposited on top of such moraines during glacial retreat. The outer extent of ice-cored moraines marks the maximum glacier advance (Etzelmüller et al., 1996).

Over time, ice-cored moraines may increase or decrease in stability. With glaciofluvial erosion and thaw-driven movement, ice is exposed to thaw, which destabilises the till. With a sufficiently thick debris cover, the ice-core will be protected from melting (Tonkin et al., 2016). Warming climate may re-initiate thaw and destabilise and degrade ice-cored moraine systems. Further destabilisation can occur from added water through rainfall or snowmelt (Gariano & Guzzetti, 2016; Humlum et al., 2003; Kokelj et al., 2017).

2.5 Slope processes

Slope processes, comprising landslides and avalanches, describe the mass movement of material under the effect of gravity (Gariano & Guzzetti, 2016; Hermanns, 2016; Highland & Bobrowsky, 2008). This applies to rocks, soil, debris, snow, and more. “Failure” is associated with most slope processes. This is a certain point of significant movement, typically when strain becomes too large for material stability. The process of movement occurs on a many scales and often through several stages. A typical landslide or avalanche occurs through pre-failure deformation, the failure itself and post-failure displacement. Such movement may occur repeatedly over time scales from seconds/minutes to years (Hungr et al., 2013).

A landslide is comprised of specific parts which are illustrated in Figure 10. Some important terms are highlighted using a rotational landslide as an example. The surface of rupture is a typically weak zone where the main body of failed material can slide over the original ground material below. Main and minor scarps are near-vertical surfaces exposed through downslope movement of adjacent material. The crown is the area directly behind the main scarp which has not failed. There are often cracks on the crown, approximately parallel to the scarp, due to strain and instability from removed adjacent material. Cracks can also occur on the main body, both transverse and radial. Flanks are located along the main body, often connected to scarps. The toe is the furthest reaching material after movement (Highland & Bobrowsky, 2008). Some other terms are also labelled on the illustration.

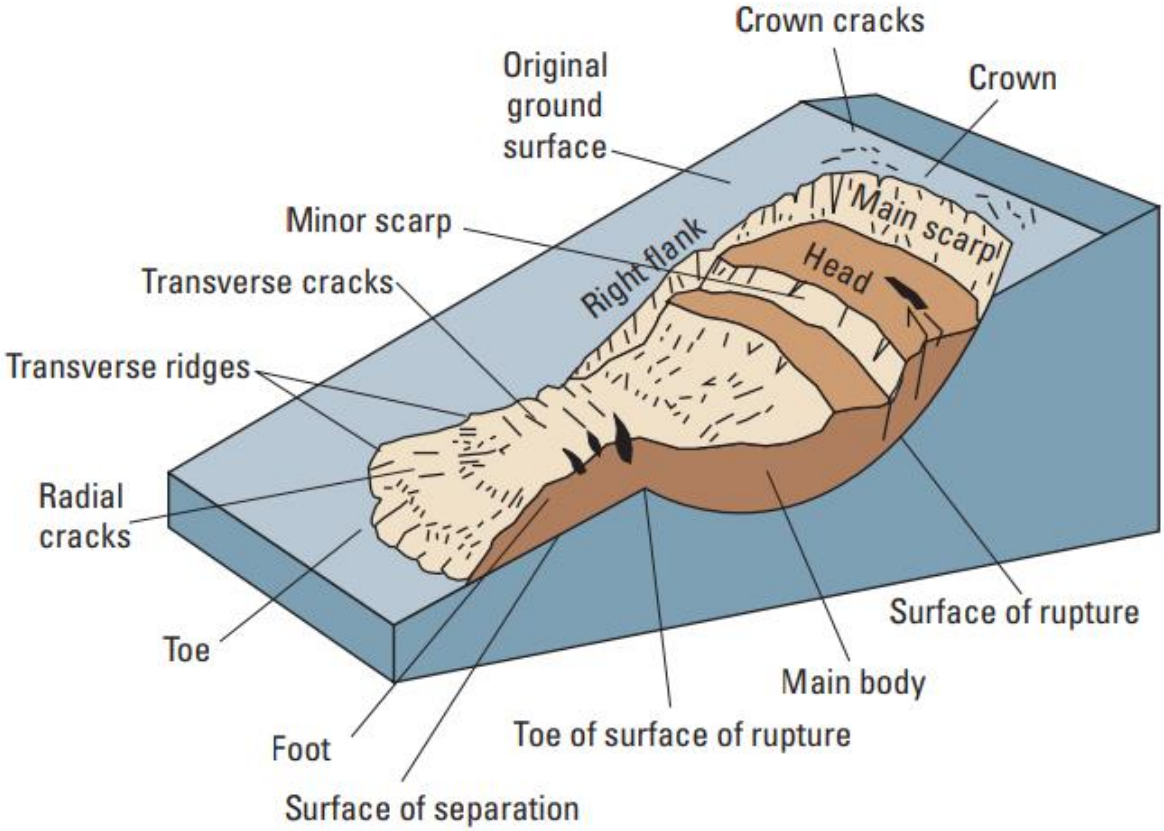

Figure 10 Simple illustration of a rotational landslide with important terms. Showing the sliding of material along the surface of rupture exposing scarps and flanks and forming cracks. From Highland and Bobrowsky (2008).

2.5.1 Types of landslides and avalanches

Landslides are classified based on the materials and movement types involved. Materials are commonly classified as rock, clay, mud, silt, sand, gravel, boulders, debris, peat, and ice. The commonly used movement types are falls, topples, slides, spreads, flows, and complex (Hungr et al., 2013). The term complex is less used in recent years, where instead the term slope deformation is applied. Snow avalanches are in most cases considered separately in classification, but in Scandinavian countries snow is considered as a material within landslide classification (Hermanns, 2016). Combining the terms for materials and movement give a large variety of landslide and avalanche types. Some of these are illustrated in Figure 11.

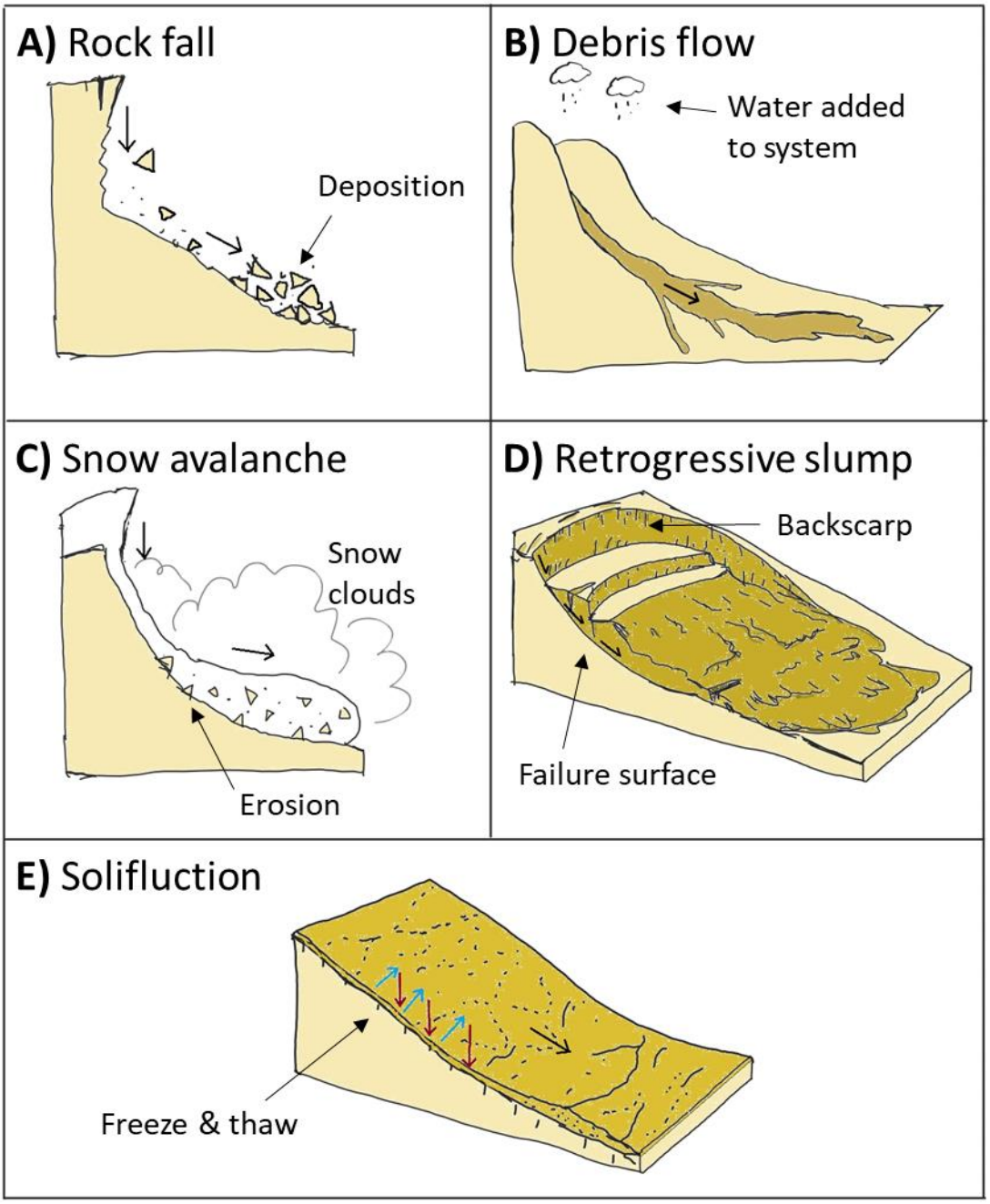

Figure 11 Diagram of some slope process types. Colours: bedrock in light beige, soil in dark beige, snow in white. A) Rock fall, B) Debris flow, C) Snow avalanche eroding and transporting rocks, D) Retrogressive slump, E) Solifluction from freeze and thaw processes, with lobes. Inspired from Highland and Bobrowsky (2008).

Rock fall

Rocks detach from cliffs by tensile cracking, bending or other, and fall abruptly downwards (Figure 11A). The rocks roll and/or bounce after striking the slope below, which can occur as single rocks or in clusters. Rocks may break into smaller pieces from impact with the ground or other hindrances. Larger rocks often travel further due to higher velocity from more weight. The roundness of deposited rocks is often angular due to the short transportation distance and breaking. The deposits are typically small in volume (Highland & Bobrowsky, 2008; Hungr et al., 2013).

Debris flow

Very rapid to extremely rapid flow of debris in channel(s) (Figure 11B). They are often triggered by the addition of water into the system from rain, snowmelt, or other. Flows will move on slopes steeper than 10°-20°. As material surges downslope, it can erode the slope material below and add it to the flow. The front of the flow can be either a concentration of boulders or a turbulent "head". Typically, debris flows occur in the same place periodically where paths have been made by previous flows. They may develop as a secondary part of a landslide process with materials from initial failures such as rock falls (Hungr et al., 2013).

Snow avalanche

Snow avalanches are masses of snow moving rapidly down steep slopes. They can erode and transport rocks, ice, vegetation, or soil during movement. The two main types of snow avalanches are loose snow avalanches and slab avalanches (Schweizer et al., 2003). Figure 11C illustrates a loose snow avalanche from the breakoff of a snow cornice hanging above a steep slope. A cornice is a leeward mass of snow growing outwards over a cliff or slope break formed from windblown snow (Burrows & McClung, 2006).

Retrogressive slump

A slump is a rotational landslide, i.e. a slide with upwards curved rupture surface (Figure 11D). These types of landslides are often triggered by the saturation of slopes from intense rainfall, rapid snowmelt, or ground-water level rise (Highland & Bobrowsky, 2008; Hungr et al., 2013). Soil slumps are characterized by a prominent main scarp. The main body sometimes has some internal deformation (Hungr et al., 2013). Concave cracks towards the movement direction often form in the main body (Varnes, 1958). Retrogressive slumps are typical in permafrost areas due to the possible saturation of a rupture surface from active layer thaw. In these cases, they are often referred to as thaw slumps/slides (Burn & Lewkowicz, 1990).

Solifluction

Solifluction is a type of creep that occurs in locations with permafrost (Figure 11E). The movement is very slow and is caused by the yearly freeze and thaw cycle in the active layer. Ground rises due to freezing and expansion, then sinks due to thaw. The process typically forms characteristic solifluction lobes (Highland & Bobrowsky, 2008; Hungr et al., 2013).

2.5.2 Slope processes in Arctic conditions

Characteristics that influence slope conditions and failure in the Arctic include permafrost, extreme low winter temperatures, yearly freeze-thaw cycles, glaciers, and snow. Failure may occur at shallower angles than usual in permafrost ground (Hanssen-Bauer et al., 2019). Seasonal thaw of the ground can temporarily oversaturate the soil, decreasing shear strength and initiating failure. Failures in permafrost regions can expose the ground below, changing what parts of the ground that may be thawed by warm air (Highland & Bobrowsky, 2008).

Failure in permafrost environments may be triggered by a localized increase in pore water pressure. This can occur due to local variability in active layer thaw depth due to e.g. variable ground materials. An uneven increase in pore water pressure leads to irregular shear strength which can trigger detachment slides or slumping (Lafrenière & Lamoureux, 2019). Other

possible trigger mechanisms include undercutting stream erosion or coastal wave erosion (French, 2007).

Some characteristic failure types in Arctic conditions are:

- Thermokarst: a broad term that describes any material released from some thaw in permafrost ground through e.g. collapse or subsidence (Etzelmüller et al., 2000; French, 2007; Lafrenière & Lamoureux, 2019).
- Retrogressive thaw slumps/flows: backwards expanding failure of saturated soil, typically large, with a steep and ice-rich scarp (Highland & Bobrowsky, 2008). Scarps are typically 1-2m tall, the failed mass may be large in volume, and the water availability is often high (Lafrenière & Lamoureux, 2019). They are often active for several decades (Lewkowicz & Way, 2019).
- Active layer detachments: downslope displacement of parts of a thawed active layer, typically with a prominent main scarp and an elongate shape in the downslope direction. Channelized drainage of meltwater may occur from larger detachments (Lafrenière & Lamoureux, 2019).

Failures such as these may further enhance the instability of ice-rich ground. For example, an active layer detachment may expose massive ice below, which promotes uneven thawing and can lead to a retrogressive thaw slump (Rudy et al., 2017).

Permafrost conditions change over time, which may change the strength and stability of slopes (Christiansen et al., 2020). The active layer may reach depths beyond its normal thickness during unusually high air temperatures in the summer. This promotes slope instability, providing conditions for sudden slope failures. This may be further enhanced by the presence of ice-rich zones (French, 2007).

Valley asymmetry may have an impact on slope failure in permafrost regions. North-east facing slopes are exposed to more solar radiation and heat due to the position of the sun, even during midnight sun in the summer. This may lead to more slope failure on these slopes than south-west facing slopes. However, this is often not the most influential factor on sediment transport in glacial catchments, where glaciofluvial erosion is considered more important (Ulrich et al., 2010).

2.5.3 Slope processes in glaciofluvial catchments

Some hydrological connectivity is necessary for sediments from erosion to impact the downstream system. This means slope processes should be immediately adjacent to active channels to directly influence the sediment yield. However, channels in braided glaciofluvial systems shift over time, such that hydrological connectivity may change daily and annually (Lafrenière & Lamoureux, 2019; Lewis et al., 2012). The contribution of sediment input from disturbed permafrost slopes may be significant in some cases, however downstream observations do not always correspond to these indications. This may be due to ephemeral behaviour, small percentage of volume from individual slopes, or temporary storage in the transportation path (Lafrenière & Lamoureux, 2019).

Glaciofluvial channels may have particularly high erosion rates in proximity to slope failures such as active layer detachments and retrogressive thaw slumps (Lafrenière & Lamoureux, 2019). Slope failures in glaciofluvial catchments may act as a positive feedback loop for

erosion, sediment transport, and further slope failure. Increased sediment load may occur with connectivity of slope failures to active glaciofluvial channels, increasing the potential river erosion. This may in turn trigger further slope instability by river bank erosion. As such, one initial slope failure may result in long-term changes in glaciofluvial morphology and sediment load (Rowland et al., 2010).

A study from the Canadian Arctic investigated the downstream impact of retrogressive thaw slumps on suspended sediment concentration in a large catchment. Rudy et al. (2017) found a clear impact of slumps, with a three order of magnitude increase in total suspended sediment compared to catchments undisturbed by slumping. They suggested that variability of downstream suspended sediments is increased with connectivity of slumps to channels. The study highlights that fluvial sediment transport will be further intensification with climate-driven thaw displacement (Rudy et al., 2017).

2.5.4 Climate change influence on slope processes

Climate change factors including increased air temperature, precipitation, and rainfall intensity have the potential to affect slope processes globally (Gariano & Guzzetti, 2016). This is especially relevant in the Arctic with active layer thaw. Increased air temperature extends the yearly period during which the active layer is thawed, and increases the possible depth of thaw. As such, landslides may occur during a longer period each year, and may occur more frequently and/or effecting larger volumes (Christiansen et al., 2020; Hanssen-Bauer et al., 2019; Lewkowicz & Way, 2019). Higher rainfall intensity also contributes to increased landslide probability, due to increased pore water pressure with infiltration (Hanssen-Bauer et al., 2019).

Thawing of permafrost may reduce the presence of interstitial ice, decreasing shear strength, which would increase the frequency of slope failures. Glacier retreat is also a possible consequence of increased air temperature. This may lower the load on the new exposed ground or steepen slopes, which can increase slope failure probability (Gariano & Guzzetti, 2016). Increased slope erosion with hydrological connectivity may increase the sediment load in rivers, which promotes river erosion. This could further destabilise and erode slope sediment (Rowland et al., 2010).

Increased rainfall can have a secondary effect on landslide occurrence. The further addition of moisture to the ground can make the top layer of permafrost more ice-rich. This can act as a barrier for thaw as a larger amount of heat is required to thaw a thicker layer of ice. Once the ice starts to thaw, the water content will be higher and thus friction will be lower. Therefore, more energy may be needed to trigger landslides, but they may occur more frequently during seasonal thaw peaks (Hanssen-Bauer et al., 2019). Rainfall may also contribute to continuing the retrogressive development of thaw slides/slumps (Lafrenière & Lamoureux, 2019).

3 Methods

Sediment sources, erosion, and transportation was observed over the melting season 2021. A range of methods were applied, with adjustments and changes done throughout the fieldwork period due to challenges arising in the Arctic environment. Some methods were continued from the established monitoring in 2018, 2019, and 2020.

3.1 Mapping of Upper Longyeardalen morphology and sediments

Upper Longyeardalen is here defined as the area from Nybyen/Sverdrupbyen to both Longyearbreen and Larsbreen Glaciers including valley side slopes. Drone photography of Longyearelva and Larsbreen and Longyearbreen moraine areas was carried out over 10 days between 07/07 and 10/09 to document the state of and changes in morphology. The aim was to use vertical drone images to create orthophotos and Digital Elevation Models (DEMs) to be used as a key dataset in ArcGIS mapping. Drone mapping was supplied by field visits with ground photography as well as angled drone photography.

3.1.1 Drone Fieldwork

Drone flights were completed from July to September, with two main missions in the mid-season (July/August) and late-season (early September). Angled photos were taken manually several times during these missions and regularly throughout the field period with the aim of observing seasonal changes. A Mavic 2 Pro drone with Smart Controller was used (Figure 12). The automatic mapping mission programme DJI Pilot PE and manual flying was used to obtain vertical photos for 3D mapping in Agisoft Metashape Pro. The mapping was done in several sections to account for pilot proximity, drone safety, and battery time. Vertical photos at 70% overlap were taken at 80m elevation above the drone home point. Mapping of areas close to the Larsbreen glacier was done partly with manual flight at varying heights due to very uneven topography and further distance from pilot. The height had to be increased to 100m for some automatic flights due to topography. However, the height limitations and difficulty of manual flight missions for 3D model purposes resulted in some areas that did not meet the overlap requirements for modelling (Appendix B).

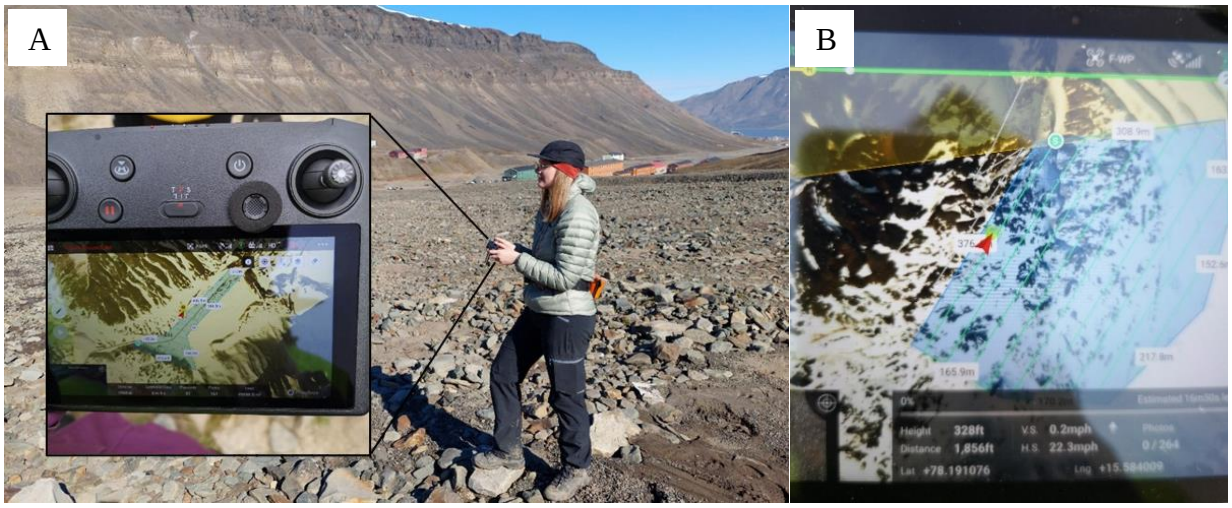

Figure 12 Drone flights using the DJI Pilot PE programme with the available basemap layer from winter. Yellow field marks flight warning zone. Blue field marks the mapping zone, and flight path as green lines. (A) Flying a small route towards Longyearbreen, (B) Planned route towards Larsbreen.

Challenges were encountered during drone photography fieldwork, including weather, wildlife, topography, flying height limitations, battery capacity, and automatic mapping limitations. All flights were authorised by the airport tower. For flights in the lower river and delta zone an online application had to be filled in each time to temporarily unlock the authorisation zone for the drone. The selection of a mission area was done on the single provided map layer which showed winter conditions, making selection inaccurate and prone to mistakes in higher elevation areas such as Larsbreen moraines (Figure 12B).

3.1.2 Constriction of orthophotos and elevation models from drone images

Orthophotos and Digital Elevation Models (DEMs) were produced of the study area for both missions. The mapping area was split into six sections for practicality of processing time. The Structure from Motion (SfM) method was used in Agisoft Metashape Professional. This method is based on resolving a 3D structure from a section of overlapping, offset images (Westoby et al., 2012). Figure 13 shows the workflow to achieve desired models. Photos were imported, aligned, and in some cases realigned. A dense cloud was built for each section, which was used to build an orthomosaic and DEM. High quality was chosen at all stages for all models. Files were exported as big TIF, as normal TIF was not large enough.

Some areas, particularly the edges of Larsbreen moraine, did not meet the conditions of 70% overlap for 3D mapping. This was due to large topography difference making the height above the ground too low when using a pre-programmed flight path. Realignment of photos in these areas were unsuccessfull and thus not included when building models (Appendix B).

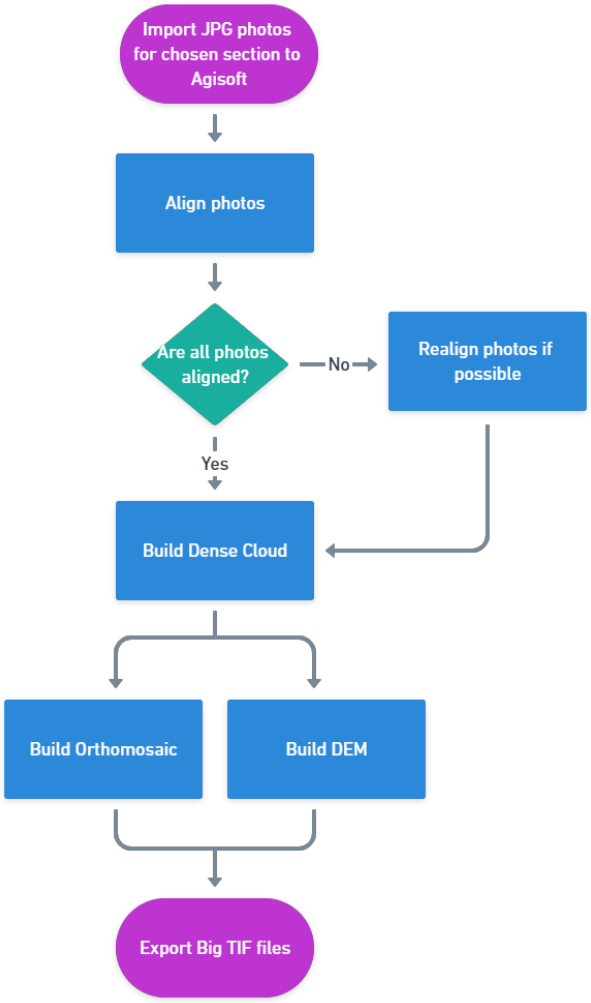

Figure 13 Workflow of Structure from Motion (SfM) modelling steps in Agisoft Metashape Pro from importing JPGs to exporting TIF files. Based on method from Westoby et al. (2012).

3.1.3 Field data collection in source areas

Field data was colleced in Longyeardalen to be used in combination with drone photography for quantification of sediment sources. The Larsbreen and Longyearbreen moraines were visited at least once during the mid-late summer season. The upper glaciofluvial system was visited at least five times from June to September to observe changes over the season. Observations of morphology, sediments, and roundness were noted. This was supplied by ground photography of backscarps, melting channels, and various source sediment deposits.

3.2 ArcGIS Mapping

Orthophotos were orthorectified using the georeference tool in ArcGIS Pro. The photos were first reprojected onto the ETRS 1989 UTM Zone 33N coordinate system to align with the NPI Toposvalbard WMTS Server with images from 2009 and 2011 (NPI, n.d.). Equivalent points were manually chosen on the 2021 and 2009/2011 photos, then aligned. Very distorted parts of the photos and noise outside the area of interest was removed at this stage. Some distorted parts were kept in the photos to avoid overly detailed and messy outlines.

This approach was repeated for an airplane photo from 2009 from NPI and a drone orthophoto from 2019 from Hanna (2019). These were used to map areas which were not covered with drone photography in 2021 and to map slumping in the moraines in earlier years. 1st order polynomial or spline georeferencing was applied, using 7-30 reference points for each orthophoto depending on size and necessity. The orthophoto of the Larsbreen moraine system from the mid-season was difficult to orthorectify due to a lack of high certainty points in both the 2009 basemap and the drone image. This image was therefore orthorectified onto the orthophoto from the late-season 2021. The increased uncertainty this causes, as well as the smaller area coverage, made the late-season images most suitable for making a map.

Mapping in ArcGIS Pro was done using NGU standards for ArcMap and adjusting were necessary (Norges Geologiske Undersøkelse, n.d.). Polylines and points were drawn onto the orthorectified photos in ArcGIS Pro. Polygons were created using the Feature to Polygon tool. Polygons, lines, and points were labelled and coloured appropriately using imported NGU symbology LYR-files. A scale of 1:7000 was chosen for the map, thereby making a digital drawing scale of 1:1750 suitable. Backscarps of slumps in the moraines were drawn in more detail to allow for area estimations and volume calculations.

3.2.1 Calculations of volumes displaced by thaw-slumps

The volume of slumped material in the Longyearbreen and Larsbreen moraine systems was calculated for 2009, 2019 and 2021. A mean vertical thickness was estimated as half of the maximum backscarp height for each moraine system; then multiplied by the horizontal surface area. This method is typically considered suitable for shallow landslides affecting soil over hard rock (Jaboyedoff et al., 2020). More detailed methods were not used in this case due to the lack of subsurface information. The complexity of ice-cored moraines makes it difficult to make more detailed assumptions with good certainty. As such, this approach was considered suitable for the study aim within the limitations.

Areas were estimated in ArcGIS Pro. Polygons were drawn over the 2021 late-season drone orthophotos of estimated initial areas of material that has slumped in the moraines. This was repeated over the 2019 drone orthophoto and 2009 NPI orthophoto. Volume was calculated by multiplying the areas with an estimated mean vertical thickness (Figure 14). One thickness was used for each moraine system consistently for all three years to avoid too many variables. This assumption is considered viable, but may give a slight overestimate of volume from earlier years if the active layer in the moraines has increased since 2009.

The maximum height of at least two backscarps in each moraine system was estimated using person-for-scale ground images. Exact in-field measurements were not done due to accessibility and safety. The average of backscarp heights was halved to give an estimated thickness of initial volume.

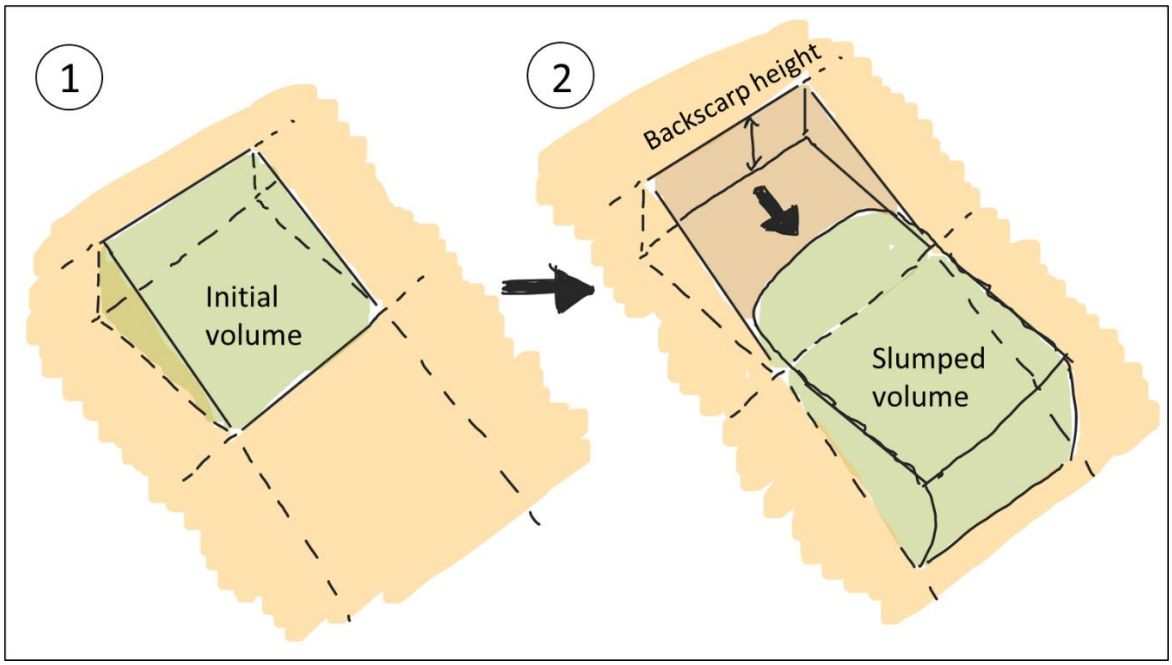

Figure 14 Simplified schematic figure of slumping volume on a slope. 1) Initial volume before slumping, as a simple triangular prism shape. 2) Volume after movement by slumping, with a visible sliding surface, backscarp, and flanks. Maximum backscarp height is labelled based on where the measurements were done from field photography. Half of the maximum backscarp height multiplied by area of initial material gives the initial volume.

3.3 Analysis of particle roundness

Roundness of rocks can indicate the length of transportation of a particle. Roundness analysis was performed in different parts of the active channels in Longyeardalen using two approaches. Rocks were observed to determine roundness on a scale of 1-6 from very angular (1) to well rounded (6) (Nichols, 2009). This was repeated for several sampling locations and profiles. Only sedimentary rocks were chosen for analysis as they are natural to the local geology (Chapter 1.3.1). Anthropogenically added rocks, such as flooding mitigation rocks, were not analysed.

3.3.1 Method 1 - Profiles

Six profiles were chosen across the river as shown in Figure 15. For each profile, at least 100 random rocks were analysed at regular intervals. Profile locations were chosen at different distances from the Longyearbreen and Larsbreen moraine systems to the delta. In total four profiles were chosen upstream of the river confluence, one along Longyearbyen, and one close to the delta. The aim of this method was to observe possible changes in roundness with distance from sources. One important factor for the lower profiles is possible anthropogenic reworking of sediment.

3.3.2 Method 2 - Squares

The second roundness method is based on a method used by Burki et al. (2010). Ten squares of about 1m^2 across a river profile close to Larsbreen moraine were defined (Figure 15). A group of five squares were selected on either side of the river deposit. The 20 largest rocks in each square were chosen for roundness analysis. The east group is below a rock glacier with a steep slope, and the west group is adjacent to inactive glaciofluvial deposits, solifluction material, and some mixed avalanche deposits. The aim of this method was to relate roundness to secondary sediment sources.

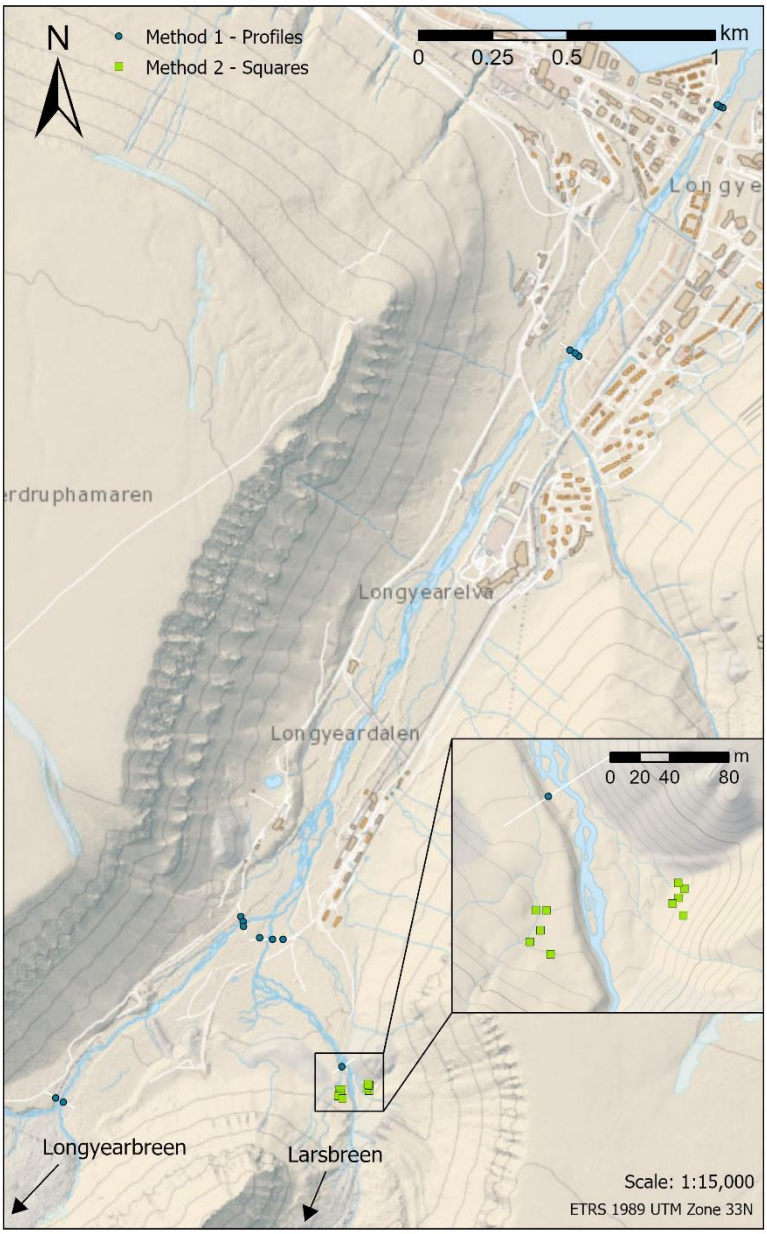

Figure 15 Map of Longyeardalen with locations of roundness analysis. Blue dots indicate profile locations for method 1. Green squares indicate locations of squares for method 2 downstream of the Larsbreen moraine system and rock glaciers. Scale 1:15000.

3.4 Hydrology and sediment transport

Hydrological monitoring in 2021 was carried out between 22/06 and 26/08. Additional photos were taken after the main monitoring period until 09/09. Most activities in this chapter were continued as part of the Longyearelva monitoring project initiated in 2018 (RiS ID 11641). Methods were adjusted based on recommendations from Løvaas (2021) and experience throughout the monitoring period in 2021, with the aim to improve the dataset. This applies to e.g. the suspended sediment sampling frequency, and choice of passive tracers.

The Longyearelva catchment was drawn in ArcGIS Pro in collaboration with Ottem (2022), twin study. This was produced based on NPI aerial photos and DEMs from 2009 and 2011 (NPI, n.d.).

3.4.1 Longyearelva river gauging station

A river gauging station was set up by Veg 600 from 22nd June to 25th August to measure pressure (to derive water level), electric conductivity (EC), and temperature, and to collect water sediment samples (Figure 16 & Figure 17). The sensors were connected to a station box from which data was transferred to a field PC at least every other week. The sensors were secured with straps, and a sign was put up to inform locals and visitors. Measurements of water level, EC, and temperature were recorded every 10 minutes and averaged every hour, resulting in an hourly data series with continual representation.

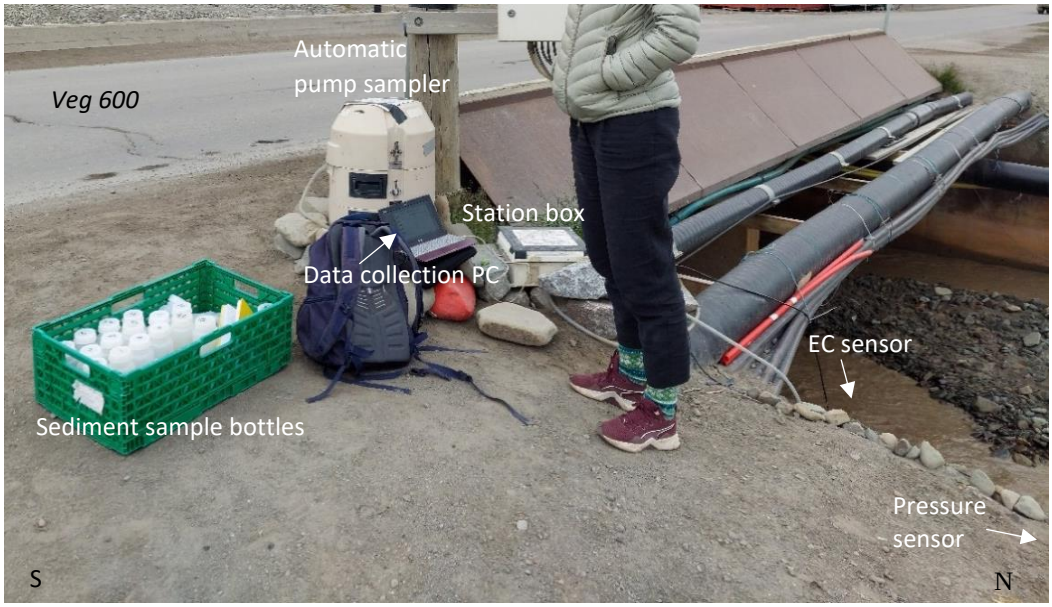

Figure 16 River gauging station by Veg 600 with an automatic pump sampler, sediment sample bottles in transport box, data collection PC connected to the station box, electric conductivity sensor, and pressure (water level) sensor location indicated.

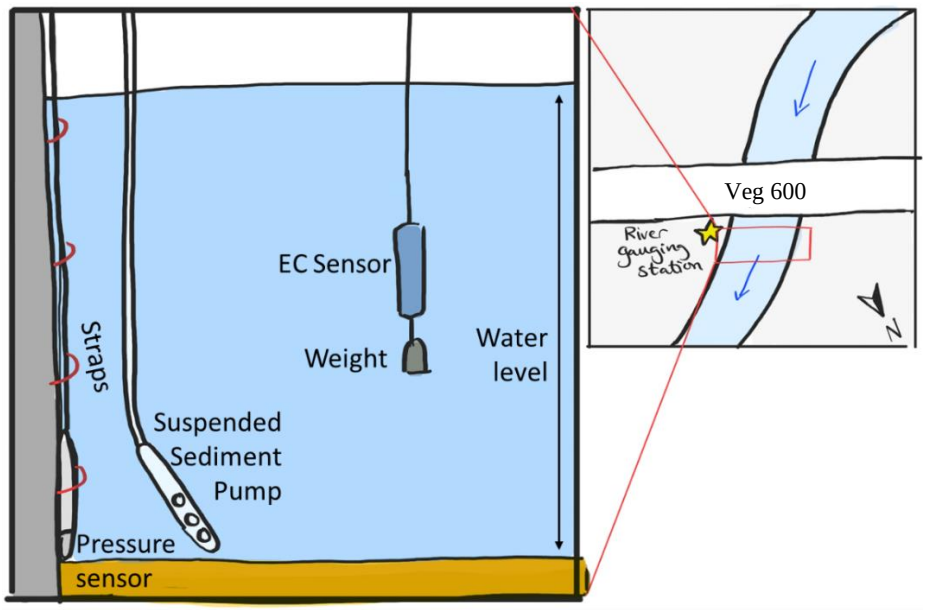

Figure 17 Cross river section of sensors at river gauging station by Veg 600. A pressure sensor was fastened to the side using straps to give consistent water level measurements. A suspended sediment pump end-piece and electrical conductivity (EC) sensor were submerged freely. A weight was used during high discharge periods to stop the EC sensor from floating.

3.4.2 Discharge measurements

Specific discharge measurements were made more than 10 times over the season using the salt dilution method with slug injection as described by Moore (2005). This method was chosen due to the turbulent, single channel stream, and a successful application of the method the previous monitoring year (Løvaas, 2021). The method uses diluted salt to measure how fast and by how much EC increases in a river. Discharge may be calculated based on this. The amount of salt injected must be high enough to produce a measurable peak in EC (Moore, 2005). Between 600g and 1500g of salt was used. The amount of salt was increased over the season as the natural ion concentration of the river water was expected to increase, requiring more salt for a low error margin (Moore, 2005).

The EC measurements were made using a handheld sensor downstream from injection at 5 second intervals during the tracer passage time. It is recommended to use a stretch of at least 25 times the length of the width of the stream (Radulovic et al., 2008). The measurement location was chosen in a single-stream part of Longyearelva, but in some cases the width was >2m. The measurement length was chosen as 60-70 m, starting with salt injection by Veg 600. Some incoherent observations in EC measurements resulted in a shift of location on July 20th upstream to a ~160m long stretch (starting at Polarriggen bridge) to promote more salt mixing. At the same time as location change, the handheld EC sensor stopped working and was therefore exchanged for a new, more reliable sensor.

Discharge Q (m^3/s) was calculated as:

$$Q = \frac{kM}{(T_2 - T_1) \times (EC_{mean} - EC_b)}$$

where k is calibration constant, M is mass of salt (g), T_2-T_1 is the duration of tracer passage (s), EC_{mean} is mean conductivity during tracer passage T_2-T_1 (µS/cm), and EC_b is stable base EC before salt injection (µS/cm). The calibration constant k was determined before each measurement by measuring the EC in five bottles of water with a known concentration of salt from 0-80 mg/L at river water temperature.

Hourly discharge was inferred based on the water level measurements and an exponential rating curve created from the specific discharge measurements. This is considered a reliable method as water level was recorded in a consistent single-channel flow (Killingtveit et al., 2003). A good fit of the rating curve was achieved with an R^2 value of >0.75.

3.4.3 Suspended Sediment Concentration

Water sediment samples to measure Suspended Sediment Concentration (SSC) were taken from 22nd June to 19th August. This was initially done manually, then after a few days an automatic pump sampler was installed by the river gauging station (Figure 18). A Sigma 900 MAX Portable sampler was used (Hach Company, 2003). Samples were taken four times daily at 02:00, 08:00, 14:00, and 20:00 until 19th August when NVE started flood mitigation work upstream in the active channel which would change the natural SSC. Manual samples were not taken at night.

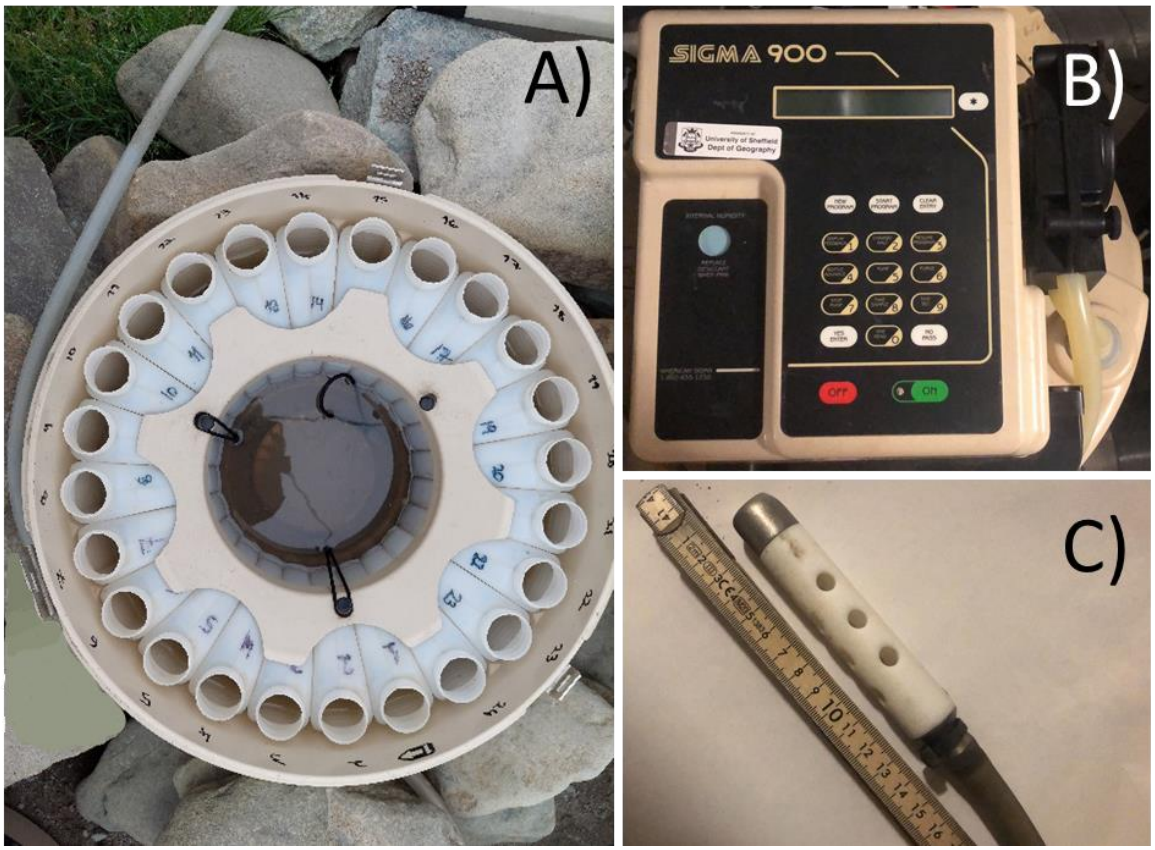

Figure 18 Sigma 900 MAX Portable sampler used for sampling water to determine Suspended Sediment Concentration (SSC). A) Inside the pump: 24 removable bottles that are filled with water samples in rotation. Water gathered in the middle from excess/spill while pumping. B) Programming setup keypad on top of the pump with options as described in the manual (Hach Company, 2003). C) End-piece of pump with 8mm in diameter holes to prevent most gravel from entering the pump.

The automatic pump sampler was programmed to take samples every six hours with a total of 24 containers with a 500mL capacity (Figure 18A). The station was visited every few days to once a week to check that the pump had taken samples as programmed. The pump battery level was checked weekly to biweekly to ensure level above 11.7mW. Once, the pump had stopped taking samples as it was automatically programmed to stop after bottle 24 despite bottle 1 being empty. This resulted in the loss of eight samples from 30/06 14:00 to 02/07 08:00. One sample was lost on 13/07 02:00 as the bottles were not emptied on time. Twelve samples on 3rd-6th July were taken at a ~1.5h delay due to a pump programming error.

At least three times (reoccurring problem), when emptying the samples, there was a lot of water in the middle (Figure 18A). This may have resulted from leaking or inaccurate filling of samples from the tube to the bottles. This resulted in smaller sample sizes in the bottles. This problem was not resolved. The pump end-piece had 8mm holes to prevent sampling of gravel (Figure 18C). However, some small gravel was sampled in the bottles.

Suspended Sediment Concentration (SSC) was found by filtering the water samples of a known volume using pre-weighed Whatman GF/F 47mm filters with a retention size of 0.7µm. An automatic pump was used with a plastic filtering bottle (Figure 19). Filtered samples were put in labelled aluminium foil packets and dried in an oven for 24h at 100°C. Filters were then weighed, subtracting the known filter paper weight for the net sediment weight (g). SSL in g/L was found by dividing this by known filtered water volume.

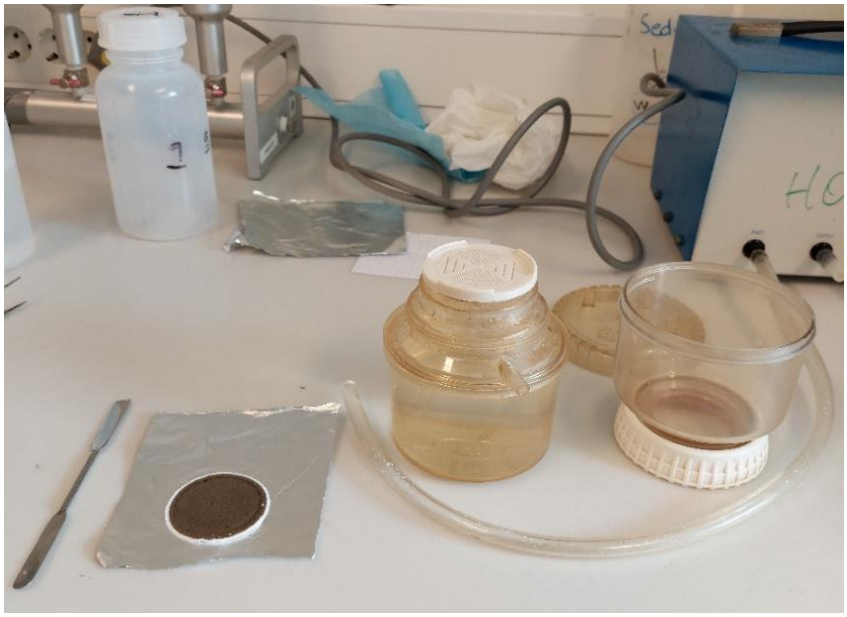

Figure 19 Equipment for filtering sediment water samples: A filtered sediment sample on aluminium foil, a filtering bottle in two parts, and a tube connected to the automatic pump in the back.

3.4.4 Bedload monitoring

Bedload monitoring was carried out using passive tracers to find river capacity. 138 rocks of known sizes were painted red and labelled with a unique number. The red rocks were placed in three different starting locations in the river, corresponding to locations used for the same method by Løvaas (2021). Rocks were placed in the river channel between 26th and 28th June. Two larger size classes were added as recommended by Løvaas based on observations from 2020, giving in total of 138 rocks of six size classes (Table 1). Ten rocks of classes 1-4 were placed across the river at each location, with the smallest size furthest downstream and 1-2 m

between each profile (Figure 20). Up to five rocks of classes 5-6 were placed across the river channel. The rocks were placed evenly across the river as bedload transport typically varies laterally, and channel flow may shift over one summer season (Ashmore et al., 2011).

Movement of the rocks was tracked over the summer by GPS and photography. Rocks that had not disappeared were removed from the river channel on 26th August and stored at UNIS for possible future use.

Table 1 Passive tracer classes 1-6, diameters in from 50mm to 400-450mm, and number of rocks placed at the three starting locations Pr-PT, Ha-PT, and Hu-PT.

		Number of rocks		
CLASS	**Diameter (mm)**	Polarriggen (Pr-PT)	Hallen (Ha-PT)	Huset (Hu-PT)
1	50	10	10	10
2	100	10	10	10
3	150	10	10	10
4	200-250	10	10	10
5	300-350	5	4	5
6	400-450	0	4	0

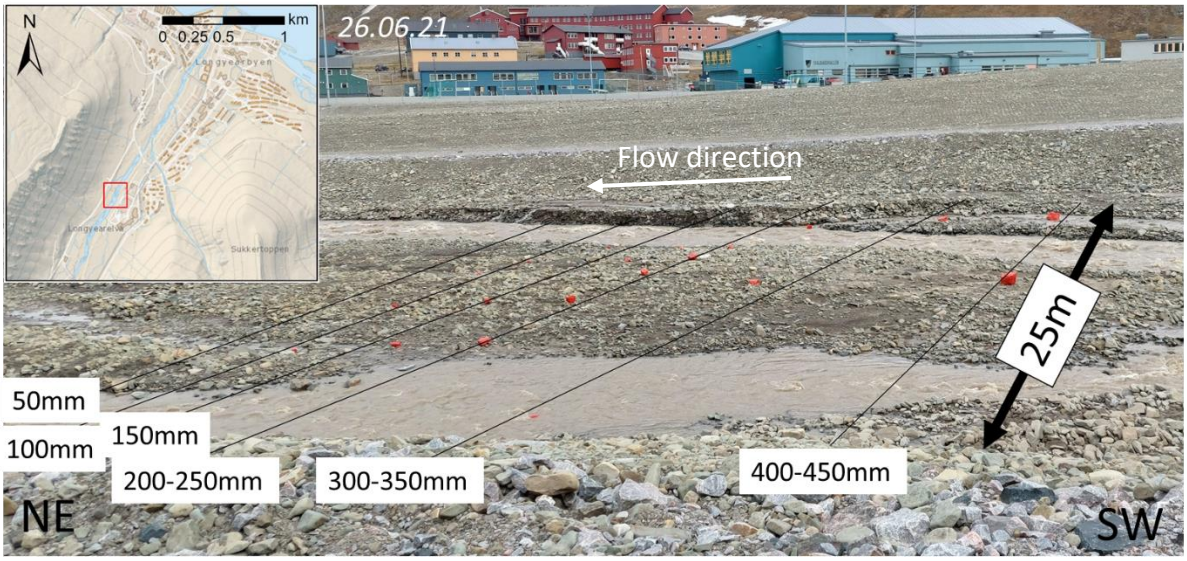

Figure 20 Passive tracers placed for bedload monitoring over a ~25m wide river stretch by Hallen (Ha-PT). Two main active channels are visible, flowing to the NE (arrow). A higher flow velocity is seen in the eastern channel (furthest from camera). Some rocks are submerged in the channels.

3.4.5 Climate data search

Temperature and precipitation data was obtained from the Norwegian Centre for Climate Services (Norwegian Meteorological Institute, n.d.). Data from the stations Svalbard Airport, Platåberget, and Adventdalen was used. Svalbard Airport has the oldest data series, providing seasonal temperature and precipitation from 1967-2021. This station was, however, missing precipitation measurements for significant periods of time over the summer 2021. This led to the usage of the Platåberget and Adventdalen stations. Measurements that were available from multiple stations at the same points in time were cross-checked to ensure that there was no systematic difference between the stations.

3.5 Monitoring of river management measures

The morphology of Longyearelva has been modified by anthropogenic construction of erosion banks and sills for safety and confinement. This has been done by the Norwegian Water and Energy Directorate (NVE) with Longyearbyen Lokalstyre (LL) (NVE, 2017). The morphology of sills and active channels was documented over the melting season. The 20 sills constructed by NVE were photographed five times over the summer from 29/06 to 27/08. This could be used along with drone mapping and compared to observations from 2020 (Løvaas, 2021). The potential subsidence of sills was investigated. The distance between sills and the gradient from the lowest point of each sill were measured using a Leica Rangemaster CRF 2800 laser.

Documentation of the river management measures is important for the long-term monitoring of Longyearelva. However, this is not a central part of the research questions for this thesis regarding source material and climate change influence. The results are therefore not presented in this thesis. The data may be of use to NVE for evaluation and planning of preventative and restricting measures in the river.

4 Results

Mapping and hydrological monitoring was done in Longyeardalen during the melting season in 2021. The study aims to improve knowledge of the primary and secondary sediment sources in the valley and the transportation of sediment. The components of sediment transportation from source to sink is shown in the flow chart and will be described in detail in this chapter (Figure 21). An overview of the distribution of sediment sources found in Upper Longyeardalen is shown in Figure 22; glacial, moraines, slumps in moraine systems, river erosion, slope processes, and anthropogenic input. Aeolian deposition (wind) is considered an external primary source of fine sediments. River erosion is a transportation source as it is enabled by the flow of water in channels and sediment transport. Observations regarding the sink (deposition and delta development) is presented in the twin study by Ottem (2022).

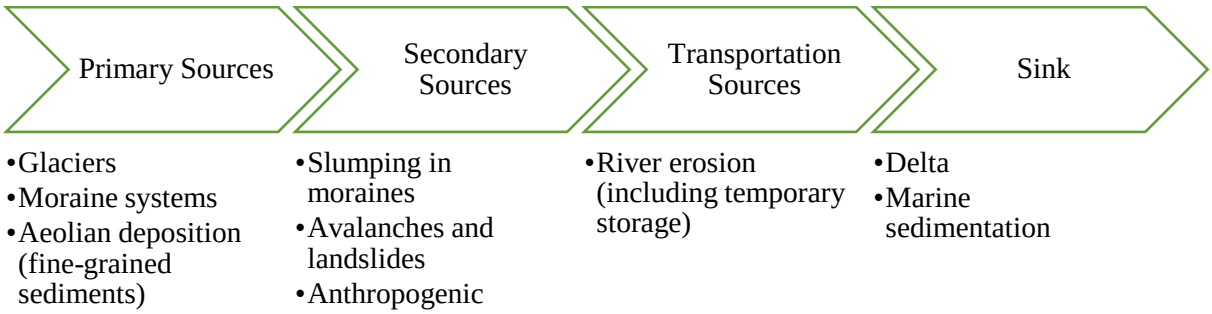

Figure 21 Flow chart of the components of the Longyeardalen source-to-sink system.

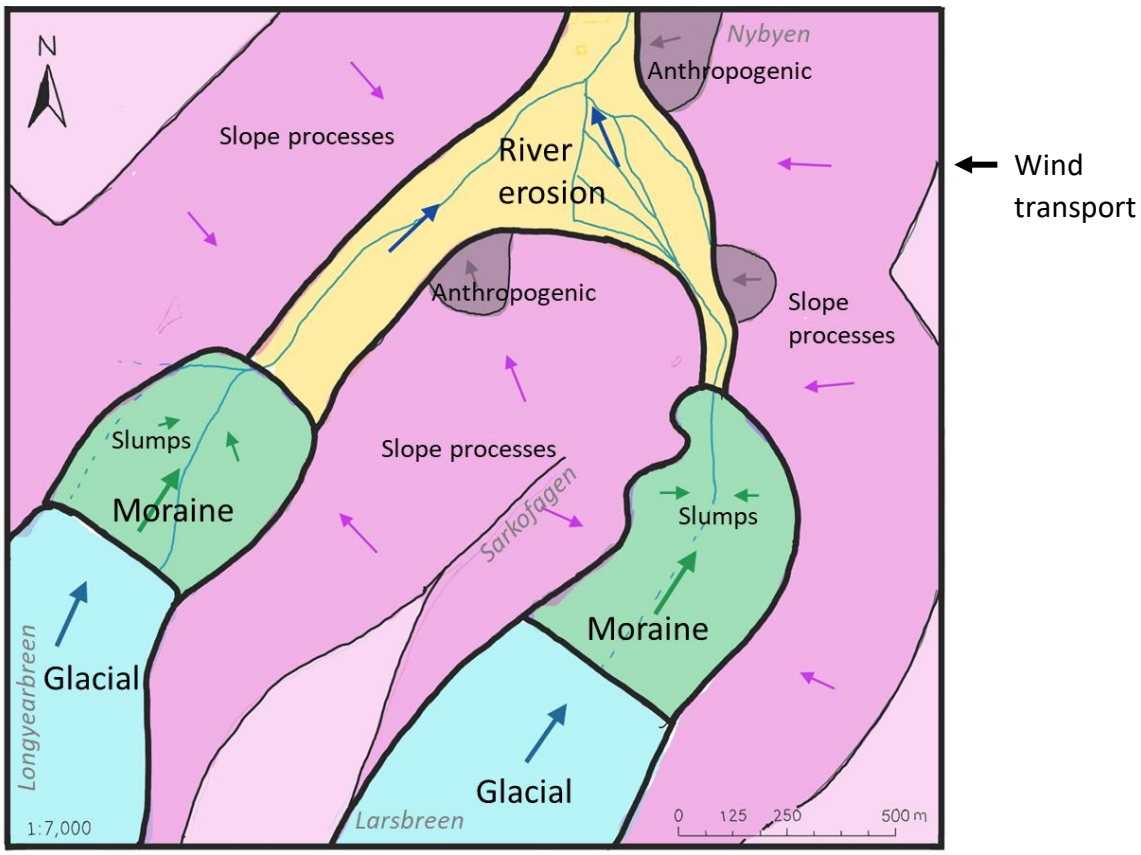

Figure 22 Map schematic illustation of the sediment sources in Longyeardalen. The primary sources are the Longyearbreen and Larsbreen glaciers and ice-cored moraines, and wind (external). Secondary sources are slumps in the moraines, avalanches, rock fall, debris flow and other slope processes, and anthropogenic material. River erosion occurs due to the transportation of sediment in the channels.

4.1 The Longyeardalen catchment

Sediment input and transport in Longyeardalen occurs within the partly glaciated catchment presented in Figure 23. The catchment was defined in collaboration with Ottem (2022), twin study, using a background map of aerial photos and DEMs combined from 2009 and 2011 (NPI, n.d.). The total area of Longyeardalen catchment was estimated to 22.9 km^2 (Figure 23). Larsbreen covers 2.7km^2, Longyearbreen covers 2.4km^2 (total glaciers 22%), and non-glacierized areas cover 17.8 km^2 (78%). Accuracy may be reduced due to the presence of photos from two years. The catchment is based mainly on the two glaciers Larsbreen and Longyearbreen. Platåbreen to the west may also add meltwater to the Longyeardalen catchment, but this is not its main drainage path.

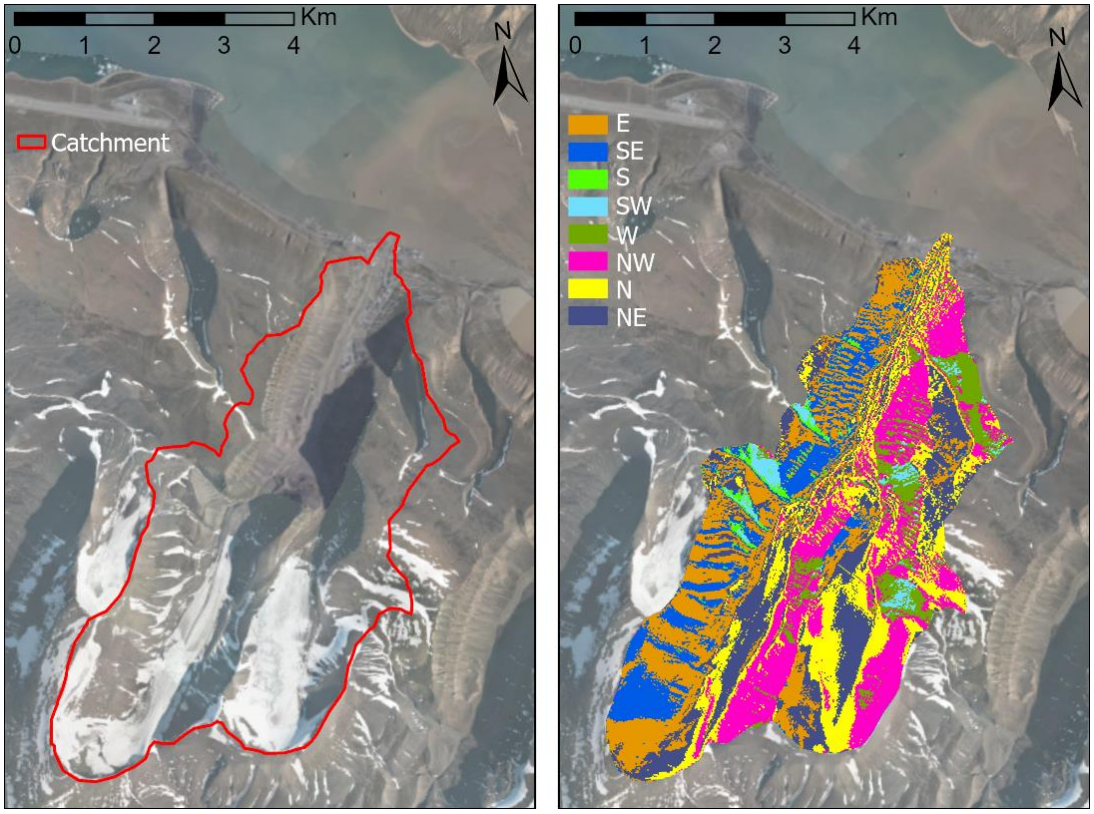

Figure 23 The Longyeardalen Catchment. A) Extent of the catchment, B) The cardinal direction of slopes within the catchment. In collaboration with Ottem (2022).

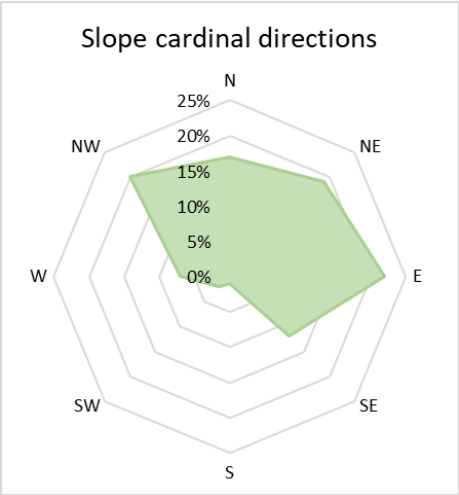

The distribution of slope cardinal directions within the catchment is shown in Figure 23B. The percentage of slopes facing each direction is detailed in Figure 24. The majority of slopes face NW-N-NE-E.

Figure 24 Percentage of slopes within Longyearelva Catchment facing each cardinal direction.

4.1.1 Temperature and precipitation

The climate in Longyeardalen is important for seasonal glacier melt, snowmelt, ground thaw. Temperature and precipitation over the past 30 summer seasons indicate how 2021 compares to past years. Summer seasonal average temperature and total precipitation in 2021, the last 5 years, and the last 30 years are presented in Table 2. The temperature during the summer season 2021 was relatively cold compared to recent years, with a 16% decrease in average temperature compared to the last 5 years, and similar to the last 30-year average. Precipitation in 2021 increased by 8% from the 5-year average, and by 15% from the 30-year average.

Table 2 Summer seasonal (June-August) average air temperature and precipitation in Longyearbyen (Svalbard Airport). Shows the 30-year seasonal average (1992-2021), the 5-year seasonal average (2017-2021), and the seasonal average in 2021. Data from The Norwegian Meteorological Institute (Norwegian Meteorological Institute, n.d.).

	Years Summer	**Temperature (°C)**	**Precipitation (mm)**
30 seasons	1992-2021	5.6	51.4
5 seasons	2017-2021	6.2	55.3
1 season	2021	5.2	60.4

The daily precipitation and air temperature in the study area in 2021 was monitored by Norwegian Meteorological Institute (n.d.) (Figure 25). Precipitation (Platåberget) occurred in repeated periods reaching a maximum daily total of 8.9mm on 18th July. Daily air temperature (Adventdalen) fluctuated within 3-10°C with a maximum of 9.8°C on 16th July.

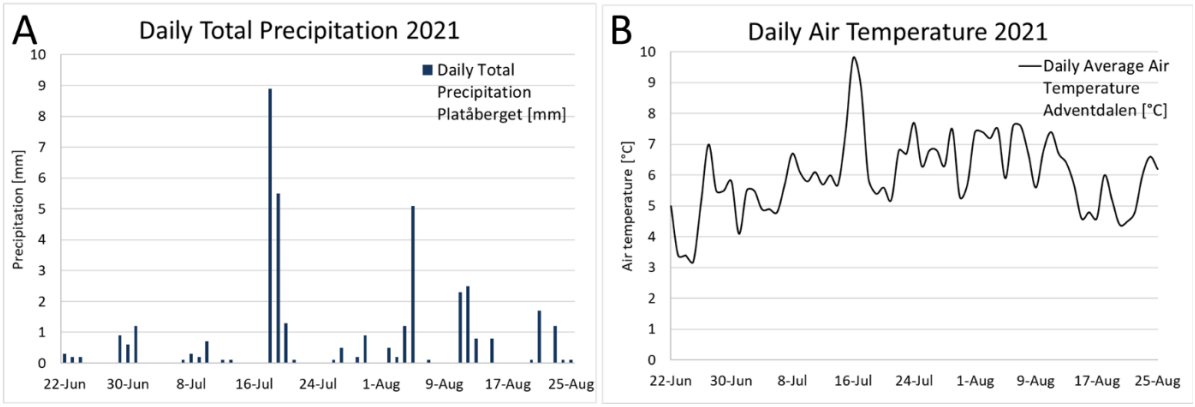

Figure 25 Weather data for the summer 2021 (Norwegian Meteorological Institute, n.d.). A) Daily total precipitation [mm] from Platåberget station. B) Daily air temperature [°C] from Adventdalen station.

4.2 The Upper System in Longyeardalen

Many sediment sources in Longyeardalen are found in the upper part of the valley. Upper Longyeardalen includes the Longyearbreen and Larsbreen glaciers, the marginal moraine systems, and the braided glaciofluvial rivers that confluence around Nybyen (Figure 26).

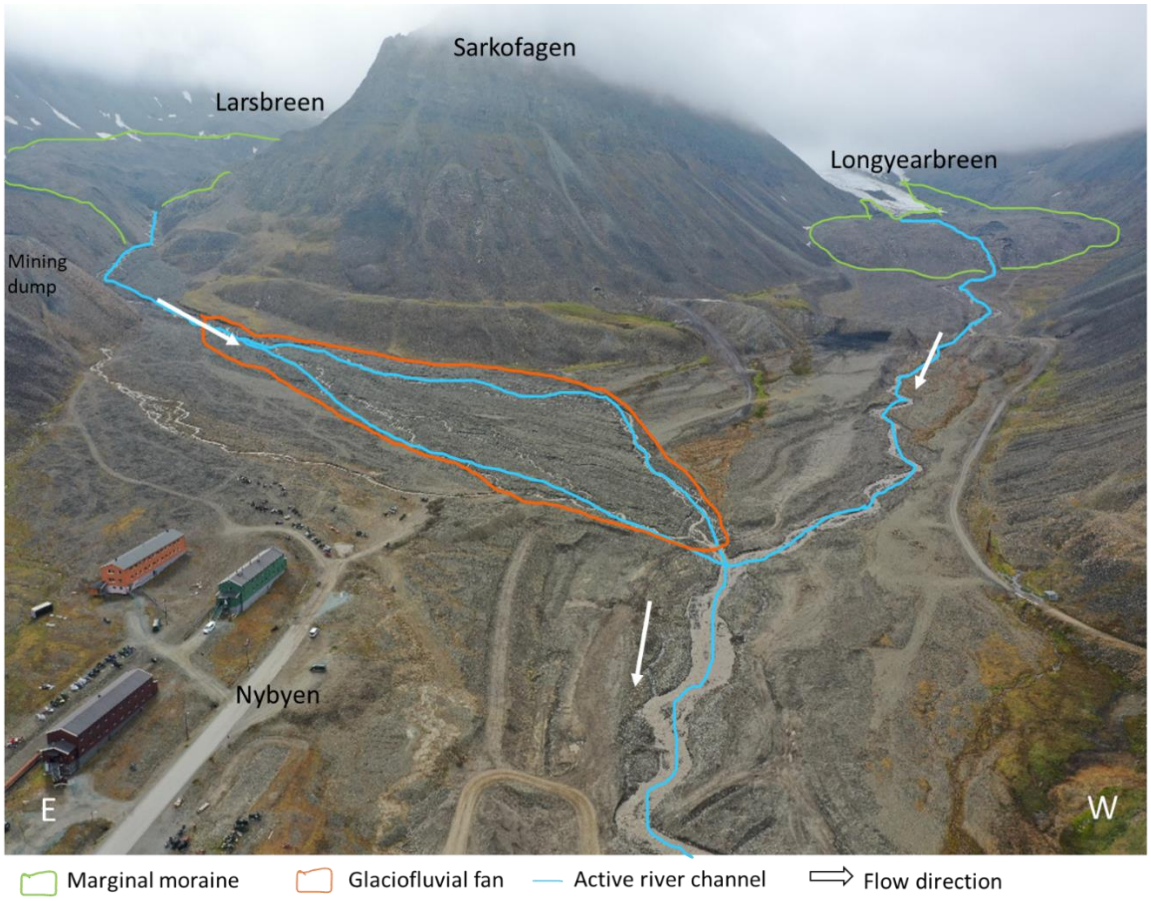

Figure 26 The Upper Longyeardalen area towards the south. Meltwater from Larsbreen and Longyearbreen glaciers pass through the moraine systems (green outline), and flows in braided river channels (blue), meeting by Nybyen. From Longyearbreen 1-2 channels are confined to an active path. From Larsbreen the meltwater channels are braided over an active glaciofluvial fan (orange).

The sources were quantified through mapping of a chosen extent covering the important sources in the upper valley (Figure 27). Quaternary deposits and geomorphological elements in Upper Longyeardalen were mapped (Figure 28) using available previous data orthophotos, field observations and photos, and a preliminary Longyeardalen Quaternary map (Rubensdotter, 2016). This was done following primarily the Norwegian SOSI standard for Quaternary geological maps. The map is underlain by a merged hillshade of 2021 Digital Elevation Models (DEMs) and a 2009 DEM (NPI, n.d.). The map shows the distribution of quaternary deposits and geomorphology in the upper valley. It defines which areas are affected by different processes, including glaciofluvial erosion and slope processes. The map covers a significant area of potential sediment sources in the Longyeardalen source-to-sink river system.

Figure 27 Longyeardalen topographical map with the defined extent of mapping in Upper Longyeardalen (Figure 28).

The Longyearbreen and Larsbreen glaciers were partially mapped in the uppermost part of the catchment (south) (Figure 28). Multiple supraglacial melting channels flow over the centre and along the sides of both glaciers. The glacier fronts and sides are partially overlain by supra-glacial till deposits, with one central deposit on Longyearbreen glacier. The two glaciers were only mapped partially since all sediment and meltwater passes through the front and the respective ice-cored moraine systems.

The ice-cored moraines are large features of old glacial ice covered with till. Longyearbreen marginal moraine stretches along the glacier down the valley to form a lobate front (Figure 28). The central part is overlain by glaciofluvial deposits with active channels. There are also active channels on the west side of the moraine. The channels flow partially below the surface of the moraine. An inactive channel is located along the eastern front and cuts into snow avalanche deposits. Some ridges run parallel to the glacier movement direction. Backscarps from slumping are located on the front part of Longyearbreen moraine. Most scarps lie adjacent or close to active channels. The active channels confluence directly in front of the moraine, forming sharp, few meters tall erosion banks. The active channels are confined to a 10-30 m wide path with 1-3 braided streams. A large part of the valley is covered by inactive channel deposits which lie slightly higher than the active channel.

Larsbreen marginal moraine is larger and lies at a higher altitude than Longyearbreen moraine. Active glaciofluvial channels flow through the central part of the moraine. Signs of degradation are prominent in the moraine, with limited original morphological structures such as ridges. This is most prominent in the lower half of the moraine, but some collapse has also occurred more proximal to the glacier. Backscarps from slumping are found along the glaciofluvially eroded river valley through the moraine. Water channels from melted ice flow from the slump scars into the active channel. Rock glaciers as three prominent, curved ridges are located along the front of the moraine between the slopes and active channel.

Large areas of active and inactive glaciofluvial deposits are located downstream of both moraines. Active channels from Larsbreen form a large glaciofluvial fan up to >250m wide at its widest with up to >10 braided active channels (Figure 26 & Figure 28). The channels in this area are a few cms up to around 3m wide at high discharge. Most channels in the glaciofluvial fan are shallow, up to a few 10s of cms. The channel paths changed frequently over the 2021 melting season within the fan. A prominent erosion scarp borders the active glaciofluvial fan and inactive glaciofluvial deposits from Longyearbreen. A secondary channel originates from the mining dump to the east, possibly from groundwater and/or meltwater from snowpacks. Some inactive channels have been anthropogenically disturbed.

Quaternary Map of Upper Longyeardalen

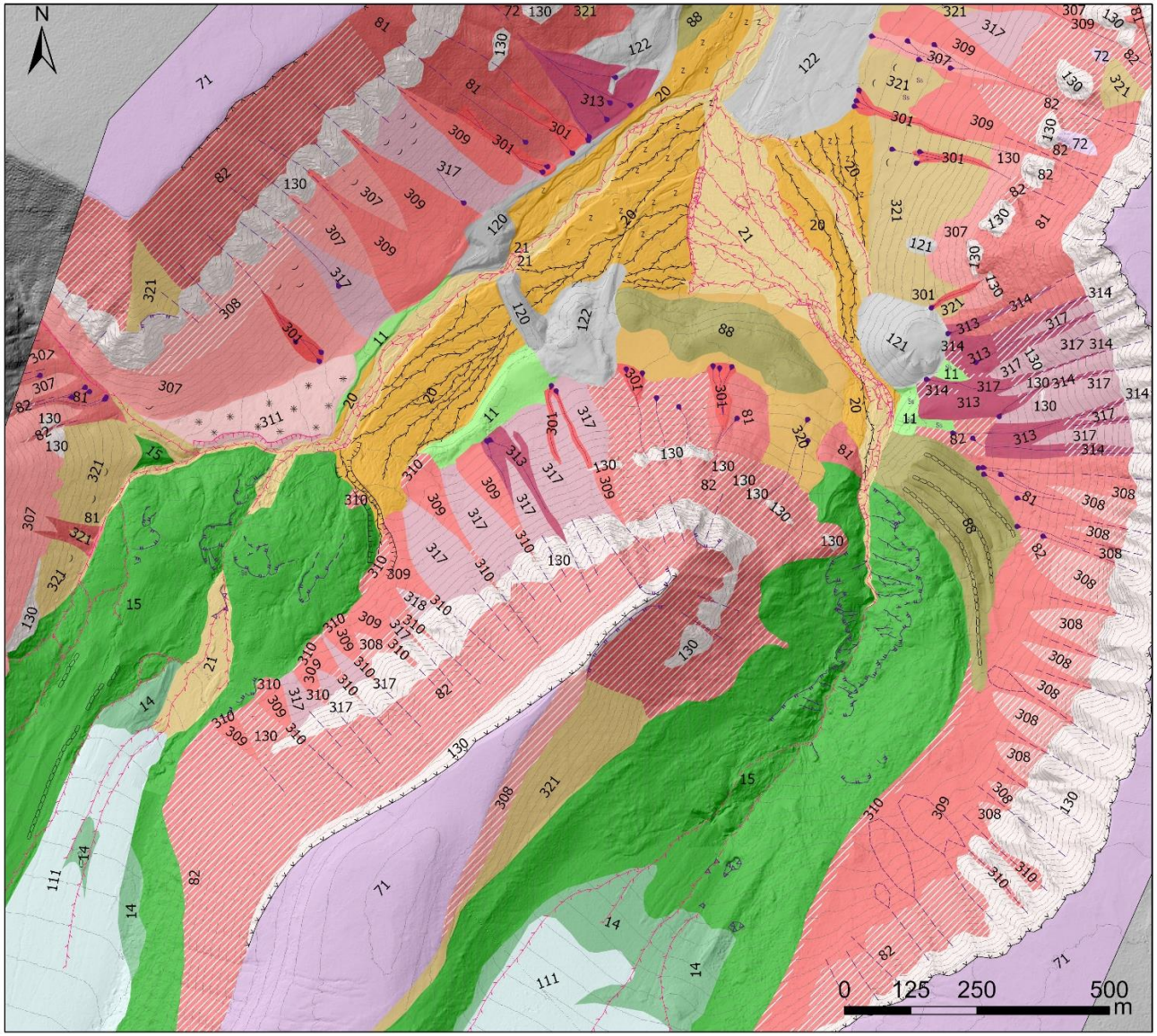

Legend

- 011-Till
- 015-Marginal moraine
- 014-Supra-glacial till
- 021-Glaciofluvial deposit, active channel
- 020-Glaciofluvial deposit, inactive channel
- 071-Weathering material
- 072-Weathering material, thin cover
- 088-Rock glacier
- 130-Bare bedrock
- 321-Stone-rich solifluction material
- 320-Solifluction material
- 120-Anthropogenic fill mass
- 121-Mining dump
- 122-Anthropogenically disturbed sediment
- 307-Rock fall deposit
- 308-Rock fall deposit, thin cover
- 309-Snow avalanche deposit
- 310-Snow avalanche deposit, thin cover
- 301-Debris flow deposit
- 311-Inactive slush avalanche/debris flood deposit
- 313-Snow avalanche and debris flow deposit
- 314-Snow avalanche and debris flow deposit, thin cover
- 317-Snow avalanche and rock fall deposit
- 318-Snow avalanche and rock fall deposit, thin cover
- 081-Mixed avalanche deposit
- 082-Mixed avalanche deposit, thin cover
- 111-Glacier
- Anthropogenically added sediment
- Solifluction lobe
- Patterned ground
- Small snow avalanche deposit
- Glaciofluvial erosion scarp
- Glaciofluvial channel
- Subsurface glaciofluvial channel
- Inactive glaciofluvial erosion scarp
- Inactive glaciofluvial channel
- Water channel from slump
- Back-scarp of slump/ slide
- Previous/stabilised backscarp
- Edge of slump scar
- Collapse edge
- Edge of avalanche fan
- General avalanche track
- Debris flow track
- Ridge
- Nivation scarp
- Contour, 10m

Hillshade generated from 2021 DEMs and NPI 2009 DEM (NW light source)

Scale 1:7,000

Figure 28 (Previous page) Quaternary map of Upper Longyeardalen with geomorphological elements. Follows primarily the Norwegian SOSI standard for Quaternary geological maps. Mapping based on field observation and photography from 2021, orthophotos from 2021[8], 2019[5], and 2009/2011[4] (Table 3), and a preliminary Quaternary map of Longyeardalen (Rubensdotter, 2016). Longyearbreen and Larsbreen glaciers are in the uppermost part of the valleys, with associated ice-cored moraines along and in front of the glaciers. Glaciofluvial deposits cover the valley bottom from the moraines downstream to the north past Nybyen. Sarkofagen mountain lies between the two glaciers and moraines. Landslide and avalanche deposits cover the valley slopes. The map is optimal in A3 format (Appendix A).

Anthropogenic sediment is mixed with much of the active and inactive glaciofluvial deposits in Longyeardalen (Figure 28). Large masses of anthropogenically disturbed sediment are located in the northern part of the map (Nybyen on the east and Sverdrupbyen on the west), and along the inactive glaciofluvial fan. A 10s of meters tall mining dump is located on the east side of the valley from Larsbreen. Some anthropogenic fill mass is found along the active channel from Longyearbreen.

Mixed and various avalanche and landslide deposits are mapped on all the slopes in Longyeardalen, with some debris flow and avalanche tracks identifiable (Chapter 2.5). Some slope material was also found on top of the moraines. Bare rock is exposed at the top or close to the top of the slopes, and weathering material covers the plateaus above. Debris flows are sometimes concentrated, e.g. north of the Larsbreen rock glaciers and northwest of the Longyearbreen anthropogenic fill masses. One slushflow deposit with a patterned, irregular ground surface is mapped northwest of Longyearbreen moraine. The transition from rockfall deposits to stone-rich solifluction material (e.g. east of Nybyen) is more gradual than it appears on the map.

The Quaternary map was created based on orthophotos created in this study and uncovered from previous studies. Orthophotos from 1936 from satellites, airplanes, and drones of were found through data search. An overview of the available data, relevant information, and source of data is shown in Table 3. Figure 29 presents the available data; A-F are previous works and G-H were produced for this study in collaboration with Ottem (2022), twin study. The photos overlay the TopoSvalbard topographical map (NPI, n.d.).

Table 3 Available orthophotos of Longyeardalen from 1936-2021 and data source.

	Time	*Info*	*Source*
1	1936	Black/white – S36	Norsk Polarinstitutt (NPI, n.d.)
2	1990	Infrared - S90 3682 (clip)	Norsk Polarinstitutt (NPI, n.d.)
3	2009	S2009 00105 (clip)	Norsk Polarinstitutt (NPI, n.d.)
4	2009/2011	WMTS 25833 – NE 2009 & SW 2011	Norsk Polarinstitutt (NPI, n.d.)
5	September 2019	From drone images	Hanna (2019)
6	June/July 2021	World imagery	Esri
7	July/August 2021	From drone images	Fieldwork (Appendix B)
8	September 2021	From drone images	Fieldwork (Appendix B)

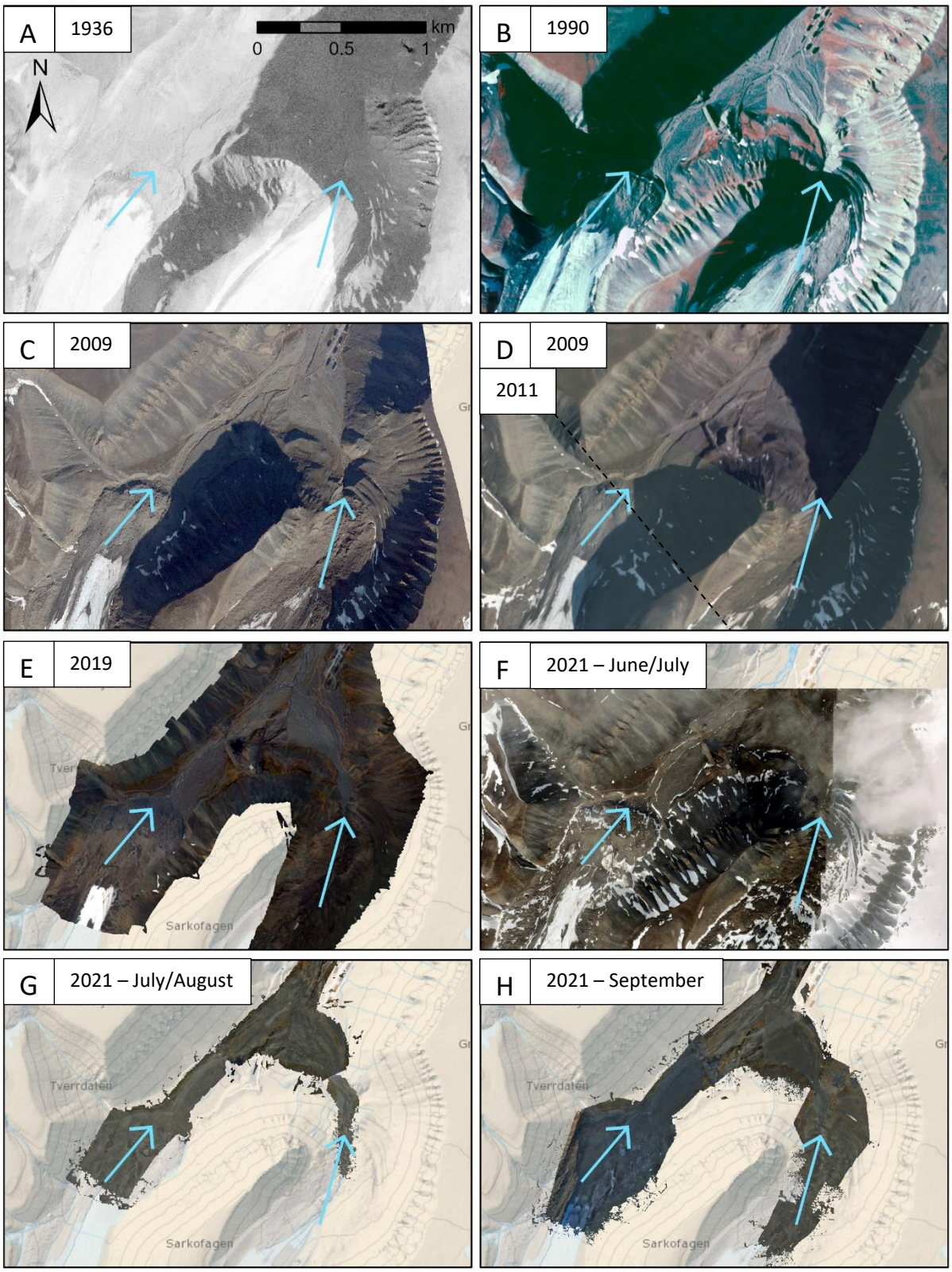

Figure 29 Overview of all raw available vertical photography data between 1936 and 2021 of Upper Longyeardalen. Blue arrows indicate glaciofluvial transport direction from the glaciers. Photos and maps have been found or produced from the years A) 1936[1], B) 1990[2], C) 2009[3], D) 2009 NE & 2011 SW[4], E) 2019[5], F) June/July 2021[6]. G) July/August 2021[7] H) 2021 September 2021[8]. Footnote citations refer to data sources in Table 3. Background map from NPI (NPI, n.d.).

4.2.1 The Longyearbreen moraine system

The Longyearbreen moraine system covers the valley north of Longyearbreen glacier (Figure 30). The ice-cored moraine has a clear lobate outer ridge and multiple wide, flat slump scars on the outer part. The forefield area shows signs of erosion, transport, and deposition of sediments, with both original morphology and signs of degradation present. Active melting channels flow over and partially below the central and west part of the moraine.

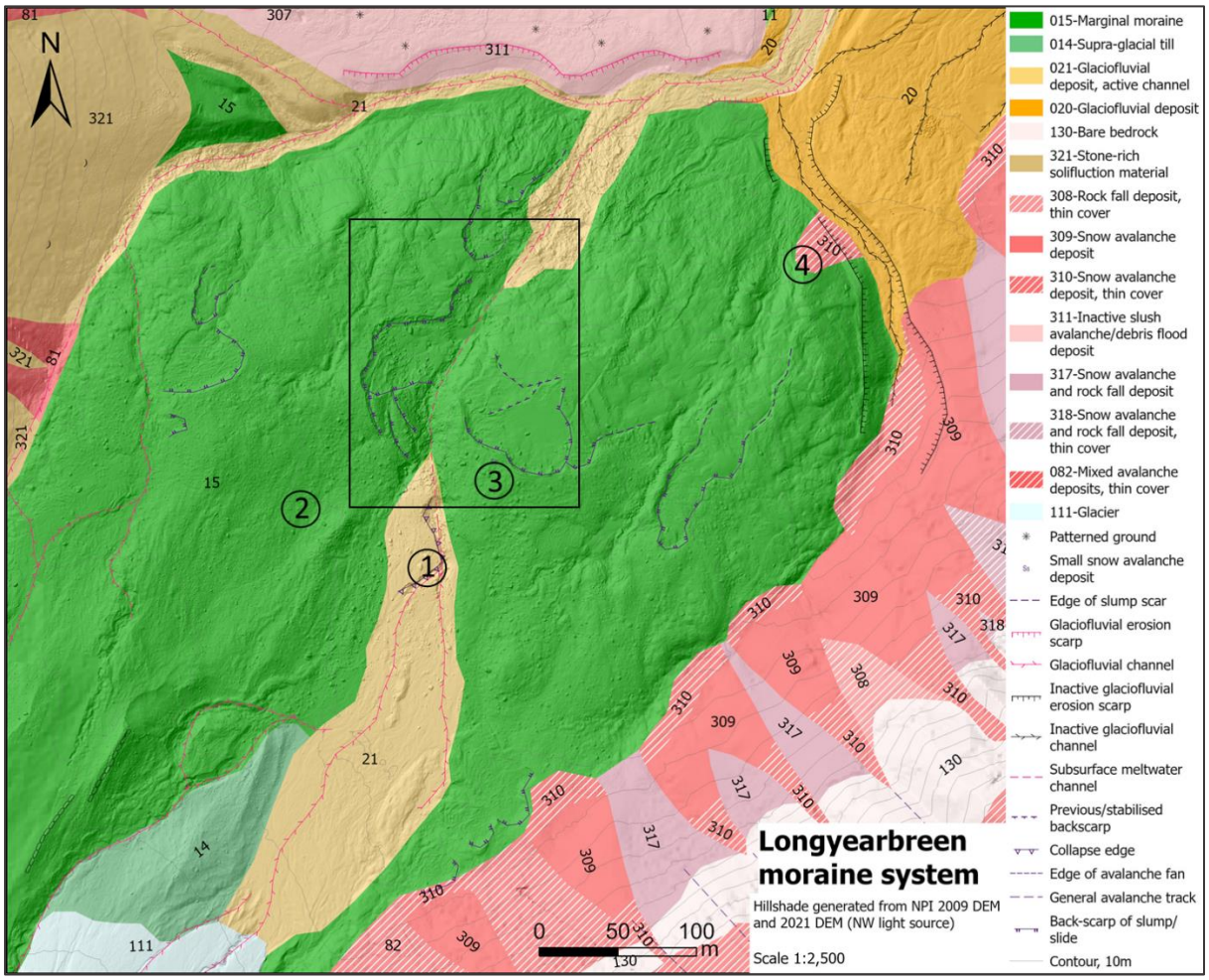

Figure 30 Quaternary and geomorphological map of Longyearbreen moraine system in scale 1:2500, a snippet of the Upper Longyeardalen map (Figure 28). Points of interest are described further in chapters 4.2.1 and 4.2.2. Black square indicates an area with multiple slumping scars by the main active glaciofluvial channel (Figure 32). 1) Collapse in glaciofluvial channel (Figure 33), 2) Location of a few well-rounded rocks (Figure 36), 3) High proportion of angular rocks (Figure 37), 4) Snow avalanche deposit (large concentration of angular rocks).

Glaciofluvial deposits are found along the central melting channels on the moraine surface. This consists of fine sediment up to large boulders and creates a flat part of the moraine, which has mostly uneven topography with ridges and some remnant meltwater channels. Figure 31 shows the glaciofluvial deposits in the foreground stretching south towards the glacier in the background, with till visible to the west. The flat, glaciofluvial deposit lies lower in the landscape than the surrounding till to the west due to glaciofluvial erosion. Supraglacial till has been deposited in the middle of the glacier, where two main supraglacial melting channels flow along the till. The supraglacial till sediments may be added to the melting channel and constitute part of the overall glacial sediment input to the system.

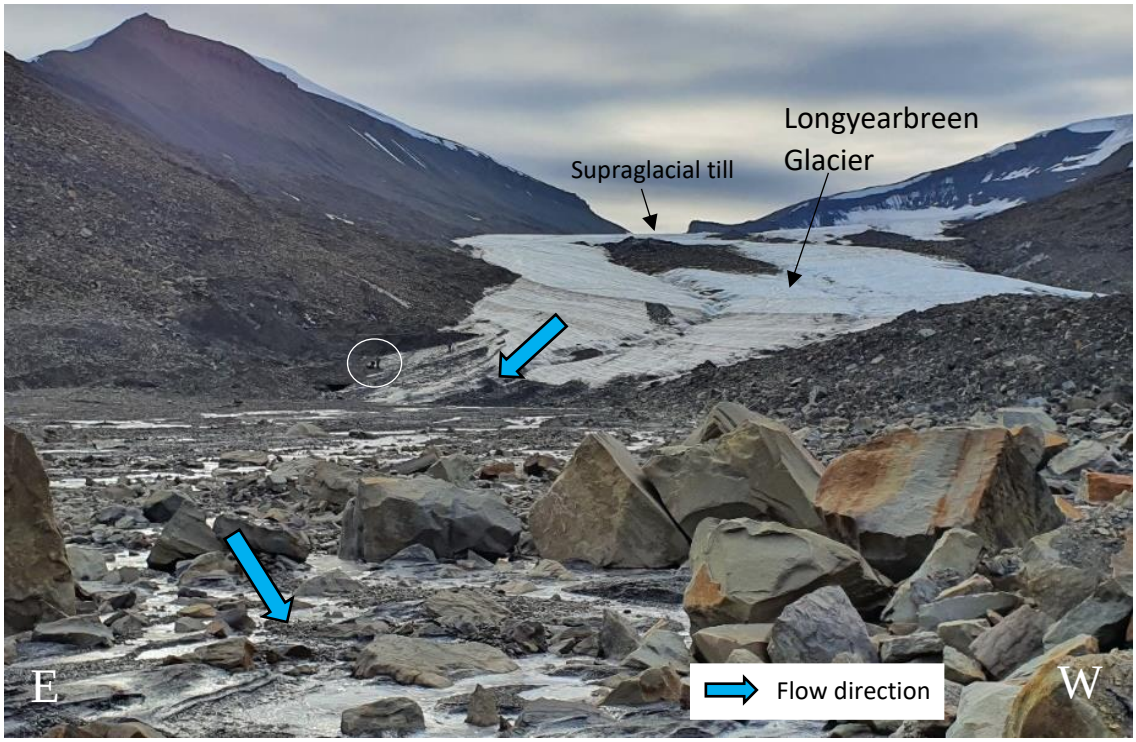

Figure 31 Longyearbreen glacier and moraine system. Glaciofluvial deposits and active channels with indicated flow direction. Till located to the west at higher topography than the glaciofluvial deposit on the east half. Large, angular to sub-angular boulders are visible. A deposit of supraglacial till on top of the middle part of the glacier, and two supraglacial melting channels visible on the glacier surface. Circle: persons for scale. (08/09/21).

Some active melting channels lie along the western edge of the moraine (Figure 30). These have mixed origin and may carry sediments from Platåbreen to the west. There was visibly lower discharge here over the summer 2021 than in the central melting channels.

Degradation in the moraine system occurs through slumping, glaciofluvial erosion, and other thaw processes. Signs of slumping were found on the outer part of the ice-cored moraine, adjacent to active and inactive melting channels. Backscarps and rupture surfaces with signs of retrogressive movement were observed. Slump scars have formed both in steep and shallow sloping parts of the moraine. Retrogressive slumping of previous scars and initial development of new slumping occurred in the mid-late melting season of 2021. The central outer part of the ice-cored moraine is pictured on four days between 05/07 and 10/09 in Figure 32A-D. Prominent slump scars are visible in the beginning of the season and fresh retrogressive scarps can be seen in the circled scars. Some new cracks have formed in August adjacent to previous scars.

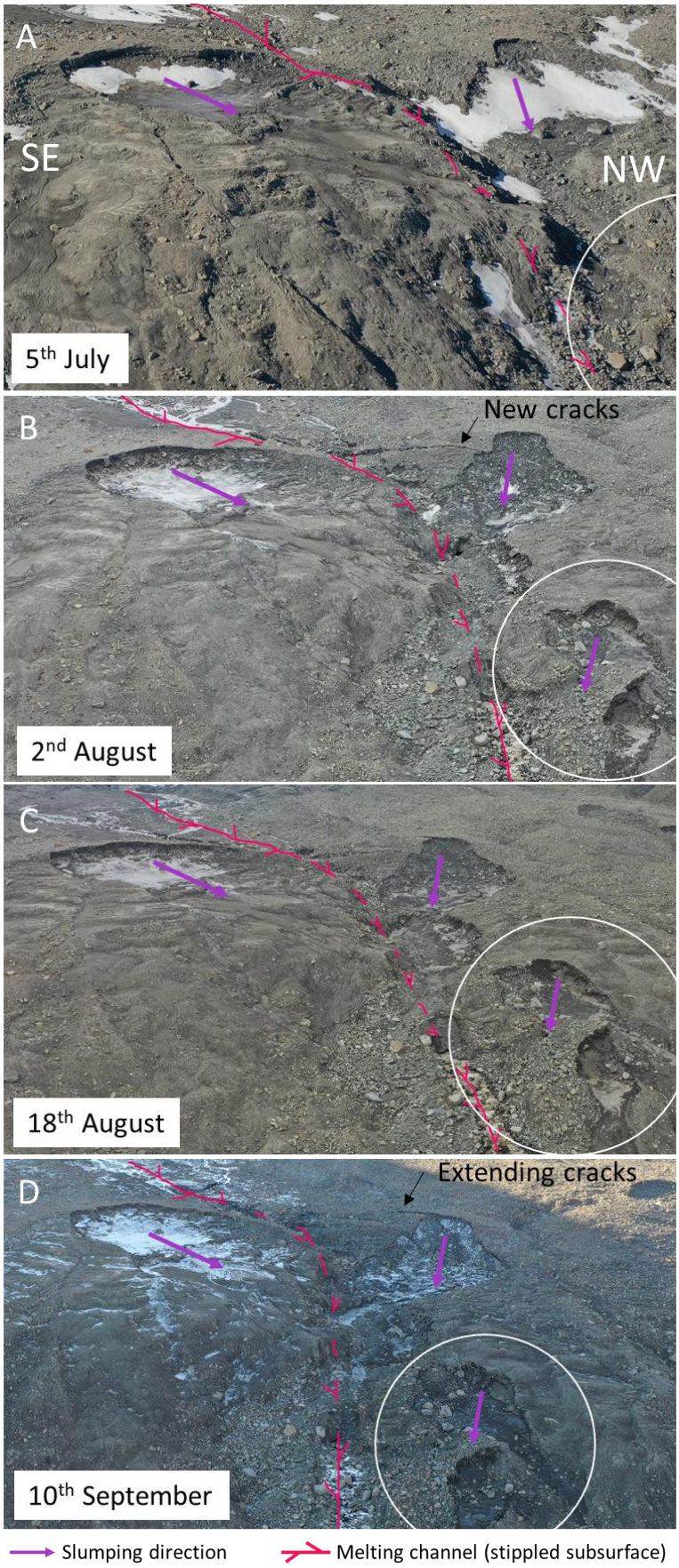

Figure 32 Backscarps from slump failure on the outer Longyearbreen moraine in 2021 (Location box in Figure 30). Active melting channel (pink) flows below the surface. This is adjacent to slumps with movement direction indicated with arrows (purple). The largest failure surface (SE) has visible ice throughout the summer. Slumping observed in circled area in the mid-late season. A darker colour indicates freshly exposed till. New cracks appeared and extended over the mid-late season. The angle of photos is slightly variable. Note variable light conditions.

A) 5th July: snow still visible in scarps formed from slumping in previous years

B) 2nd August: scarps in circled area, meltwater in active channel, new cracks start to form.

C) 18th August: retrogressive development of scarps in circled area, meltwater in active channel.

D) 10th September: ice on the surface as freeze-up starts, some retrogressive development since 18th August in circled area, cracks further extended by the top scarp.

Other degradation processes occur in the moraine system and glaciofluvial deposits, in addition to slumping. One example is shown in Figure 33, where a collapse occurred in the glaciofluvial channel at some point between 16th August and 8th September. The collapse location is shown in the white outlined area. Reference crosses indicate coinciding features on both days. Fine sediment up to large boulders were observed in the collapse area. The collapse exposed vertical sides of till/glaciofluvial deposits up to >90cm height (Figure 34).

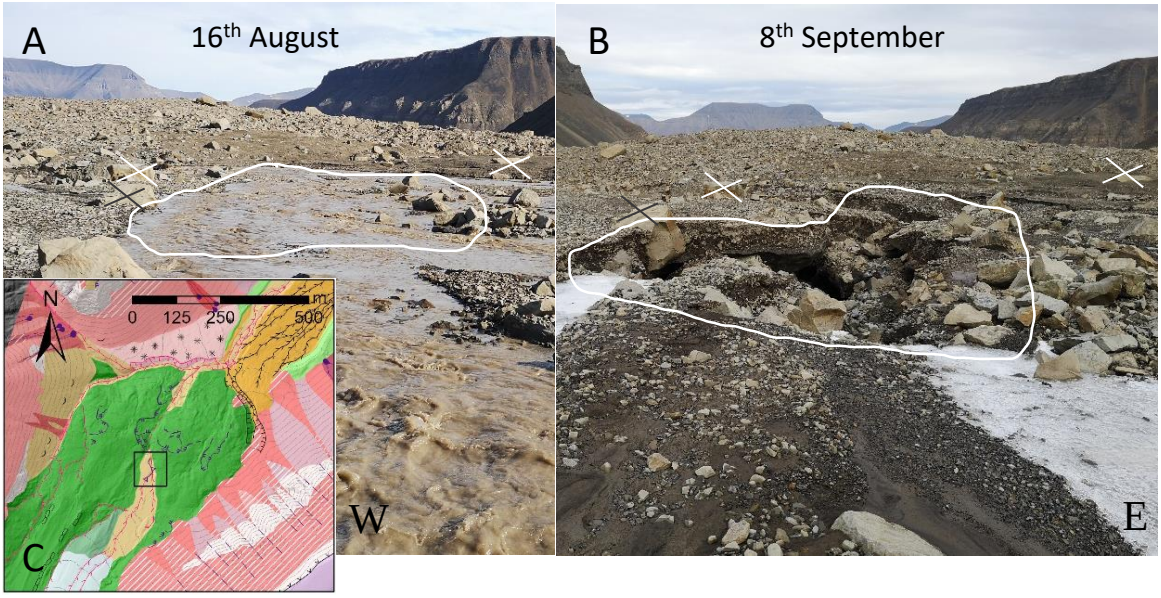

Figure 33 Collapse in glaciofluvial deposits on Longyearbreen moraine system in the late-season in 2021. The white outline indicates the same approximate area in both photos. Crosses mark coinciding points on the photos. A) 16th August: high discharge and sediment concentration, B) 8th September: no surface discharge in the main channel and a collapse hole has appeared in the channel. Slightly different camera positions were used for A and B. C) Location of collapse on Longyearbreen moraine (see point 1 in Figure 30).

Figure 34 Exposed vertical surfaces of till/glaciofluvial deposit in the collapse in Figure 33, in location 1 on the Longyearbreen moraine system map (Figure 30). A) ~50cm thick vertical surface with an open space underneath where meltwater can flow. Ice is seen below the exposed section. Loose, subangular to very angular boulders on the surface. B) ~90cm thick vertical surface. Some rounded to subrounded rocks.

4.2.2 Sediment sources and transport on Longyearbreen moraine

A key to understanding the sediment sources and transportation in the moraine systems is to observe roundness of rocks. Particles become gradually more rounded through transport (Chapter 2.2.3). There may be multiple degrees of roundness and multiple sources of the same degree of roundness present in the same general area. The origin of angular rocks on Longyearbreen moraine are till and slope processes, including avalanches and rock fall (Figure 35). Roundness may be increased through transportation or degradation through slumping. The roundness of rocks further downstream is presented in chapter 4.3.

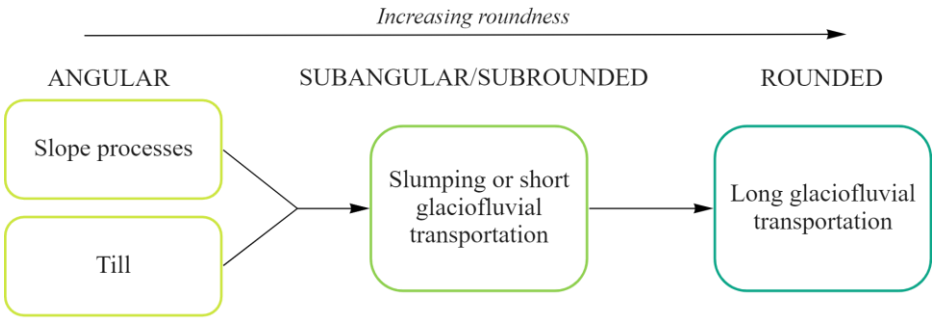

Figure 35 Flow chart of transportation processes and deposits increasing roundness of rocks in Longyeardalen from the Longyearbreen moraine system. Multiple processes may result in the same degree of roundness. Slope processes includes snow avalanches and rock fall. Angular rocks become more rounded with transportation distance. Slumping may partially round rocks.

Rocks from various sources with multiple degrees of roundness were found on the surface of the Longyearbreen moraine. Some rocks are transported through englacial channels to the moraine. Sediments are glaciofluvially eroded, transported, and deposited on the Longyearbreen forefield. The forefield is characterized by both original and degraded morphology, and hence primary and secondary erosion and transport of sediment. The sediment characteristics in this area are therefore important to consider as sources in the Longyeardalen catchment. Grainsize varies from mud to boulders, and roundness varies from well rounded to very angular. The large variability in sediment size and roundness is due to various sources and the complex glacial sediment transport system. Finer sediment is found prominently in small streams and glaciofluvial channels, as well as in till.

Rocks may become well rounded through transportation in meltwater channels supraglacially or englacially, i.e. on top of or inside of the glacier, and later become part of the moraine (Bennett & Glasser, 2011). Figure 36 shows a few well rounded rocks on the surface of Longyearbreen moraine.

Figure 36 Three well rounded rocks on the surface of the Longyearbreen moraine from glacial transport found at location 2 in Figure 30. Most of surrounding sediment is subrounded to angular loose till. (08/09/21)

Most surface material on the moraine system is till. This consists of unsorted rock with typically subangular to very angular grains (Figure 34). Some piles of rocks of homogeneous size and morphology are located on the moraine piles (Figure 37). Piles of angular to very angular rocks are likely deposited by snow avalanches onto the moraine. These are found on the eastern side of the moraine system (towards Sarkofagen). Snow avalanche deposits and some rock fall deposits are most common on the Sarkofagen slopes (Figure 30).

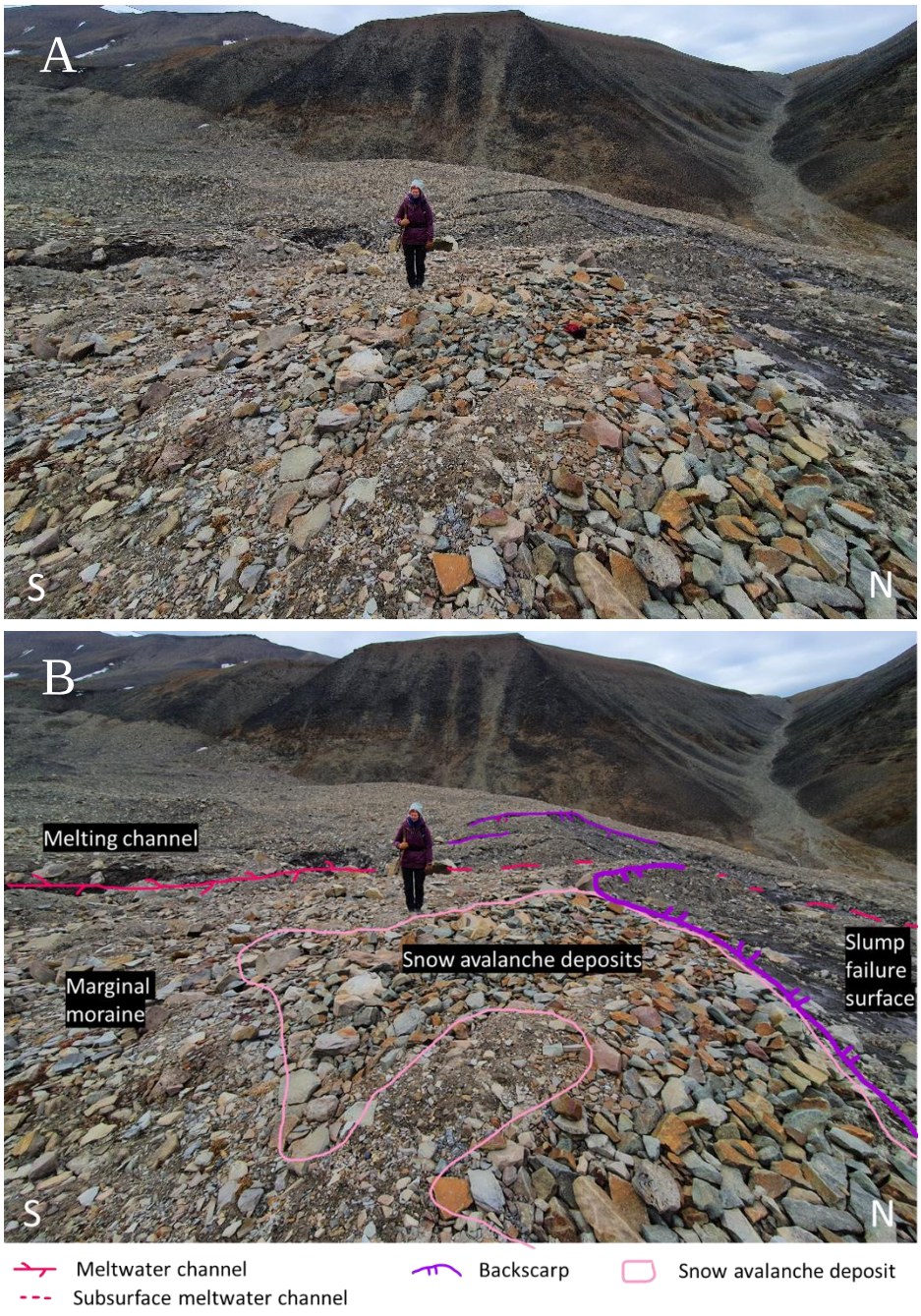

Figure 37 A small deposit of concentrated angular rocks at location (3) on the Longyearbreen Quaternary map (Figure 30). Mapped as snow avalanche material. The deposit is cut by the backscarp of a retrogressive slump. The active melting channel transports meltwater from Longyearbreen glacier northward, partly beneath the surface. The photo appears distorted at the front due to a photo effect. Person for scale ~180cm. A) Original photo, B) Annotated and sketched photo. (08/09/21).

A large deposit of homogeneous, angular rocks was observed on the edge of the moraine system, adjacent to an inactive meltwater channel (Point 4 in Figure 30). Multiple snow avalanche deposits lie on the other side of the inactive channel along the Sarkofagen slope. Inactive glaciofluvial erosion scarps cut through the deposits on both sides of the channel. The channel was active in 2019, and inactive in 2020 and 2021 (Hanna, 2019; Løvaas, 2021).

4.2.3 The Larsbreen moraine system

The Larsbreen moraine system is characterized by an ice-cored moraine covering the narrow valley north of Larsbreen glacier, cut by an active glaciofluvial channel (Figure 38). The active channel cuts through the centre of the moraine and has formed a narrow, steep river valley. The incised river valley slopes are heavily affected by slumps and other gravitational processes (Figure 38 & Figure 39). Scarps are found almost continuously along the slopes facing the channel on both sides. Sediment from slumps/slides in this area may be added directly to the active channel and transported downstream.

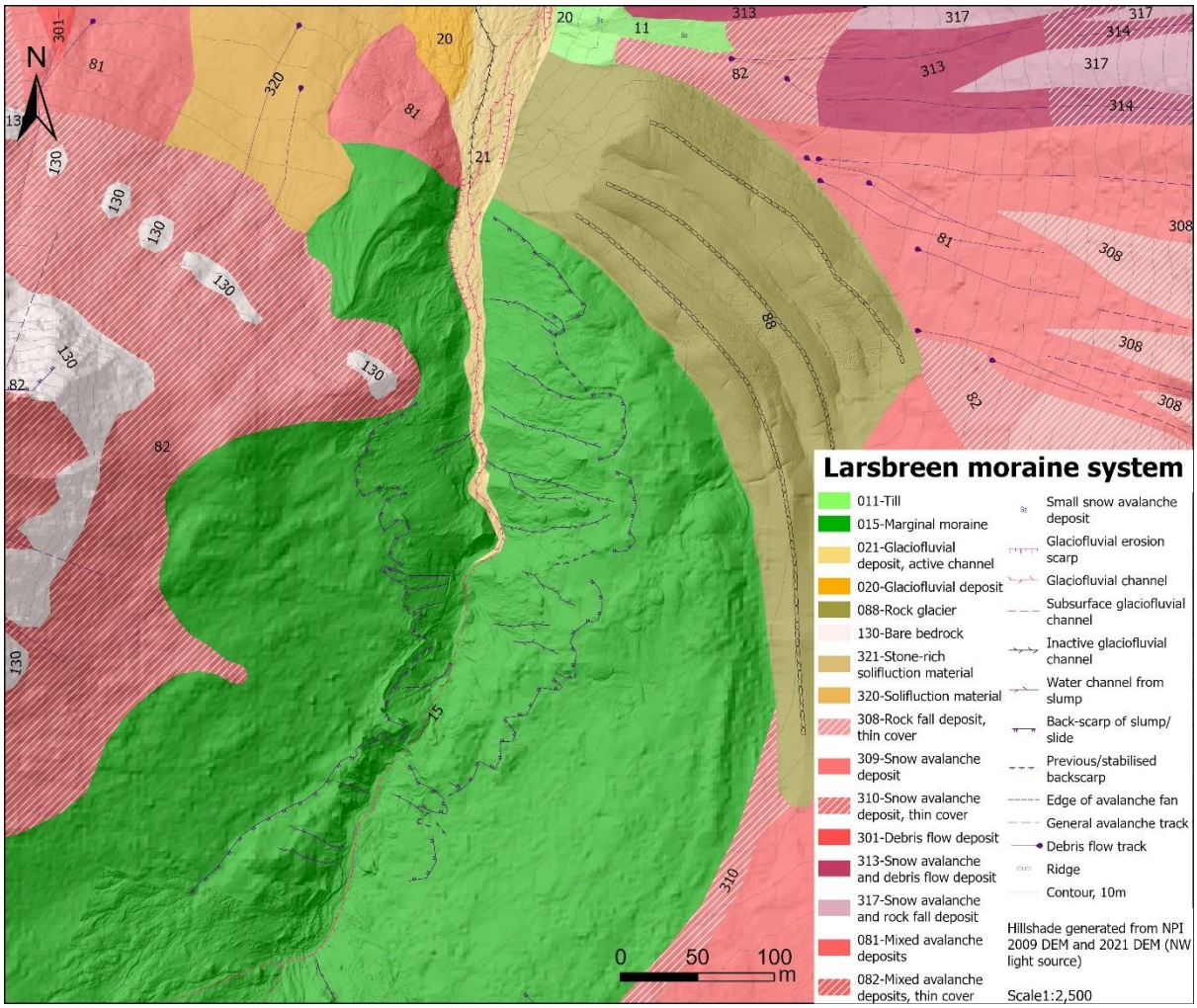

Figure 38 Quaternary and geomorphological map of the lower part of the Larsbreen moraine system in scale 1:2500, a snippet of the Upper Longyeardalen map (Figure 28). Backscarps of retrogressive slumps/slides are mapped on the ice-cored moraine along both sides of valley formed by the active glaciofluvial channel. Meltwater from slumps flow in small streams from the scars. Three parallel, curved ridges of rock glaciers lie in front of the moraine.

There is little original morphology (e.g. ridges) present in the Larsbreen moraine system. Rupture surfaces are exposed and cover most of the area down to the active channel. This results in a significantly large total area affected by slumps in the moraine (Chapter 4.2.4). Degradation in the form of slumping and other gravitational processes has occurred in the outer half of the moraine system. Backscarps in Larsbreen moraine are up to at least 165cm in height. In most cases backscarp height decreases gradually towards the edges of scarps.

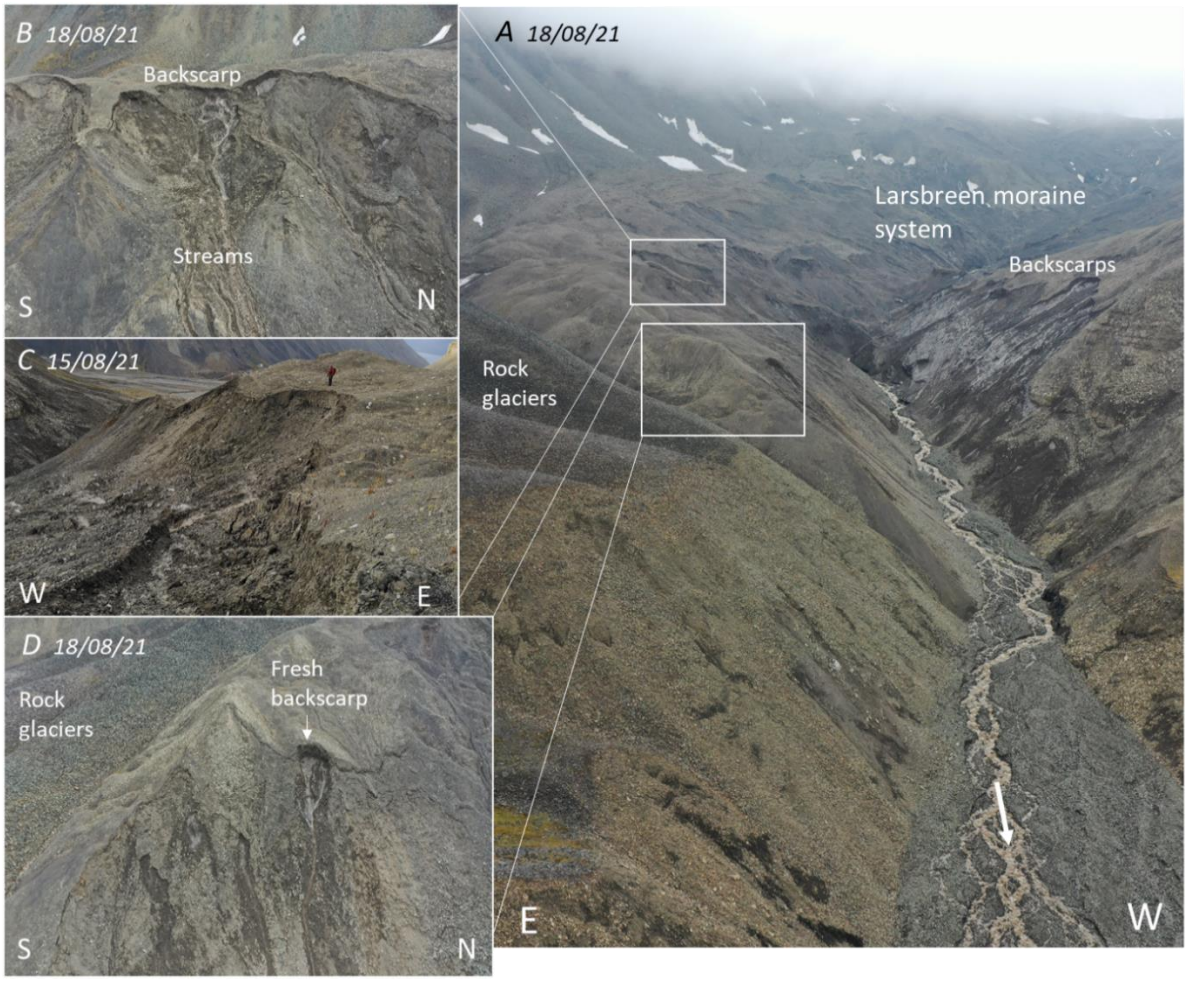

Figure 39 The Larsbreen moraine system and upper glaciofluvial channels with slump scars located along the slopes in the moraine, August 2021. A) Larsbreen moraine system with an active glaciofluvial channel cutting through with meltwater flowing downstream (flow direction indicated). Backscarps can be seen on both sides of the meltwater channel valley, where several failed surfaces have a dark colour with ice ice. Ridges of rock glaciers are on the east. B) A backscarp of several 10s of meters in width, with some ice melt streams downslope from the scar. C) Part of the backscarp in B with an uneven failure surface of slumped material, with person for scale (~160cm). D) A fresh, dark coloured backscarp with melted ice paths. Rock glaciers to the south are coarser on the surface.

Some features were identified in the slump scars in the Larsbreen moraine system. In many places, the movement of sediment has exposed a lot of ice at the surface, resulting in a smooth surface with some loose sediment on top. Some rupture surfaces have dried plants and signs of weathering, suggesting that these scarps are >1yr old. Some rupture surfaces are darker in colour, i.e. not weathered, and show no sign of plant growth. This suggests that these occurred earlier during the same year. The western side of the meltwater channel valley has mostly dark coloured failure surfaces, while the eastern side has more variability in rupture surface colour and characteristics.

The warmest mid-day temperatures and highest sun angle is from the north. The Sarkofagen slope down to Larsbreen moraine is slightly more shielded from the sun than the other side. However, both sides are exposed to a similar amount of sun and heat. The E side of the moraine has more visible >1yr slump scars, whilst the other side is steeper and mostly new scars are seen with a lot of exposed ice during the summer.

Some rupture surfaces have defined thin (a few 10s of cms) paths of meltwater from exposed moraine ice following slumping (Figure 39). Cracks parallel to backscarps are found on the crown along several backscarps, up to a few 10s of cms above the scarp, with openings up to a few cms (Figure 40). The ground above the scarps is uneven, with some undulations in the ground parallel to the backscarps suggesting slow movement or creep.

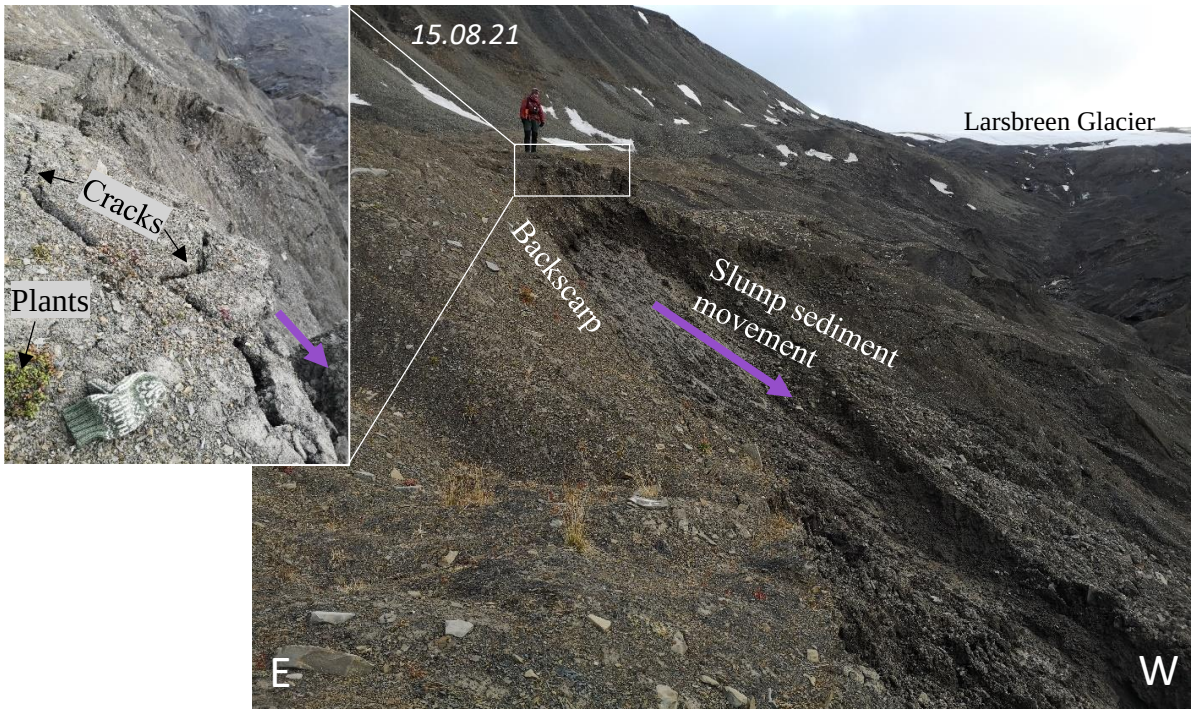

Figure 40 Top of a backscarp on the eastern side of the Larsbreen moraine system. Sediment has slumped down to the west towards the active channel through the moraine system. Purple arrows indicate slump sediment movement direction. The crown has plant growth and a light colour, with scarp-parallel cracks. The rupture surface has a darker colour with some slumped material still located in the lower part of the photo. Location: Figure 39B&C.

4.2.4 Volume of sediment from slumping in moraines

Quantification of sediment input from specific sediment sources over time can provide valuable information on changes in the source-to-sink system. Slumping was observed in the Upper Longyeardalen moraine systems in 2021. Volume calculations of slumping was done to quantify this secondary sediment source in the catchment. Calculations were done for 2009, 2019, and 2021. The three years of reference represent slumping of the ages:

- >10yr – 2009
- >2yr – 2019
- <2yr – 2021

The volumes that were calculated includes all slump activity from the years of reference as well as the previous years. This approach was taken within the limitations of discerning past activity from present observations. The calculations could then be compared to find slumping of the ages above.

Signs of slumping in the moraine systems were observed in the field and through past photography. In these calculations, "slumping" is used as a broader term to include slumping and other thaw failures, including thaw slides and detachment slides. Slump scars and backscarps cover a significant area in both moraine systems in Longyeardalen. This was not observed on orthophotos from 2009 and older. In 2009 <1% of the surface area in the Upper Longyeardalen marginal moraines had been moved from slumping/sliding. In 2021 this had increased to around 5% of the total area.

The total initial area affected by slumping was estimated based on orthophotos and DEMs from 2009, 2019 and 2021, and assisted by field observations (Table 4). The areas where most of the slumping occurred in the moraines are marked in Figure 41. Areas of slumped material in Longyearbreen moraine system was in the outer part of the ice-cored moraine (Figure 42). New slumps in 2021 have occurred adjacent to the main active melting channel in the central part of the moraine. Areas of slumped material in the Larsbreen moraine system was very limited in 2009, but found along the entire v-shaped valley in 2019 and 2021 (Figure 43). Table 5 shows estimated areas as seen in the figures, and calculated volumes.

Calculations of volume of slumped material were done using area estimations and backscarp measurements. All calculations are assumed a 20% uncertainty due to the estimation of past material, quality of available photos, and scarp height based on measurements from 2021. A different height of backscarps was found in Longyearbreen and Larsbreen moraine. The areas and volumes for 2021 are presented in Table 4. The ½ heights of backscarps were used as thickness of slumped volume as measured backscarps represent the maximum height of slump scars.

Table 4 Area and volume calculations of initial slump material in Longyearbreen moraine and Larsbreen moraine. Backscarp height as measured from scaled photos. ½ height from assumption for volume calculations (Chapter 3.2.1).

Location	**Backscarp height (cm)**	**½ height (cm)**	**Total area (m^2)**	**Volume (m^3)**
Longyearbreen moraine	170	85	$13 \pm 3 \times 10^3$	$1.1 \pm 0.2 \times 10^6$
Larsbreen moraine	158	79	$22 \pm 4 \times 10^3$	$1.7 \pm 0.3 \times 10^6$

The areas of initial material were estimated for both moraines from 2009, 2019, and 2021 (Table 5). Areas overlapping in multiple years are assumed to be from slumps occurring before the oldest photo they are visible on. The volume of slumped material was largest in Larsbreen with $1.7 \pm 0.3 \times 10^6$ m^3 in 2021. Slumping in Larsbreen moraine increased the most per year from 2009 to 2019. In Longyearbreen moraine slumping increased the most per year from 2019 to 2021. The total volume of slumped sediment in 2021 was $2.8 \pm 0.6 \times 10^6$ m^3.

Table 5 Area estimations and volume calculations using ½ backscarp height for 2009, 2019 and 2021 in Longyearbreen moraine, Larsbreen moraine, and both combined. The distributions of areas in the moraines are shown in (Figure 42 & Figure 43).

	Longyearbreen		**Larsbreen**		**Total**	
	Area (m^2)	Volume (m^3)	Area (m^2)	Volume (m^3)	Area (m^2)	Volume (m^3)
2009	$4 \pm 1 \times 10^3$	$0.3 \pm 0.06 \times 10^6$	$2 \pm 0.4 \times 10^3$	$0.2 \pm 0.03 \times 10^6$	$6 \pm 1 \times 10^3$	$0.5 \pm 0.1 \times 10^6$
2019	$8 \pm 2 \times 10^3$	$0.7 \pm 0.1 \times 10^6$	$16 \pm 3 \times 10^3$	$1.3 \pm 0.3 \times 10^6$	$24 \pm 5 \times 10^3$	$2.1 \pm 0.4 \times 10^6$
2021	$13 \pm 3 \times 10^3$	$1.1 \pm 0.2 \times 10^6$	$22 \pm 4 \times 10^3$	$1.7 \pm 0.3 \times 10^6$	$35 \pm 7 \times 10^3$	$2.8 \pm 0.6 \times 10^6$

The volume of material that has slumped in the moraine systems of the defined ages are shown in Table 6. Most of the slump activity is more than 2 years old. A total of $0.9 \pm 0.2 \times 10^6$ m^3 of material is <2yr old. This equates to almost 1/3 of the total slumped sediment in the moraines. The development over time was further assessed by calculating the average yearly volume of slumps from 2009-2019 and 2019-2021 (Table 7). The average volume of slumping per year has doubled from 2009 to the past two years.

Table 6 Volume of slumped material in the two moraine systems of the ages >10yr, >2yr, and <2yr.

	Volume of slumped material (m^3)		
Age	**Longyearbreen**	**Larsbreen**	**Total**
>10yr	$0.3 \pm 0.06 \times 10^6$	$0.2 \pm 0.03 \times 10^6$	$0.5 \pm 0.1 \times 10^6$
>2yr	$0.7 \pm 0.1 \times 10^6$	$1.3 \pm 0.3 \times 10^6$	$2.0 \pm 0.4 \times 10^6$
<2yr	$0.4 \pm 0.08 \times 10^6$	$0.5 \pm 0.1 \times 10^6$	$0.9 \pm 0.2 \times 10^6$

Table 7 Change in volume from 2009-2019 and 2019-2021, and average volume of slumped sediment in moraines per year in the two periods.

Year range	**Volume difference (m^3)**	**Average volume per year (m^3)**
2009-2019	$2.4 \pm 0.5 \times 10^6$	$0.2 \pm 0.1 \times 10^6$
2019-2021	$0.8 \pm 0.2 \times 10^6$	$0.4 \pm 0.1 \times 10^6$

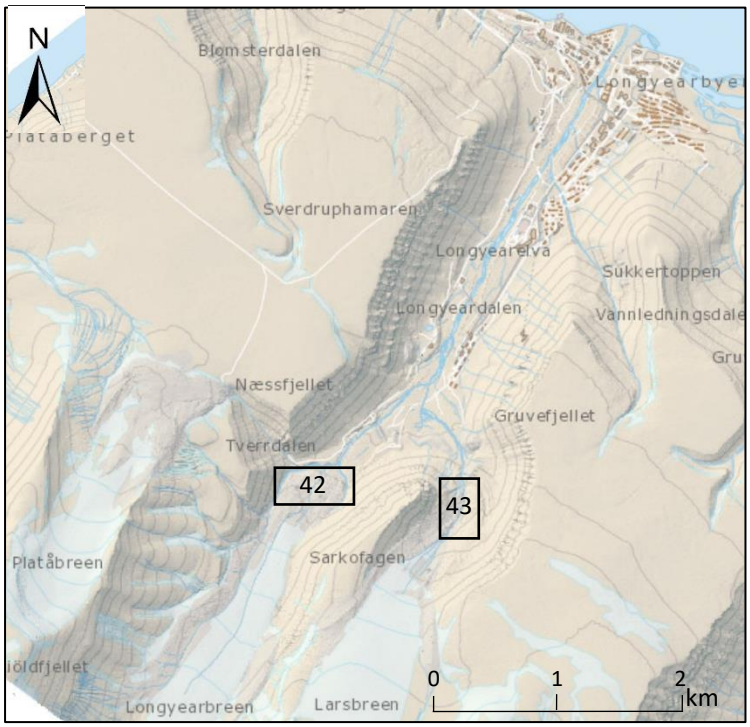

Figure 41 Overview map of Longyeardalen with locations of areas of slumped material in Longyearbreen and Larsbreen moraine systems. The estimated areas within each moraine system are shown in Figure 42 & Figure 43.

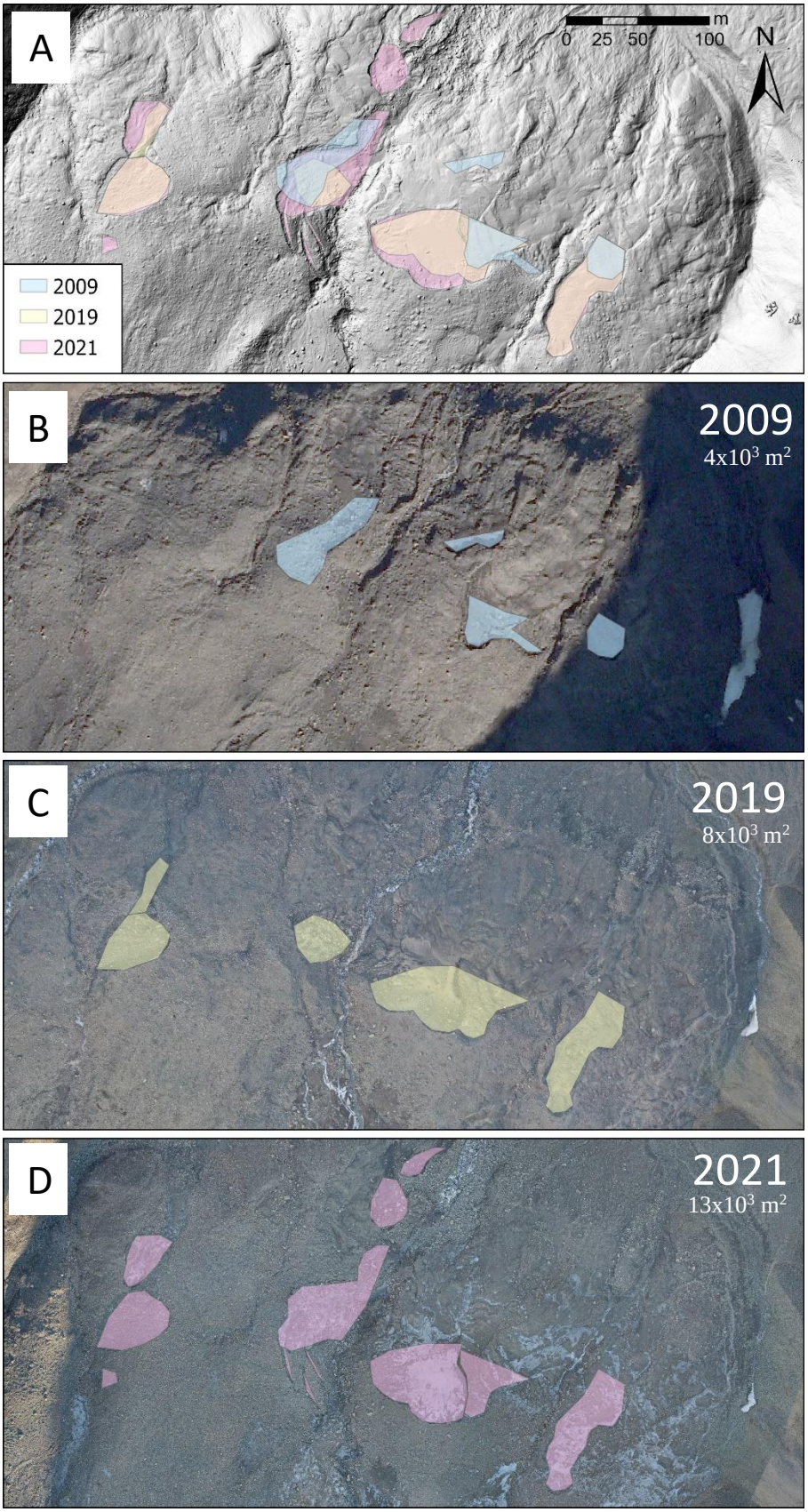

Figure 42 Area of slumped material in the Longyearbreen moraine system in 2009, 2019 and 2021. Location marked on Figure 41. A) All areas on 2021 hillshade, B) Total area of $4x10^3$ m^2 on 2009 orthophoto (NPI, n.d.), B) Total area of $8x10^3$ m^2 on 2019 orthophoto (Hanna, 2019), D) Total area of $13x10^3$ m^2 on 2021 orthophoto (Appendix B).

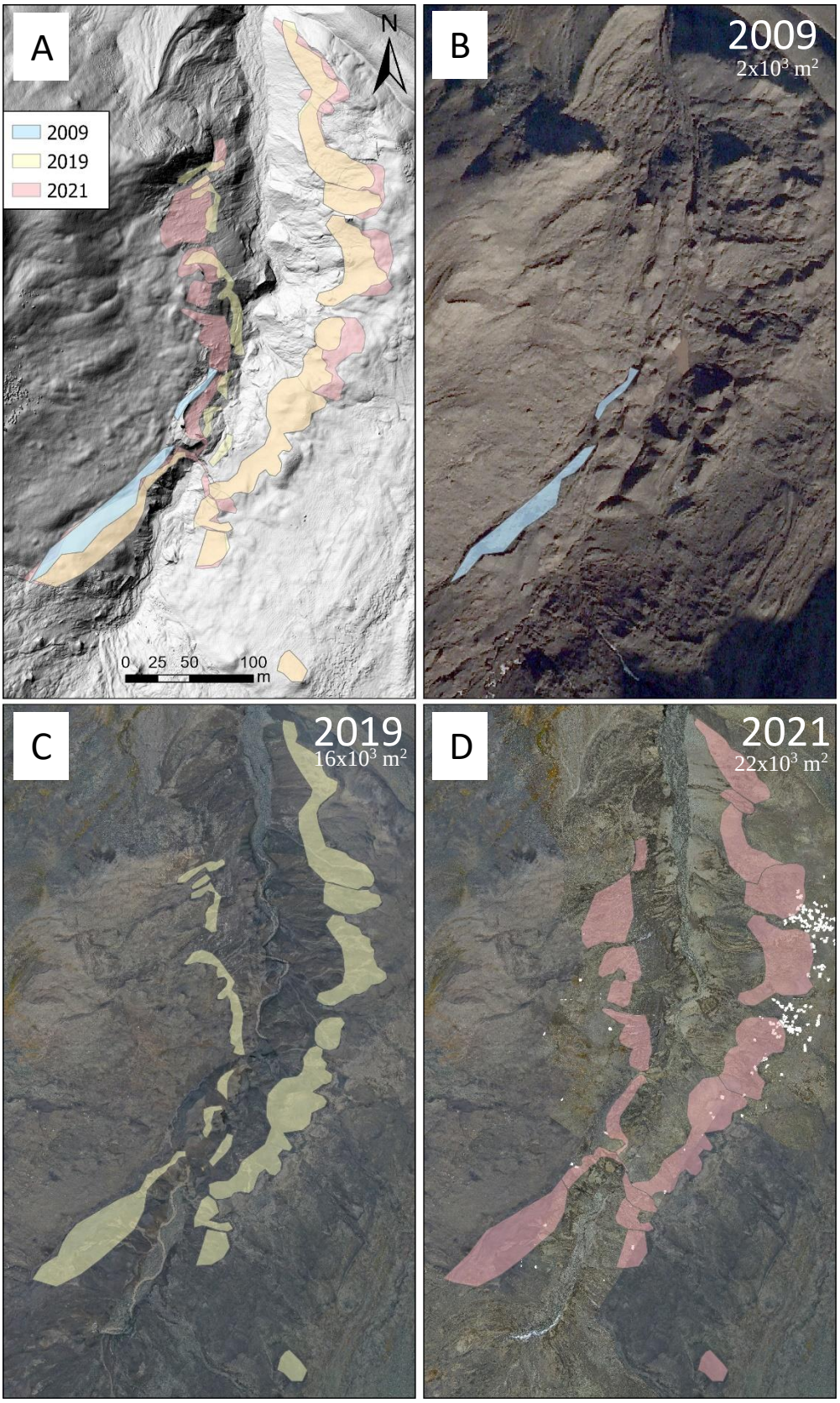

Figure 43 Area of slumped material in the Larsbreen moraine system in 2009, 2019 and 2021. Glaciofluvial v-valley formed between 2009 and 2019. Most slumping occurred after 2009. Location marked on Figure 41. A) All areas on 2021&2019 merged hillshade, B) Total area of $2x10^3$ m^2 on 2009 orthophoto (NPI, n.d.), B) Total area of $16x10^3$ m^2 on 2019 orthophoto (Hanna, 2019), D) Total area of $22x10^3$ m^2 on 2021 orthophoto (Appendix B).

4.2.5 Larsbreen rock glaciers and snow avalanche deposits

The Larsbreen moraine system is partially overlain by and adjacent to rock glaciers and snow avalanche deposits. These are both secondary sediment sources that may supply angular, coarse rocks to the Longyeardalen source-to-sink system. Snow avalanche deposits are also found along Longyearbreen moraine system and further downstream. The deposits by Larsbreen are presented due to the unique rock glaciers and the high amount of slope processes in this area with possible hydrological connectivity.

Three parallel ridges of rock glaciers are located along the outer edge of the Larsbreen marginal moraine. They have a curved morphology following the front of the moraine. Transverse cracks are visible on some parts, suggesting movement in a NW direction. Some of the rock glaciers connect to active avalanche deposits on (Figure 38).

Coarse, angular rocks were observed on the rock glaciers. This differs from finer material on the surface of adjacent moraines (Figure 39A). The rocks are of variable light to darker colours. The rocks close to the eastern slopes have little to no vegetation growth, whilst rocks further from the slopes (to the west) have moss growing on them and show signs of discolouration from weathering. This suggests that the rock glaciers are gradually older to the west. The rock glacier location, shape, and rock characteristics suggest they have been formed from repeated snow avalanche deposits from the eastern slope.

Snow avalanche deposits are found in the area around the rock glaciers. These deposits are loose, very angular, poorly sorted rocks (Figure 44). Such deposits are mapped along the slope above the rock glaciers until the mining dump (Figure 28). The furthest extent of snow avalanche deposits in this area is close to active glaciofluvial channels.

Figure 44 Snow avalanche rocks. Loose, very angular, and poorly sorted rocks. Small rocks <5cm lie on top of larger rocks >10cm, as rocks have stacked during melting based on their position in the snowpack.

Another rock glacier was mapped north of Sarkofagen (Figure 28). This is at a lower elevation than the till by the mining dump. This rock glacier has similar characteristics to the till. The lower elevation indicates movement and sinking due to ice movement inside of the till, resulting in its current position and topography.

4.2.6 River bank erosion

River erosion in Longyeardalen occurs as bank erosion and bottom erosion. River bank erosion is most easily observed and has the most influence on shifting channel course and possible changes in sediment source input. This is because river bank erosion may occur both in glaciofluvial deposits and other deposits such as slope deposits.

River erosion seems to be a prominent secondary source of sediment in the Longyeardalen source-to-sink system. Braided active and inactive meltwater channels were mapped in the moraine systems and in the open braided channel system (Figure 28). Significant river bank erosion was observed on the northern and eastern edges of the glaciofluvial fan over the melting season. The erosion has formed erosion banks up to 2.2m tall (Figure 45). The largest active channel erodes anthropogenically disturbed fluvial sediments to the NE.

River bank erosion occurred within and along the edges of the glaciofluvial deposits. An example of this is erosion of solifluction material with vegetation cover along the southern edge of the glaciofluvial fan. Erosion scarps up to >1.5m with vegetation overhang were formed. The position of the glaciofluvial to solifluction deposit border shifted visibly over the summer 2021.

Some brightly orange coloured smaller channels run separately from the main glaciofluvial channels. The colour is assumed to come from iron hydroxides/oxides in the water. It is likely that groundwater is the source of runoff in these channels. These channels may also transport sediments to the system. The relatively small size of these channels suggest that they amount for a much smaller total sediment input than the meltwater channels. It is likely that these channels do not contribute to significant river erosion. However, it may be important to note in the discussion of fine sediment sources. The amount of groundwater added to the system was not measured, and so quantified comparisons are not made.

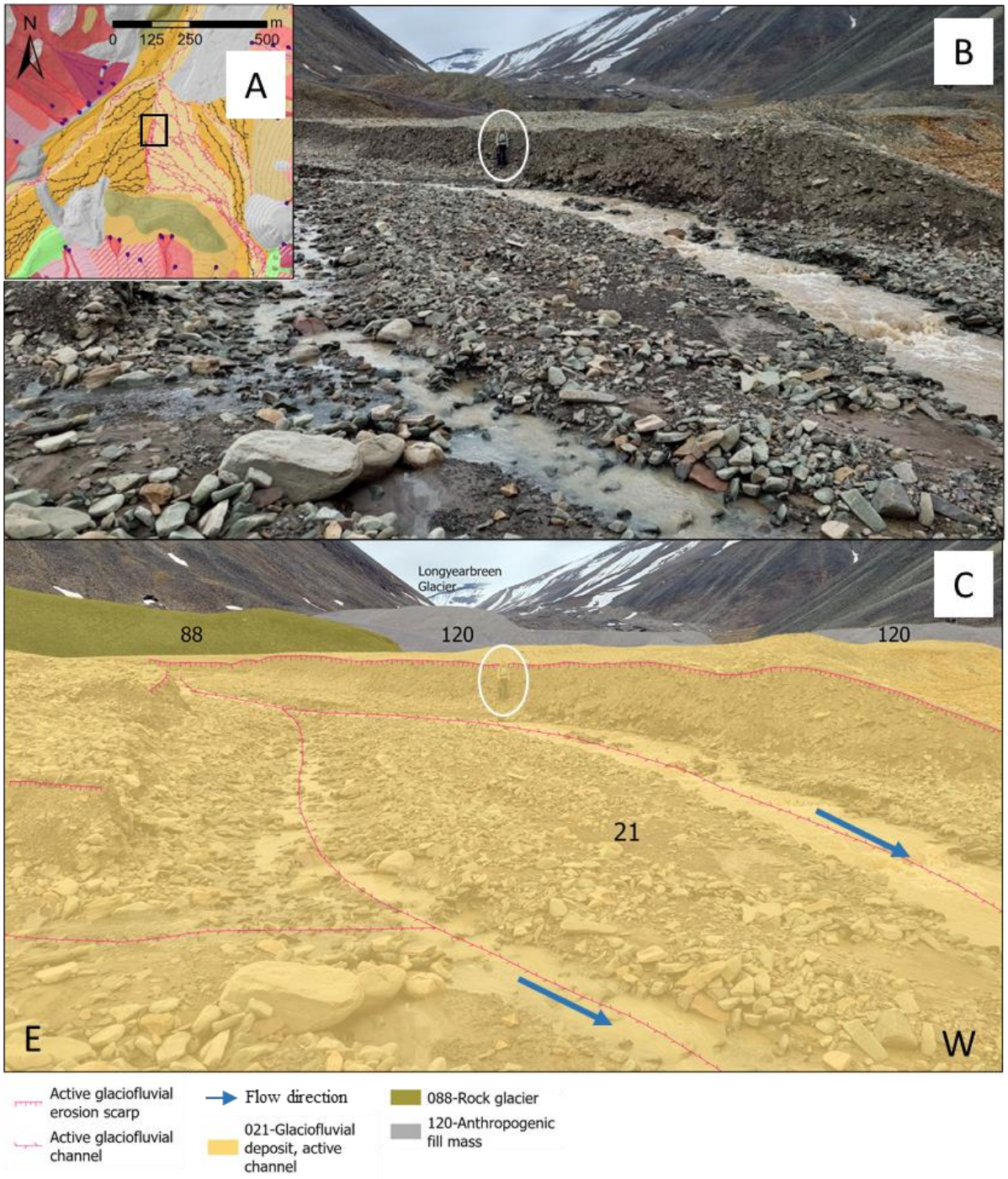

Figure 45 Glaciofluvial channels in the lower part of the active glaciofluvial fan. River bank erosion occurs on the NW side of the channels. Person for scale ~180cm indicated in white circle. A) Overview map (Snippet from Figure 28), B) Original photo: a lower sediment concentration is visible in the small channel merging from the East. The largest, western channel has a more turbulent flow. Subrounded rocks are common, with grainsize from mud to boulders. C) Quaternary and geomorphological features mapped onto the photo: River bank erosion has occurred of partially anthropogenically disturbed glaciofluvial sediment, forming a long, active glaciofluvial erosion scarp. (20/07/21).

4.3 Roundness of rocks to detect sediment sources

The degree of roundness of rocks can be used to infer sources and transportation distances. A certain degree of roundness can in Longyeardalen be attributed to multiple sources and processes (Figure 46). Angular rocks were observed in deposits from slope processes, rock glaciers, and till. Subangular to subrounded rocks were observed in slumped material and glaciofluvial deposits. Rounded rocks were observed in englacial and further transported glaciofluvial deposits.

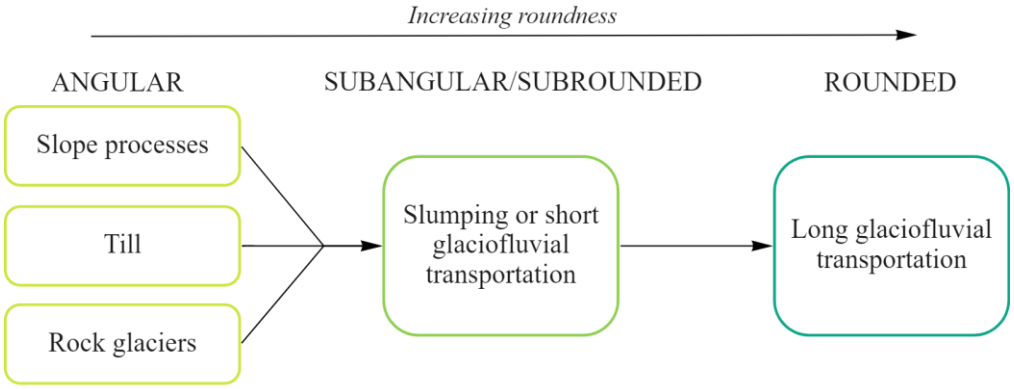

Figure 46 Flow chart of transportation processes and deposits increasing roundness of rocks in Longyeardalen. Multiple sources can have the same degree of roundness. Slope processes includes snow avalanches and rock fall. Angular rocks become more rounded with transportation distance. Slumping may partially round rocks.

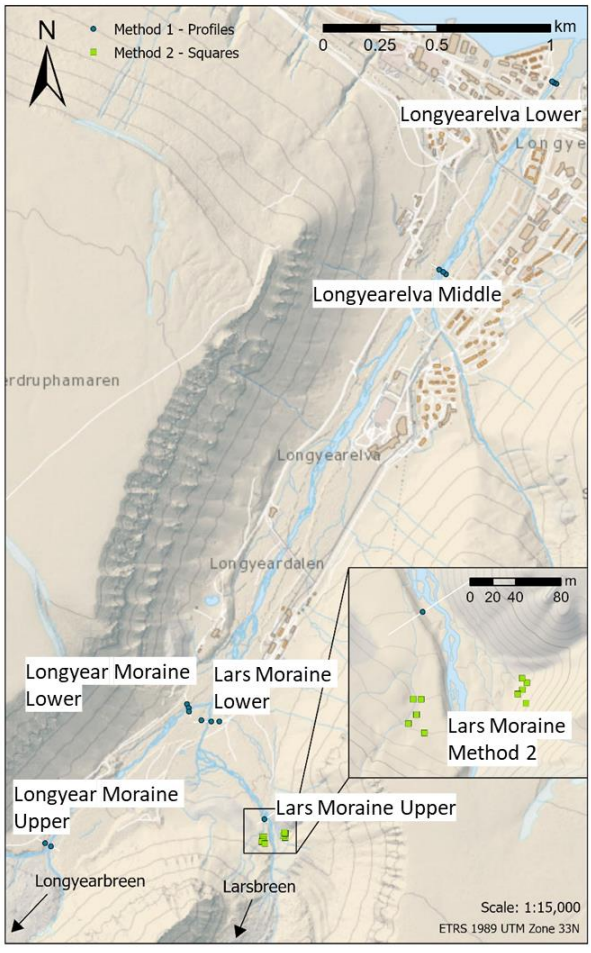

The aim of the roundness analysis was to test if there was an increase of roundness with transportation distance in Longyearelva, and to detect possible variation in roundness from different sediment sources. The roundness of rocks was determined at multiple locations between the moraine systems and the sea (Figure 47). This was done using larger rocks of at least a few cms in diameter found on the surface of active glaciofluvial deposits. Selected squares and profiles were chosen for analysis (Figure 48). The degree of roundness was determined from very angular to well rounded (Chapter 2.2.3). Detailed results of degree of roundness at each location can be found in Appendix C.

Figure 47 Map of Longyeardalen with locations of roundness analysis. Profile location names marked adjacent to blue dots. Green squares indicate locations for method 2 by Larsbreen moraine. Scale 1:15000.

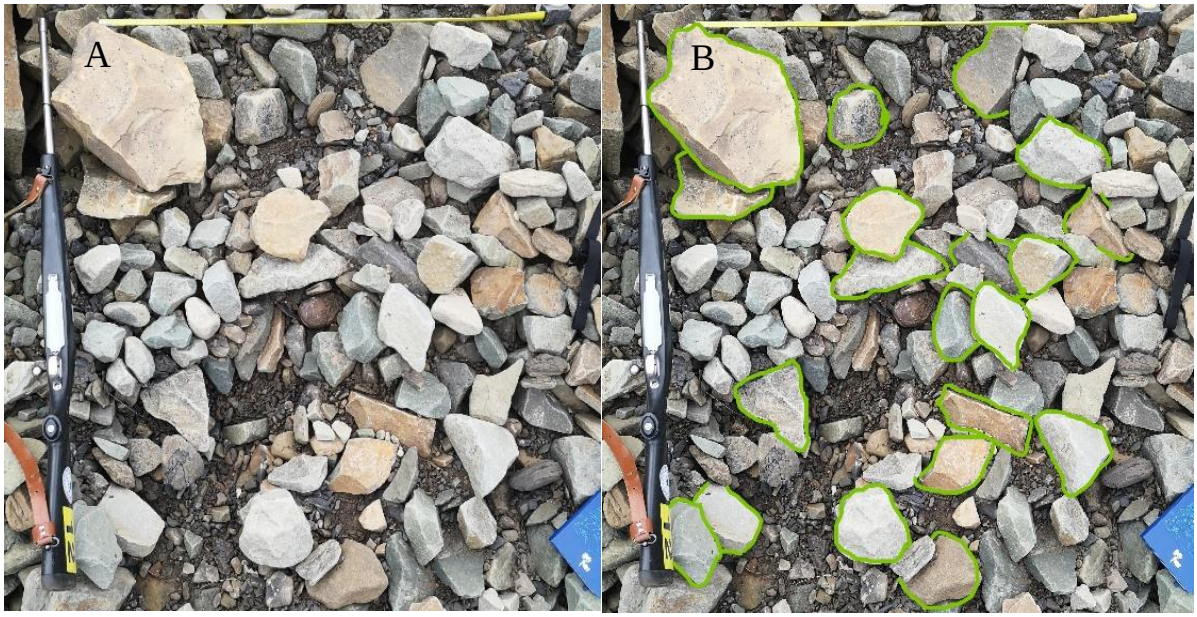

Figure 48 Example of a 1m^2 square used for roundness analysis. A) Top down photo. B) Same photos with green outlining the 20 largest rocks chosen in this square.

Roundness analysis showed a general trend of increased roundness with transport distance (Figure 49). At least three classes of roundness were observed at each sampling location. Very angular rocks were found in the upper parts of the valley. Well rounded rocks were found both in the upper and lower parts. The most common degree of roundness was subrounded. The spread in degree of roundness was largest downstream of the Longyearbreen moraine system.

The roundness of rocks directly downstream of the Larsbreen moraine system was investigated in more detail. Rounded to very angular rocks were found on both sides of the active glaciofluvial deposit (Figure 50). The most common degrees of roundness were subangular and subrounded. A larger amount of very angular to subangular rocks were found closest to the rock glaciers by the Larsbreen moraine system (East of river, proximal).

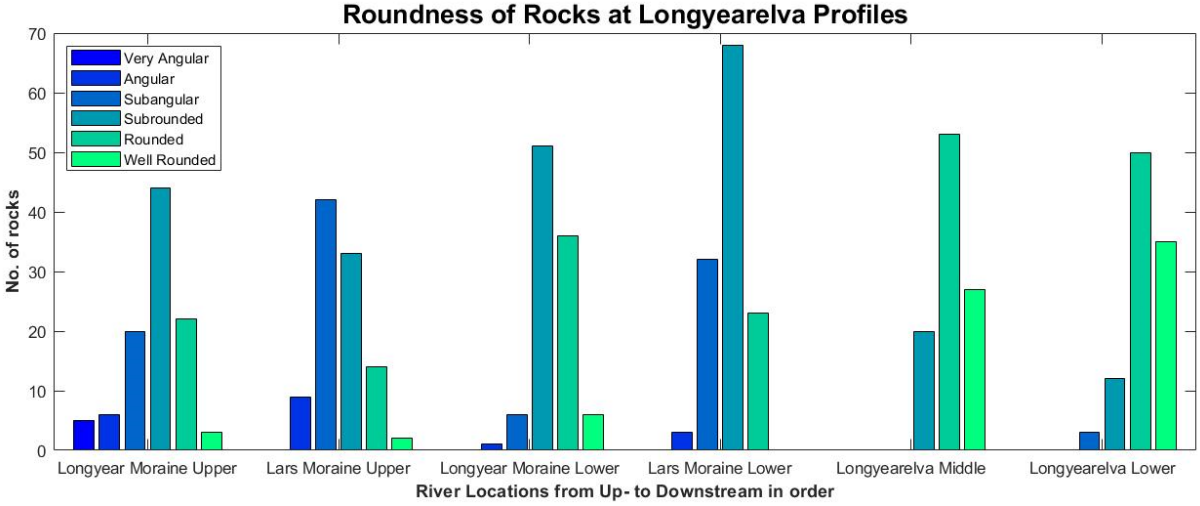

Figure 49 Roundness of rocks at six profiles across Longyearelva from directly downstream of Longyearbreen and Larsbreen moraine systems until directly upstream of Longyear delta (Longyearelva Lower). Increase in rounded rocks with transportation distance from source to sink.

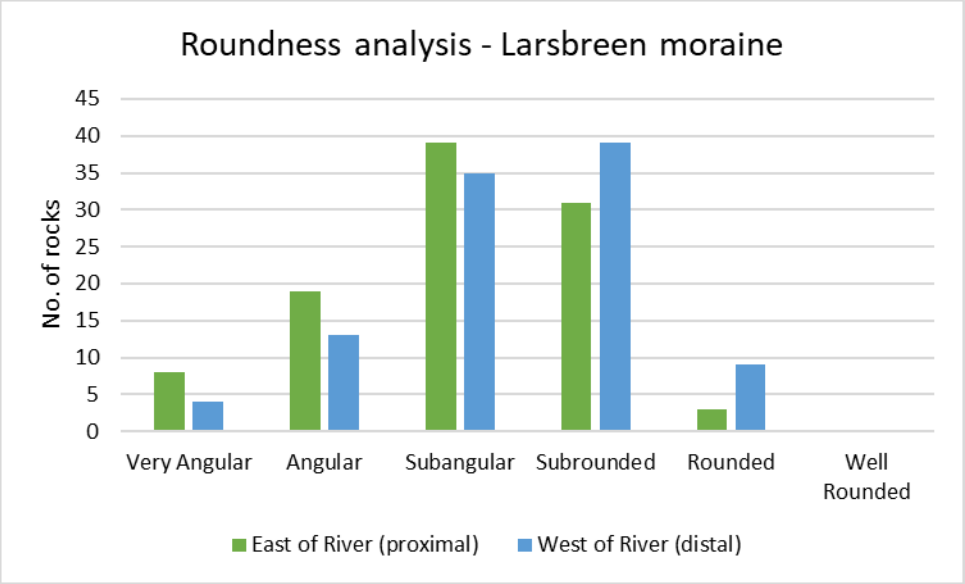

Figure 50 Roudness of rocks at squares on both sides of active glaciofluvial deposit directly downstream of Larsbreen glacier. The East of River location was adjacent/proximal to rock glaciers. The West of River location was more distal to the rock glaciers, adjacent to solifluction and mixed avalanche deposits (Figure 38).

4.4 Discharge and sediment transport

Discharge and sediment transport was monitored in Longyearelva over the melting season 2021. This provides important information on the amount of source material that is transported in the river on a daily and seasonal scale. Both bedload and suspended sediments were considered. Suspended sediment concentration is mainly controlled by sediment input and can therefore be used as a measure of input (Hodgkins et al., 2003). The size of rocks transported as bedload can be related to discharge and river erosion rates. Results regarding discharge and sediment transport are based on observations and measurements from the locations marked in Figure 51.

Key findings summer 2021:

- Mean Discharge from 22/06-25/08 was 1.3 ± 0.1 m^3/s
- Maximum Discharge on 08/07 of 3.2 ± 0.3 m^3/s
- Maximum Suspended Sediment Concentration on 10/08 of 8.1 ± 0.8 g/L
- Total Suspended Sediment Load (SSL) of 11×10^3 tonne
- The competence of Longyearelva river is at least 300-350 mm in diameter rocks

Figure 51 Overview of field locations used for discharge and sediment transport monitoring. The river gauging station is on the eastern side of the river. Marks the stretch of specific discharge measurements using the salt dilution method, and the three starting locations for passive tracers (bedload monitoring).

4.4.1 Discharge

Discharge in Longyearelva increased in periods over the melting season in 2021 with variable daily fluctuations. Hourly discharge in Longyearelva between 22/06 and 25/08 was calculated using water level measurements and a rating curve based on specific discharge measurements. Water level measurements were taken at the river gauging station by the bridge at Veg 600 (Figure 51).

Visual changes in discharge and river morphology were observed just upstream of the gauging station (Figure 52). One main channel was consistent on the SE side at the location. A small stream was visible on the NW side of the river in July and August. Erosion and change in river bar morphology was observed over the season. High discharge was observed on 6th July and 11th August (Figure 52B&C). Low discharge was observed on 4th September (Figure 52F).

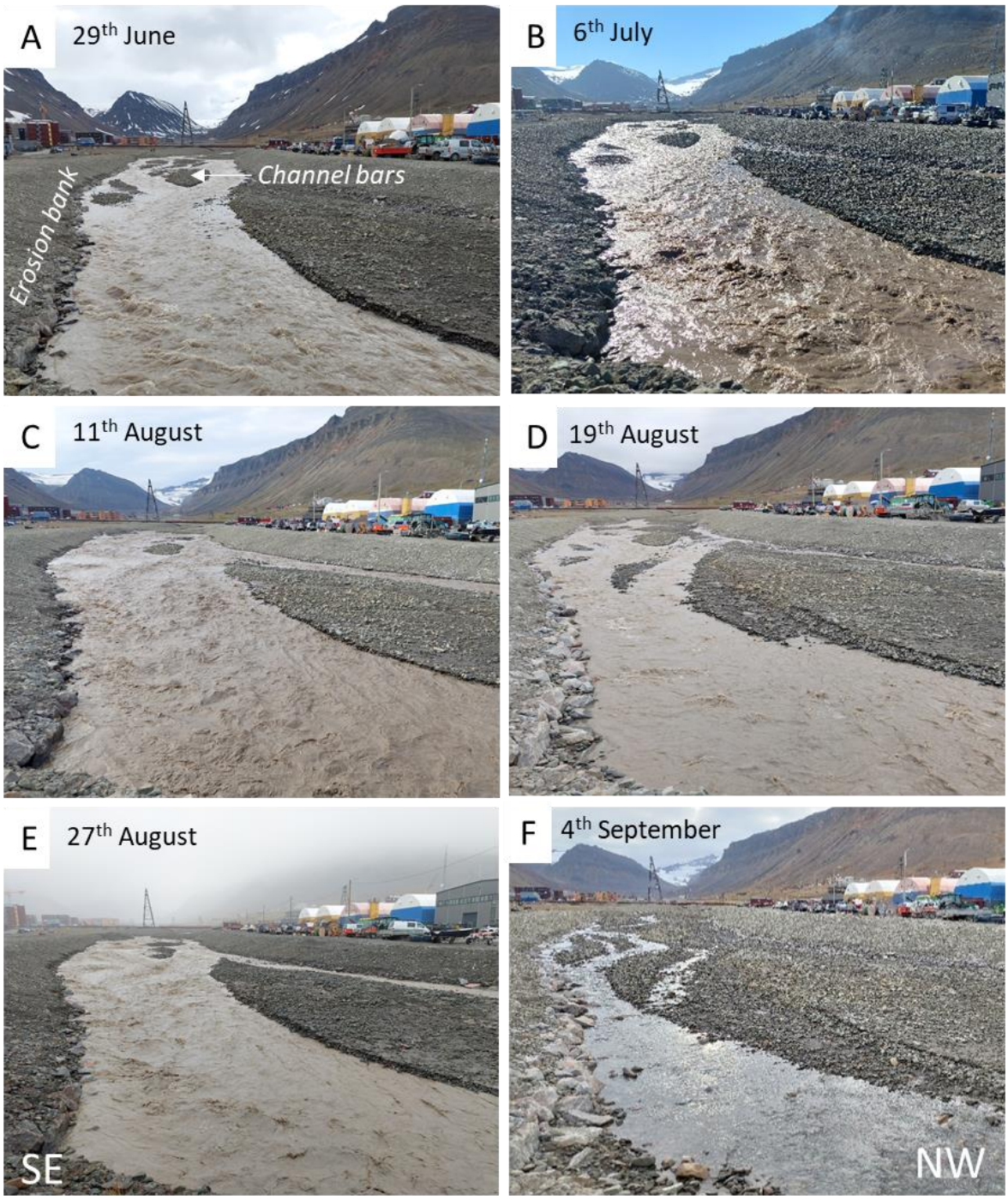

Figure 52 Varying discharge and suspended sediment concentration (SSC) in Longyearelva looking upstream from the river gauging station over the summer 2021. A) 29/06: discharge 1.5m^3/s, SSC 0.6g/L, B) 06/07: discharge 1.7m^3/s (two days before maximum), SSC 2.8g/L, C) 11/08: discharge 2.1m^3/s, SSC 7.1g/L, D) 19/08: discharge 1.0m^3/s, SSC 1.4g/L, E) 27/08: high discharge, medium SSC, F) 04/09: low discharge, very low SSC. Photos A-D were all taken around 14:00-15:00.

It is possible to observe daily and seasonal variations in hourly discharge data (Figure 53). In the beginning of the monitoring period discharge was consistently around 1.5m^3/s with a little diurnal variation. One peak of 2.4m^3/s occurred in June. From around 4th July and towards the end of July discharge is characterized by varied pattern with high, irregular diurnal variability and a seemingly weekly cycle from 1 to >3 m^3/s. The highest peaks in July were 3.2m^3/s (8th July) and 3.1m^3/s (16th July), and the lowest discharges between each peak in July were 1.2m^3/s (11th July) and 1.0m^3/s (21st July). Discharge decreased to 0.7m^3/s at the end of July. From the beginning of August the discharge pattern seems to change to a more regular diurnal variability with one excursion around 11th August with high values reaching a peak of 2.7m^3/s. Towards the end of monitoring, discharge stabilized around 1m^3/s with slightly decreasing diurnal variation.

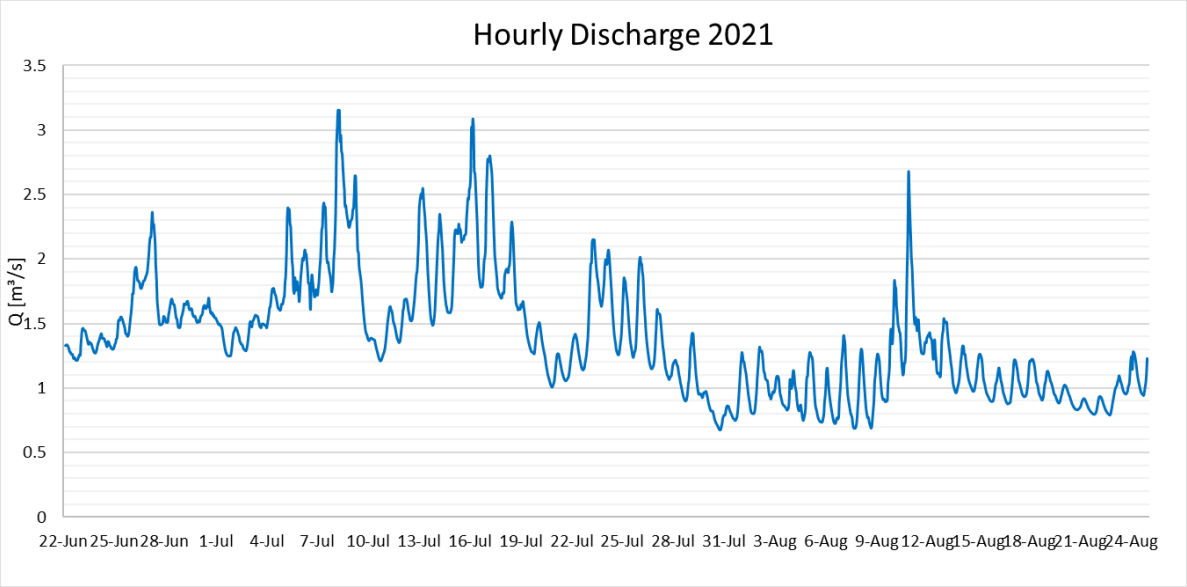

Figure 53 Hourly discharge in Longyearelva from 22nd June to 25th August 2021. The beginning of the season is characterized by a little diurnal variability and one excursion. July is characterized by weekly cycles between 1 and >3 m^3/s, and high, irregular diurnal variability. Maximum discharge of 3.2m^3/s on 8th July. From August diurnal variability is more stable but still significant, with discharge around 1m^3/s except for an excursion of 2.7m^3/s.

Daily average and daily maximum discharge are plotted in Figure 54. Seasonal variability as described for hourly discharge can also be seen in the daily average. Daily fluctuations are shown here as variable difference between average and maximum discharge. Large and variable difference is seen in July. The approximate weekly cycle in discharge in July has three main phases. The first phase has a long rising limb and short falling limb. The second phase has medium rising and falling limbs. The third phase has a short rising limb and a long falling limb. The peak in August has a short rising limb and long falling limb. This peak has the largest daily increase (i.e. largest difference between average and maximum discharge).

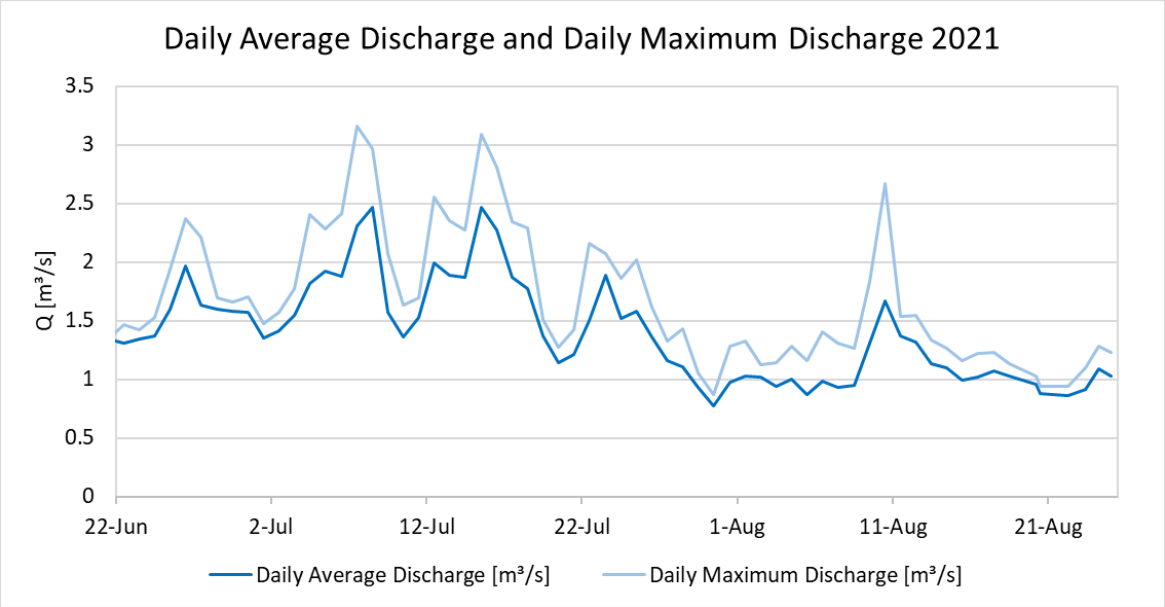

Figure 54 Daily average discharge and daily maximum discharge [m^3/s] from 22nd June to 25th August 2021. In June there is a small difference between average and maximum daily discharge. High discharge measurements generally have a larger difference between average and maximum daily discharge. The peak in August shows the largest discharge increase from the daily average to max.

4.4.2 Transport of suspended sediments

Suspended Sediment Concentration (SSC) varied daily and seasonally in 2021. SSC was measured up to four times daily from 23rd June to 19th August. at the same location as the discharge measurements (Figure 51). The sample times were 02:00, 08:00, 14:00, and 20:00. All SSC measurements are plotted in Figure 55.

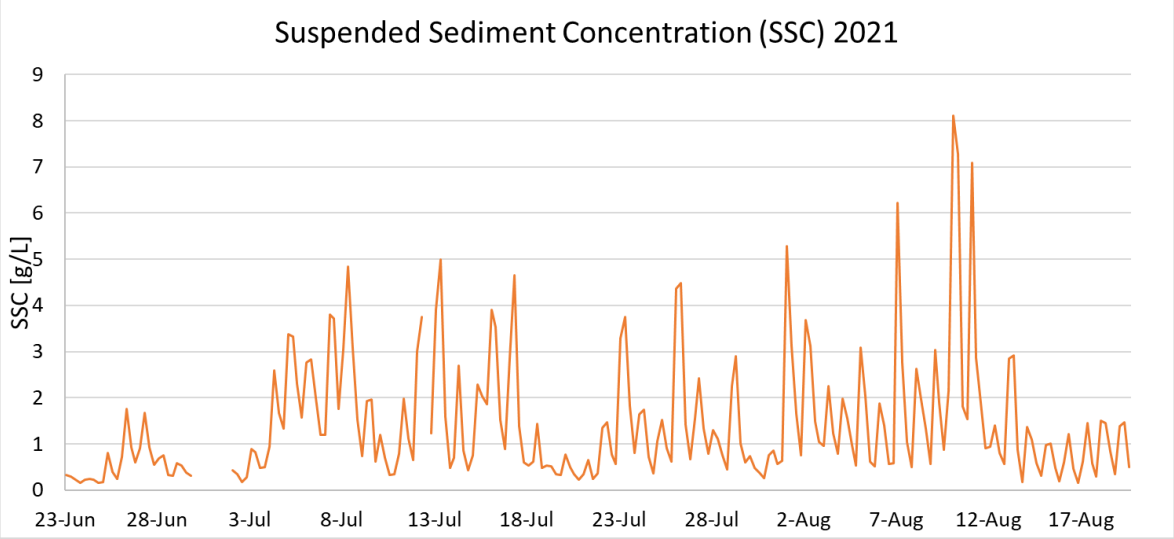

Figure 55 Suspended Sediment Concentration (SSC) [g/L] four times a day from 23rd June to 19th August 2021. SSC is low <2g/L in June. Phases of high SSC are seen in July with irregular daily fluctuations from <0.5 to 5 g/L. Consistently large daily fluctuations seen in August with increasing peaks up to a maximum of 8.1g/L on 10th August. From 14th August SSC is <2g/L. A few samples are missing in the end of June and mid-July (gaps in curve).

The beginning of the season is characterized by low SSC <2g/L with low diurnal variation. From around 4th July there was a pattern of highly fluctuating SSC between <0.5 and 5 g/L until the end of July, with significant, irregular daily fluctuations. From August the daily fluctuations seem more regular and on average larger, and peaks are >5g/L up to the maximum SSC 8.1g/L on 10th August. From around 14th August the SSC lowered to <1.5g/L with some daily fluctuation until the end of monitoring.

Maximum daily SSC occurred at different times of the day over the season in 2021. Figure 56 shows the maximum SSC values and time of occurrence. In June and July the peak was most common in the evening (20:00). Maximum SSC in July was 5.0g/L on 13th July. In August the peak was most common in the afternoon (14:00). The four days with highest maximum SSC were in August and all occurred in the afternoon. Some peaks occurred at night (02:00), but only for low SSC days (<3g/L). No daily maximum SSC occurred in the morning (08:00).

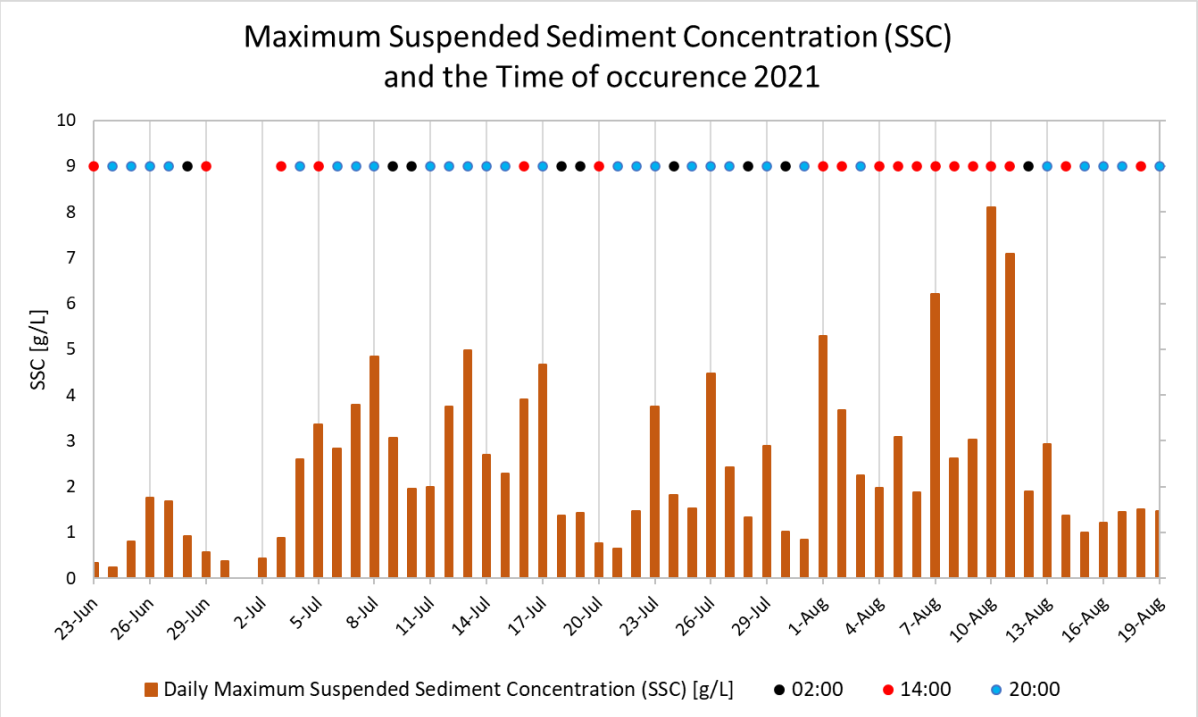

Figure 56 Maximum Suspended Sediment Concentration (SSC) [g/L] (orange bars) each day from 23rd June to 18th August 2021 and the time of occurrence (coloured dots). Max SSC at 02:00 in black, 14:00 in red, and 20:00 in blue. Max SSC was low in June, peaking in the evening. Max SSC was medium to high in July, peaking mostly in the evening. Max SSC was medium to very high from 1st to 11th August, peaking mostly in the afternoon. Highest maximum SSC of 8.1g/L occurred on the afternoon of 10th August. Towards the end of August SSC stayed < 2g/L with peaks in the afternoon/evening. Peaks at 02:00 are only observed on days with max SSC ≤ 3g/L.

Suspended Sediment Load (SSL) was calculated from daily SSC and daily average discharge (Figure 57). In June the daily SSL was <200 tonne. The highest daily SSL was 686 tonne on 10th August. A total of at least 11 x 10^3 tonne of suspended sediment was transported in Longyearelva in 2021 during the measurement period. In the Longyeardalen catchment (22.9km^2) this equates to a minimum Suspended Sediment Yield (SSY) of ~500t/km^2/yr.

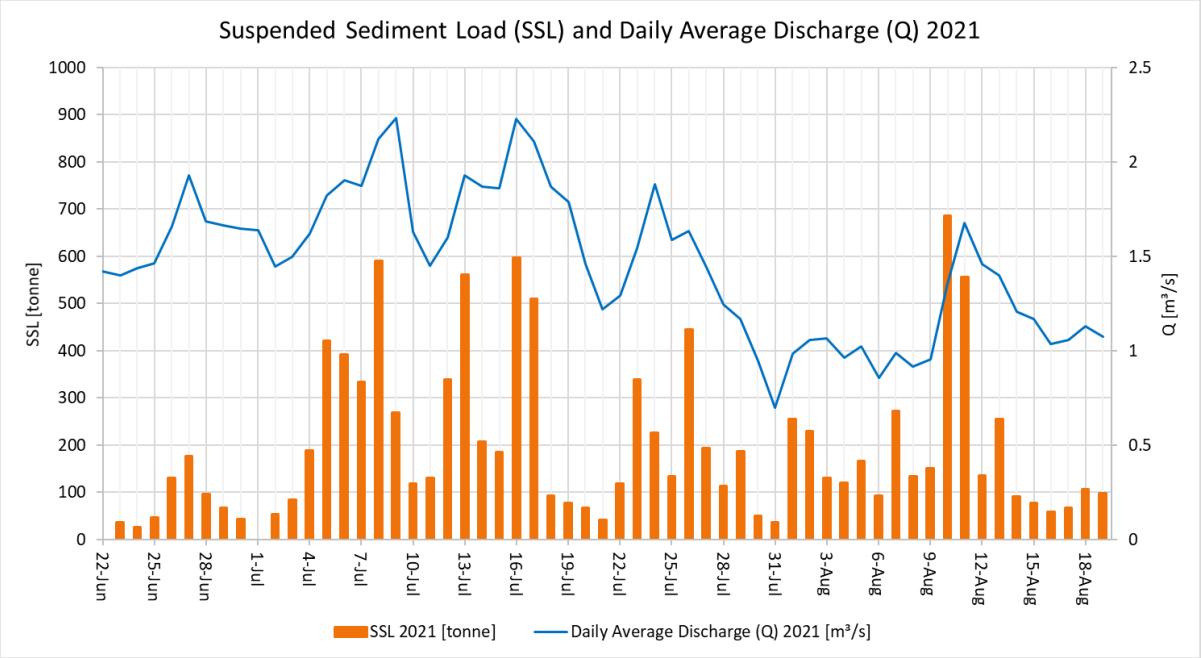

Figure 57 Daily Average Discharge [m^3/s] and Suspended Sediment Load (SSL) in tonne/day in Longyearelva 2021. Maximum SSL on 10th August of 686 tonne/day. In total more than 11x10^3 tonnes of suspended sediment was transported over this time.

4.4.3 Transport of bedload sediments

Transport of passive tracers in three locations in Longyearelva was observed during the melting season of 2021 (Figure 51). The largest sized rock with tracked movement >1m was 300-350 mm in diameter. Rocks of larger size were observed in approximately the same location in the early- and late-season (June and September 2021). The following observations were made at the three monitoring locations Hu-PT, Ha-PT, and Pr-PT:

- Hu-PT (Huset): The largest number of rocks with movement was observed here. At least two braided river channel paths shifted several times over the season. This exposed a larger number of red rocks to flow. The largest transported rock, of size 300-350 mm, was transported 65m downstream. The furthest transported rock, of size 200-250 mm was transported 74m.
- Ha-PT (Hallen): A few rocks were transported but the channel did not shift much during the season, meaning a lot of rocks were consistently above the surface. The largest rock that was observed after movement was 200-250 mm large and was transported around 21m downstream.
- Pr-PT (Polarriggen): Most rocks were above the surface throughout the season, where one well-defined channel did not change its course significantly. All the rocks that were submerged in the channel were missing at the end of the season. The largest missing rock was of size 300-350 mm.

5 Discussion

There is a large range of primary and secondary sediment sources in the Longyeardalen source-to-sink system (Figure 58). Sediment transportation in the river relies on seasonal glacial meltwater and input of sediment from moraines, slopes, river erosion and other processes. This is influenced by seasonal thawing of the active layer in the ground. The secondary sediment sources are complex and inconsistent, transporting and depositing sediment sporadically over time. The relative importance of sediment sources varies over time; on a daily, seasonal, and long-term scale. The moraine systems may be particularly important sediment sources as most meltwater travels directly through or along the two moraines in the upper system. River erosion through transportation is also considered an important and seasonally readily available sediment source. These sources both consist of fine and coarse grains.

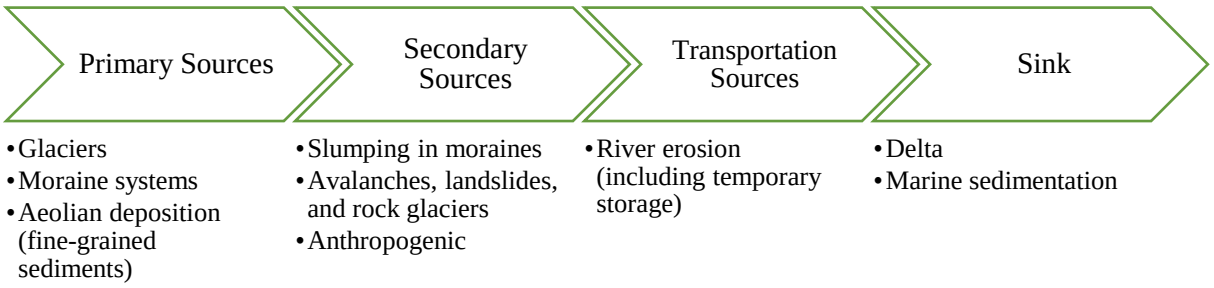

Figure 58 Flow chart of the source-to-sink system in Longyeardalen.

5.1 Primary sediment sources

The primary sources of sediment in Longyeardalen are glaciers, moraine systems, and aeolian deposition. The glaciers and moraines are thought to be important contributors of sediment to Longyeardalen. These systems are changing every year due to melting of ice, ground thaw, shifting melting channels, gravitational driven movement, and input of secondary sources. Changes in primary source systems are important to consider for their sediment contribution over time.

5.1.1 Glaciers

The two glaciers in Longyeardalen are important controls on discharge in the melting season. Glacial sediment is considered an important source of sediment input in glacial catchments (Hanssen-Bauer et al., 2019). As such, it would be expected that there is correlation between discharge and sediment concentration. This was observed in the midseason, but only partially in the late season. This suggests that glacial sediment is not the main contributor of sediment throughout the melting season. Meltwater was observed in supraglacial channels through the central parts and along the sides of both glaciers. As such, the possible glaciofluvial input from the glaciers consists of sediment from different parts of the glaciers. Sediment may be added in the glacial channels from the slopes on the side of glaciers as well as from the central parts of the glaciers.

The glaciers have previously been defined as cold-based with possible temperate patches (Etzelmüller & Frauenfelder, 2009; Yde et al., 2008). This is consistent with surface observations of significant meltwater contribution from supraglacial channels. It is expected

that for cold-based glaciers the sediment availability is controlled by ground thaw. Increase in sediment transport in Longyearelva towards the late season is consistent with this assumption. Possible temperate patches would allow for englacial transport of sediments in the glaciers. The presence of well-rounded rocks in Longyearbreen moraine system supports the presence of temperate patches. The presence of temperate patches in the glacier would promote a larger range of roundness of sediment transported in Longyearelva. However, surface observations are not sufficient to determine the scope of this. Future increase in glacier temperatures has the potential to increase sediment erosion from the glacier base.

5.1.2 Moraine systems

The Longyearbreen and Larsbreen moraine systems are ice-cored moraines in a degradational state. The glaciers have a large influence on sediment transport through the moraine systems as glaviofluvial channels cut through both systems. The moraine systems can be described as a temporary storage system with contemporaneous deposition, transportation, and erosion. Thus, these systems are an important influence on fine and coarse sediment input to Longyearelva. Larsbreen moraine has previously been suggested as an important source of sediment with expected future increase (Hanssen-Bauer et al., 2019). This is supported by field observations, mapping, and volume calculation of slumped material in 2021.

The sediment input from the Larsbreen and Longyearbreen moraine systems, respectively, vary in total amounts and type of source material. This includes till, snow avalanche deposits, rock glaciers, and englacial sediment. Various roundness of rocks was observed on the surface of and downstream of both moraine systems. Well-rounded glacially transported rocks to very angular snow avalanche rocks were observed. This shows the range of possible sediment sources that may have deposited rocks in the moraine system.

The moraine systems can be described as storage areas for sediments. Rocks from glacial and secondary sources are deposited on the moraines and may stay there for short or very long periods of time. Glaciofluvial sediment is eroded, transported and deposited in the moraine systems. The moraine systems are therefore both a direct and indirect source of sediment. The distribution of sediment sources that are transported in Longyeardalen varies over time due to shifting active channels. Shifts will change what sediment deposits are hydrologically connected and available for glaciofluvial erosion.

The two moraine systems show characteristics that suggest they are in different phases of degradation. Longyearbreen moraine system has a lobate front and a developed forefield. The forefield is asymmetrical in cross-profile with a glaciofluvial flat on the eastern side, and more preserved morphology on the western side. Multiple active channels flow over and through Longyearbreen moraine system. One previously active channel on the east side has been abandoned since 2020. No prominent inactive channels were found in the Larsbreen moraine system. As such, the active source input sediment from Longyearbreen moraine system may have changed more with shifting active channels during the past years.

The development of the two moraine systems seems to be influenced greatly by the surrounding topography. Larsbreen moraine reaches further away from the glacier but is confined in a narrower space between the slopes than Longyearbreen moraine. This restricts the possible meltwater flow paths and promotes vertical erosion. The melting channel has cut vertically through the moraine over the past 10 years, and created a steep, fluvial v-shaped valley. This development can be seen in difference in orthophotos from 2009 and 2019/2021.

5.1.3 Aeolian deposition

Aeolian deposition of fine sediment is a primary source of sediment input to the catchment. However, it can be seen as a small contributor of sediment. Wind transports fine sediment over long distances, mostly in the fall and winter when precipitation is generally lower and wind rates higher (Chapter 2.1). Aeolian sediment is deposited directly into channels, and on adjacent slopes and deposits. Thus, this may be a direct or indirect source of fine sediment. Aeolian sediments are available for transport from the beginning of the season as this is not frozen in the ground by permafrost. It is expected that the source may be depleted in active channels over the melting season. However, aeolian sediments may be mixed with other sediment sources, such as snow avalanche deposits and till. This may therefore constitute a small part of secondary sediment input throughout the melting season.

5.2 Secondary and transportation sediment sources

Secondary and transportation sediment sources are potential indirect inputs of sediment to the Longyeardalen source-to-sink system (Figure 59). These sources are slumping/thaw deformation in moraines, snow avalanches, landslides, rock glaciers, river erosion, and anthropogenic sources.

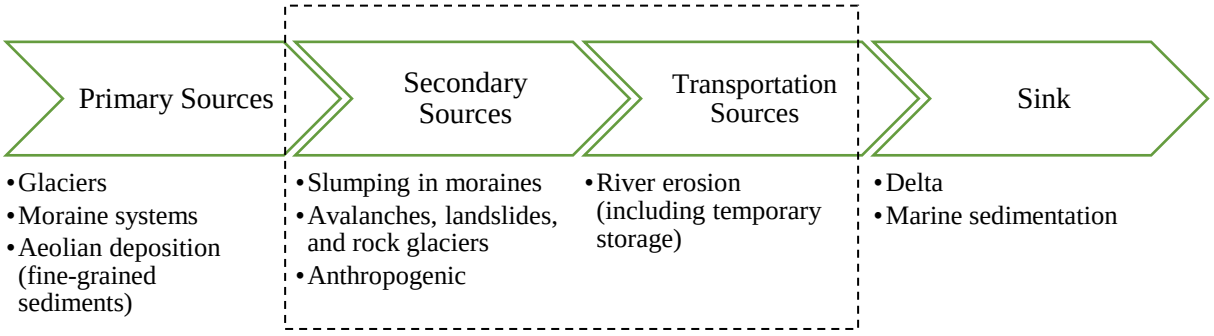

Figure 59 Flow chart of the source-to-sink system in Longyeardalen. Highlights the focus of this chapter: secondary and transportation sources.

Anthropogenic sediment is not discussed in detail as this is mixed with the other sources, and is not directly influenced by warming of the Arctic. However, it is important for the sediment transport in Longyearelva. Fresh anthropogenic sediment is loose and therefore not restricted by frozen ground before seasonal thaw. Anthropogenic reworking of sediment in Longyearelva has been done in the past years and more is planned for future years. This may cause irregular sediment transport unrelated to daily, seasonal and long-term natural changes. Some sediment transport recorded in the melting season 2021 is likely a result of anthropogenic activity.

5.2.1 Slumping in moraines as sediment source

One of the main aims of this study was to quantify the slumping of sediments in the moraine systems of Longyeardalen. This is important due to the sensitivity to degradation of the ice-cored moraines with a changing climate. Slumping may account for direct or indirect sediment input to Longyearelva, depending mainly on the path of active channels. Slumping in the moraines has occurred for more than 10 years and is expected to continue in the future.

Slumping in the moraine systems has occurred in large scales since at least 2017. This is known from previous drone mapping of the Larsbreen moraine system (Mannerfelt, 2017a)

and the Longyearbreen moraine system (Mannerfelt, 2017b). His calculations of removal and deposition of mass showed a net loss of material from both moraine systems. In Larsbreen moraine, most of the removal is due to slumping on the slopes of the v-valley (Figure 60). This suggests that slumping is an important source of sediment from Larsbreen moraine system to Longyearelva.

Mannerfelt (2017a, 2017b) also calculated net loss of sediment in the broader Longyeardalen moraine system (Figure 61). Removal of material is seen as slope processes along the moraine system, in glaciofluvial channels, and as slumping on the moraine surface. Removal and deposition of sediment from slumping over a short distance was observed (Figure 61B). This supports the idea of temporary storage in the moraine system. This slump scar has developed retrogressively in stages from 2017 to 2021 (Figure 42). The sediment deposited in 2017 can be assumed to have since been eroded or buried by new slumps. It is likely that this sediment has or will in the next few years be transported downstream in Longyeardalen. This is argued based on the adjacent active channel, and observations of subsurface erosion and collapse in glaciofluvial deposits adjacent to this scar in 2021.

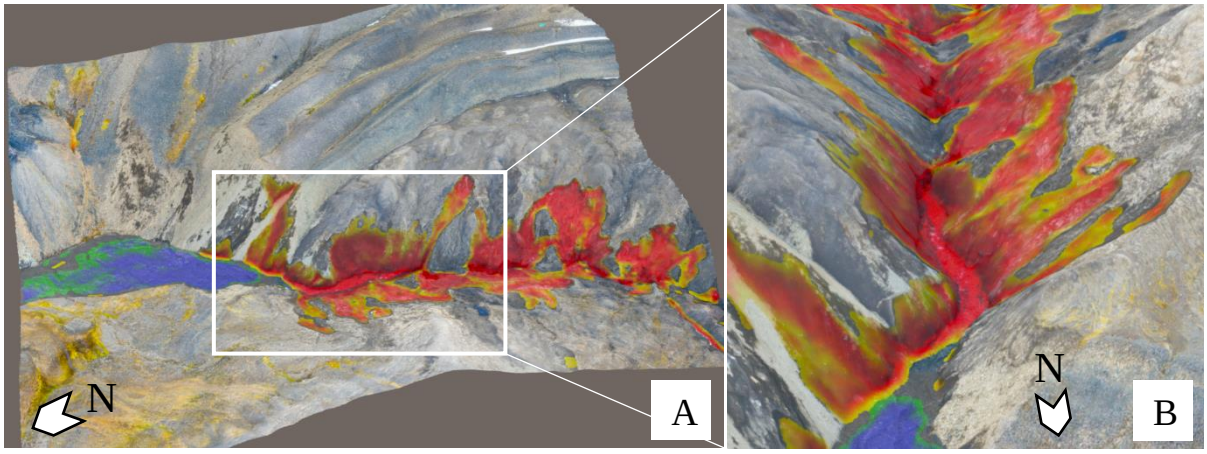

Figure 60 Larsbreen moraine system July-September 2017. Red-yellow areas indicate removal of mass and blue-green areas indicate deposition. A) Lower Larsbreen moraine, rock glaciers, and upper part of glaciofluvial fan, B) Upstream view of mass removal in the valley (Mannerfelt, 2017a)

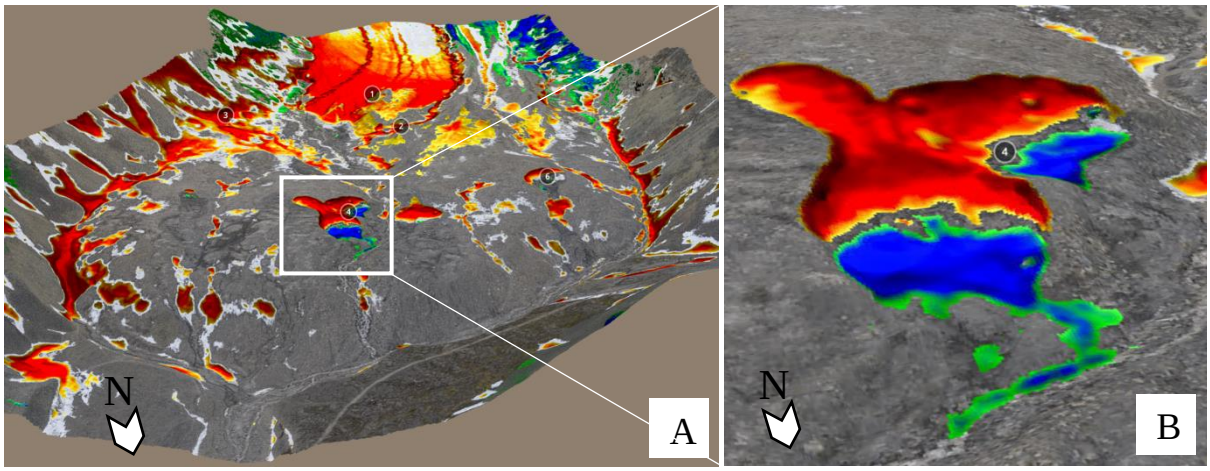

Figure 61 Longyearbreen moraine system July-September 2017. Red-yellow areas indicate removal of mass and blue-green areas indicate deposition. A) Longyearbreen glacier, moraine system and surrounding slopes, B) Slump scar with removal and deposition of sediment (Mannerfelt, 2017b).

Almost $3x10^6$ m^3 of sediment has been displaced by slumping or other thaw driven gravitational processes in the Longyearbreen and Larsbreen moraine systems from 2009 to 2021. Calculations of volumes from 2009, 2019 and 2021 suggest a doubled rate of slumping from 2009 to 2021. This indicates that the process of slumping has accelerated over time. This does not account for possible active layer thickness increase. However, if increased thickness was assumed, the acceleration would have been more intense. This is suspected to be likely due to the recent past increase in temperature and precipitation (Chapter 2.1.1). Acceleration of slumping may be driven by steepening of slopes due to vertical glaciofluvial erosion, an increase in active layer thickness, or the exposure of ice-core to heat and rainfall.

The development of slumps and exposure of old ice-core in moraine systems is illustrated in Figure 62. After an initial slumping event, the old, sediment-filled ice is exposed. Thawing may occur during the summer season. This releases sediment that was previously locked in the ice. Further slumping is promoted as the till above the scarp has less support and is more exposed to heat from the side. Thawing of internal ice and solifluction movement promotes formation of new cracks, which makes it easier for water from rainfall or snowmelt to reach the ice/till boundary. The retrogressive slumping observed in both Longyearbreen and Larsbreen moraine may be a result of this exposure to heat and surface water. As the ice below the till continues to thaw through exposure from repeated slumping, more sediment becomes available and may be eroded or added to new slumps. More water from thawed ice is also added to the till from below, which increases pore pressure and instability. This process can create a positive feedback loop to encourage degradation of the moraines and increased available sediment for input to Longyearelva. The development is supported by the volume calculations of accelerating slumping during the past years of warming.

Previous studies have found that slumps with hydrological connectivity may increase suspended sediment transport by some orders of magnitude (Rudy et al., 2017). The retrogressive development of slumps and acceleration of degradation observed in the two moraine systems was in many cases located in or along active glaciofluvial channels. This hydrological connectivity may lead to high variability and event-based sediment transport from slumps. Warming and increased rainfall is expected to further intensify this as sediment-filled ice-core is exposed and destabilised as illustrated (Figure 62).

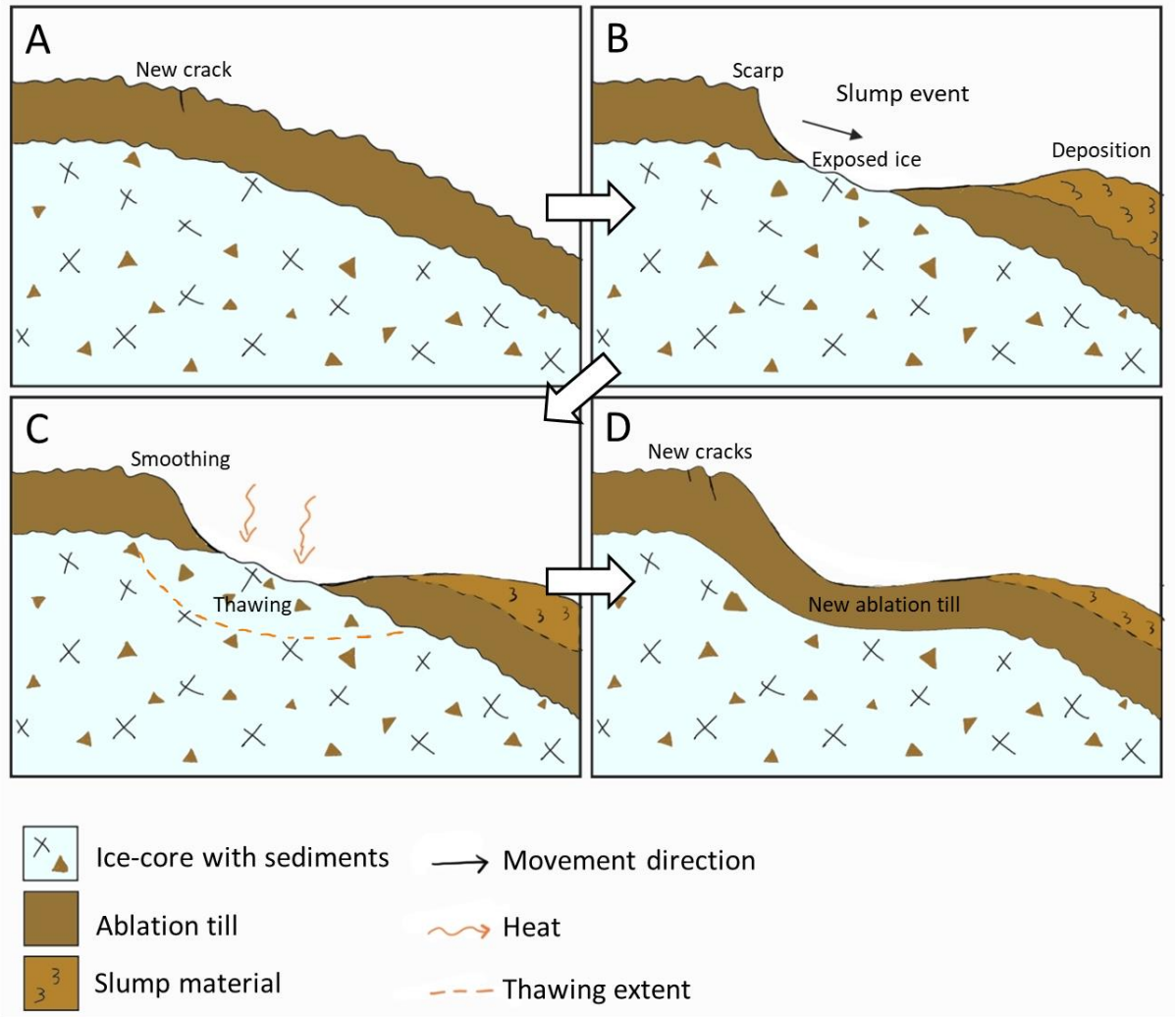

Figure 62 Schematic figure of progressive slumping in an ice-cored moraine system. A) Till cover overlaying old glacial ice is unstable. New cracks open and possibly deepen with added surface water down to the ice/till boundary B) Slumping is triggered due to increased pore pressure from added water in the ice/till boundary from melting ice and/or precipitation. A scarp is formed at the top and slumped material is deposited downslope. C) Old glacial ice is exposed to heat and thawing occurs. Thawing of internal ice and solifluction causes smoothing of fine geomorphology over time. D) New ablation till is formed from sediment released from melted ice-core. This is thinner than the initial slumped till as ground sinks when the melted ice is removed. New cracks form at the crown. Heat/precipitation may trigger retrogressive slumping later.

The different characteristics of the two moraine systems are important to note in terms of their potential as sources of sediment. They are both influenced by the same general environment, however with slightly different elevation. The higher elevation of the Larsbreen moraine system may cause slightly lower temperatures and later thaw here. Assuming the active layer is the same thickness in both moraines, and the sediment characteristics are approximately the same, a climate event could influence the two systems very similarly. An event of high precipitation could increase the pore pressure in the ground. This could trigger slumping or collapse in both moraine systems, which could cause a large, sudden increase in loose sediment in active channels in Longyeardalen.

The two moraine systems could also respond differently or at different times to the same climate event. This can make the sediment input to Longyearelva more difficult to predict. For example, an increase in temperature may initially cause retrogressive slumping in the Larsbreen moraine system, and later in Longyearbreen moraine system. This could occur due to a larger area of slumped material at Larsbreen moraine, which has exposed a larger area of ice-core to heat and water. Another factor is that the slopes along the active channel in Larsbreen moraine system are steeper, thus promoting gravitational driven movement. In the Longyearbreen moraine system, the active channel partially flows below the surface in the outer parts of the moraine. Loose sediment from slumps may therefore not be directly added during the slump event, but temporarily stored until further collapse or subsidence. The shift of active channels in the Longyearbreen moraine system also provides possible delays in sediment input from initial source availability.

5.2.2 Snow avalanches as sediment source

The input to Longyearelva from secondary sediment sources includes snow avalanches. Snow avalanches are common along the slopes of Longyeardalen and are responsible for downslope transportation of rocks. Deposits from snow avalanches are thought to be an important sediment source in the early- and mid-season when the snow is melting. Snowmelt most easily transports fine snow avalanche sediment to active channels. Coarse, angular rocks may be stored for multiple seasons as potential sediment sources.

Snow avalanche deposits were mapped on and below the slopes along both the moraines and along active and inactive melting channels. This sediment may be added to Longyearelva directly or indirectly. Directly added sediments include snow avalanches reaching into an active channel. Indirectly added sediments are, for instance, an older snow avalanche deposits eroded by a new or shifted melting channel. Snow avalanche deposits on the slopes in Longyeardalen are mostly not in direct contact with melting channels, with some exceptions. Snow avalanche deposits have also been seen to form rock glaciers in Longyeardalen, which may also be considered as long-term temporary storage of snow avalanche deposits.

An example of hydrologically connected snow avalanche deposits were mapped along the Longyearbreen moraine system (Figure 30). These are located directly along a currently inactive channel on the eastern side and front of the moraine. This channel was active in 2019 (Hanna, 2019), and inactive in 2020 (Løvaas, 2021) and in 2021. A smaller, separate snow avalanche deposit was mapped on the other side of the inactive channel on top of the moraine front. It is interpreted that this has the same source as the deposit on the slope side. This indicates that the snow avalanche(s) depositing these rocks occurred before 2019, and at one point a large snow avalanche deposit covered the channel. Meltwater has eroded the snow avalanche sediments from the channel path during its active time, leaving tall erosion banks. After abandonement, the main active channel has shifted to the middle of Longyearbreen moraine. This has changed some sediment input from snow avalanche deposits to till. In 2021, the favoured input in the Longyearbreen moraine system was till and slump sediment. This illustrates interannual variability in sediment sources.

5.2.3 Rock glaciers as sediment source

The contribution of sediments from rock glaciers to Longyeardalen depends on the movement of rock glaciers and the shifting of active channels. The rock glaciers in front of the Larsbreen moraine system show signs of movement towards the active channel. This suggests that rock glaciers are and may continue to be important secondary sediment sources. Snow avalanches around the Larsbreen moraine system have been shown by Humlum et al. (2003) to supply significant amounts of rock debris and snow/ice to the rock glaciers. The morphology of the Larsbreen rock glacier is curved outwards, due to being pushed in a northward direction by the Larsbreen glacier during the Little Ice Age (Humlum et al., 2007). Thus, the main snow avalanche sources for the rock glaciers are suggested as closer to the glacier position than the current slope source. This is due to the presence of large snow avalanche deposits along the slopes closer to the glaciers, whereas directly adjacent to the rock glaciers the snow avalanche deposits are smaller. The age of rocks on the rock glacier increases from the slope towards the active channel, which is interpreted from the colour and vegetation in the deposits.

The Larsbreen rock glaciers are in contact with the active melting channel (Figure 28). During the summer season some rocks in rock glaciers are released as thawing occurs (Humlum et al., 2007). This is supported by the roundness analysis results, where more angular rocks were observed on the rock glacier side of the Larsbreen melting channel. The transverse cracks that were observed on the rock glaciers indicate movement to the NW towards the active channel. The active channel erodes parts of the rock glacier during the melting season, and the movement of the rock glacier will ensure further addition of sediment to the active channel in future melting seasons. The magnitude of rock glacier sediment input is limited due to the relatively low percentage of this type of deposit in the valley. However, it is thought that rock glacier sediment will continue as a consistent sediment source to Longyearelva due to the position of active channels from Larsbreen confined by the surrounding slopes and moraine.

5.2.4 River erosion as sediment source

River erosion sediment input is thought to increase over the melting season due to thaw releasing sediment in frozen ground. Sediment input by river erosion is difficult to quantify as it is assumed to occur throughout the extent of the melting channels and river until the sea. The process adds sediments from many initial sources, mainly glacial, glaciofluvial, moraine, anthropogenic, and slope processes. One significant observation in Upper Longyeardalen is the extensive amount of inactive glaciofluvial deposits (Figure 28). The shifting course of multiple channels over time changes the sediments that are available for erosion on the river banks. The origin and type of sediment added through river erosion would therefore shift between e.g. solifluction material, anthropogenic fill mass, and rock glacier material.

A significant amount of river erosion was observed in the Larsbreen glaciofluvial fan, both within the glaciofluvial deposits and on the edges of adjacent deposits. Orthophotos from 1990, 2009 and recent years show that the morphology around the braided channels has shifted. For instance, some areas that previously had solifluction material are mapped as glaciofluvial deposits in 2021. River bank erosion is likely an important contributor to this change. This illustrates the significance of river erosion on sediment input to Longyearelva and the morphological development of the river.

Anthropogenic disturbance has also resulted in changes in the flow pattern in the upper part of Longyearelva, upstream of Nybyen. Parts of the river path has been restrained, which promotes flow in fewer braided channels, as seen in the narrow active channel from Longyearbreen. This enhances river bottom and bank erosion as discharge increases when meltwater is more confined (Ashmore et al., 2011).

5.2.5 Relative sediment source contribution

The sediment sources in Longyeardalen are important for the downstream transportation of sediment to the sink (Figure 63). The main sediment sources are glaciers, moraine systems, slumping in moraines, and river erosion. Slumping and river erosion are especially subject to seasonal increase due to active layer thaw. These sources are also considered the most sensitive to warming and rainfall. Aeolian deposition, avalanches, landslides, and rock glaciers likely contribute a smaller total amount of sediment to the system. Slope processes, slumping, and anthropogenic input are considered the most irregular sources of sediment and might result in more events of high sediment transport. Glaciers, moraine systems, avalanches, rock glaciers, and river erosion are responsible for the coarse grained sediment input.

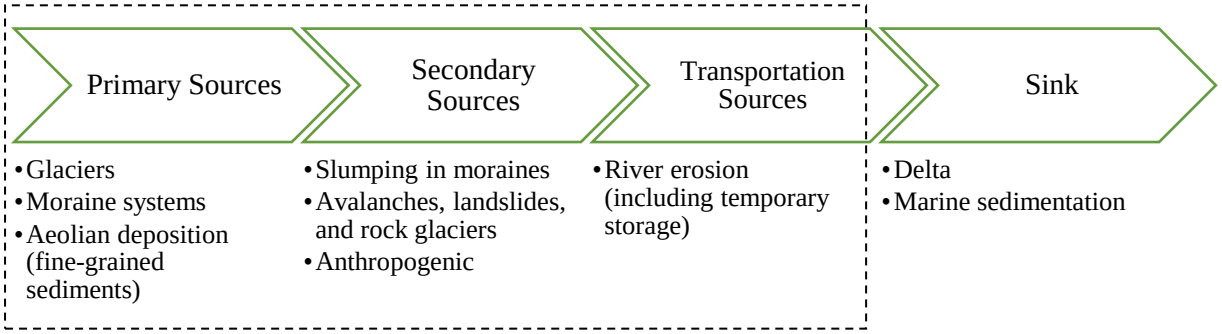

Figure 63 Flow chart of the source-to-sink system in Longyeardalen. Highlights the focus of this study: sources.

5.3 Sediment transport

Sediment transport in Longyearelva was measured as suspended sediment concentration (SSC) and bedload transport of passive tracers. Discharge was also monitored as an important factor for sediment transport with runoff from glacial meltwater, snowmelt, rainfall, and possibly groundwater.

Three modes were defined for the monitoring period in 2021 based on trends in hourly discharge (Figure 64). This was done in collaboration with Ottem (2022), twin study. The intention of dividing the seasonal data into modes was to highlight patterns and seasonal changes. The conditions of the modes are thought to be related to the seasonal glacial meltwater input and thawing of the active layer releasing sediment for erosion. The modes are defined with the following characteristics:

- Mode 1 (22/06-04/07): Low discharge with minimal daily fluctuations, one peak <2.5m^3/s
- Mode 2 (04/07-31/07): Low to very high discharge in weekly cycles with an overall linear decrease from start to end. Two peaks of discharge >3m^3/s. High and irregular diurnal fluctuations.
- Mode 3 (31/07-25/08): Low discharge with a nearly flat trend. High and somewhat regular diurnal fluctuations that decrease towards the end. One significant peak with a short rising limb and long falling limb.

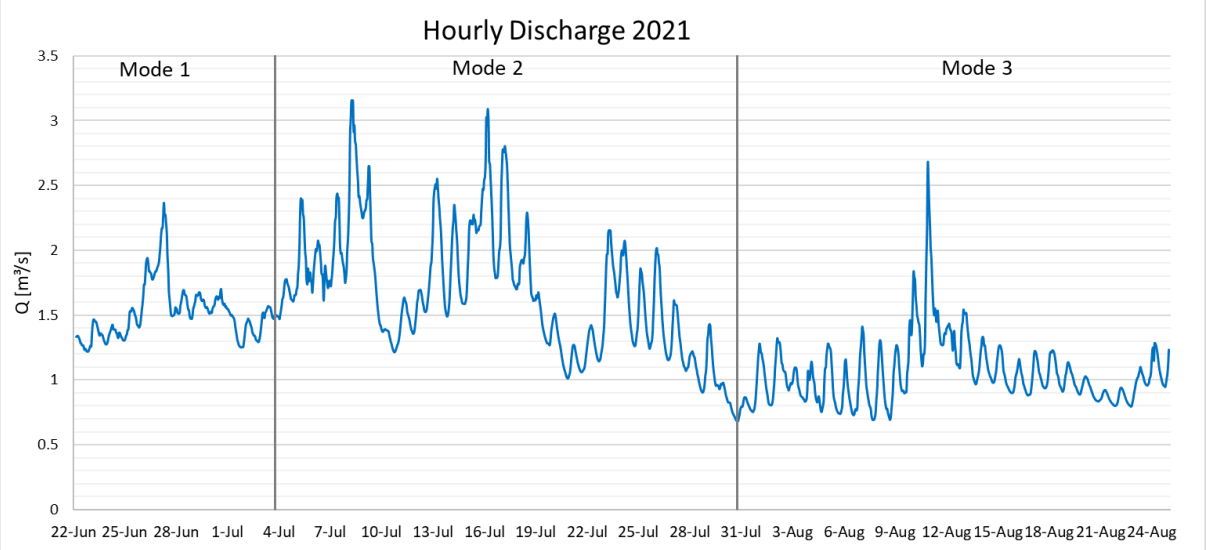

Figure 64 Hourly discharge in Longyearelva from 22nd June to 25th August 2021. Three modes were defined based on trends/patterns in the data. Mode 1 has low discharge with a small peak and little diurnal fluctuations. Mode 2 has three peaks with different lengths of falling/rising limbs and high, with irregular diurnal fluctuations. Mode 3 has the lowest median discharge, high diurnal fluctuations decreasing towards the end, one significant peak, and an overall flat trend.

5.3.1 Discharge and transport of suspended sediments

SSC can be studied in relation to changes in discharge and weather over the melting season (Figure 65 & Figure 66). Discharge was the main control on sediment concentration in the beginning and middle of the melting season (modes 1 & 2). SSC does not seem to be controlled by precipitation in mode 1 & 2 (Figure 66). This is supported by a significantly low SSC that was observed immediately after the largest rain event in mid-July.

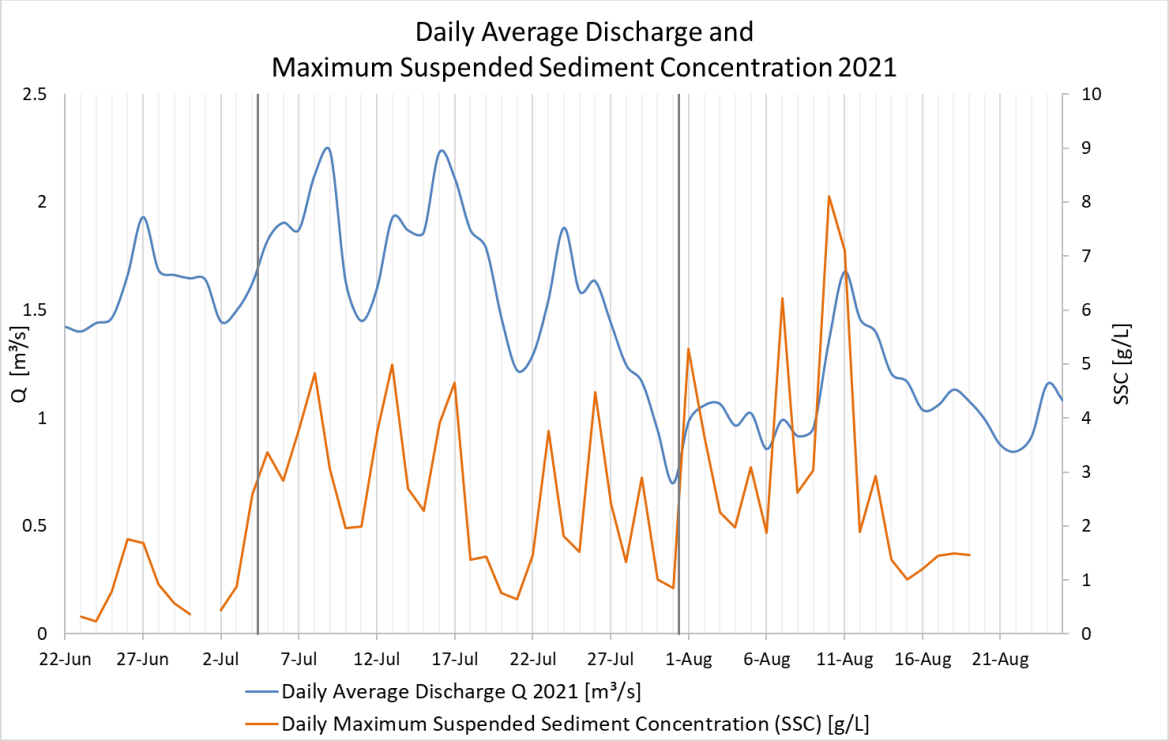

Figure 65 Maximum Suspended Sediment Concentration (SSC) [g/L] and daily average discharge [m^3/s] in 2021 through modes 1, 2 & 3. SSC has mostly good correlation with discharge in modes 1 and 2. The highest SSC coincided with the mode 3 small peak in discharge.

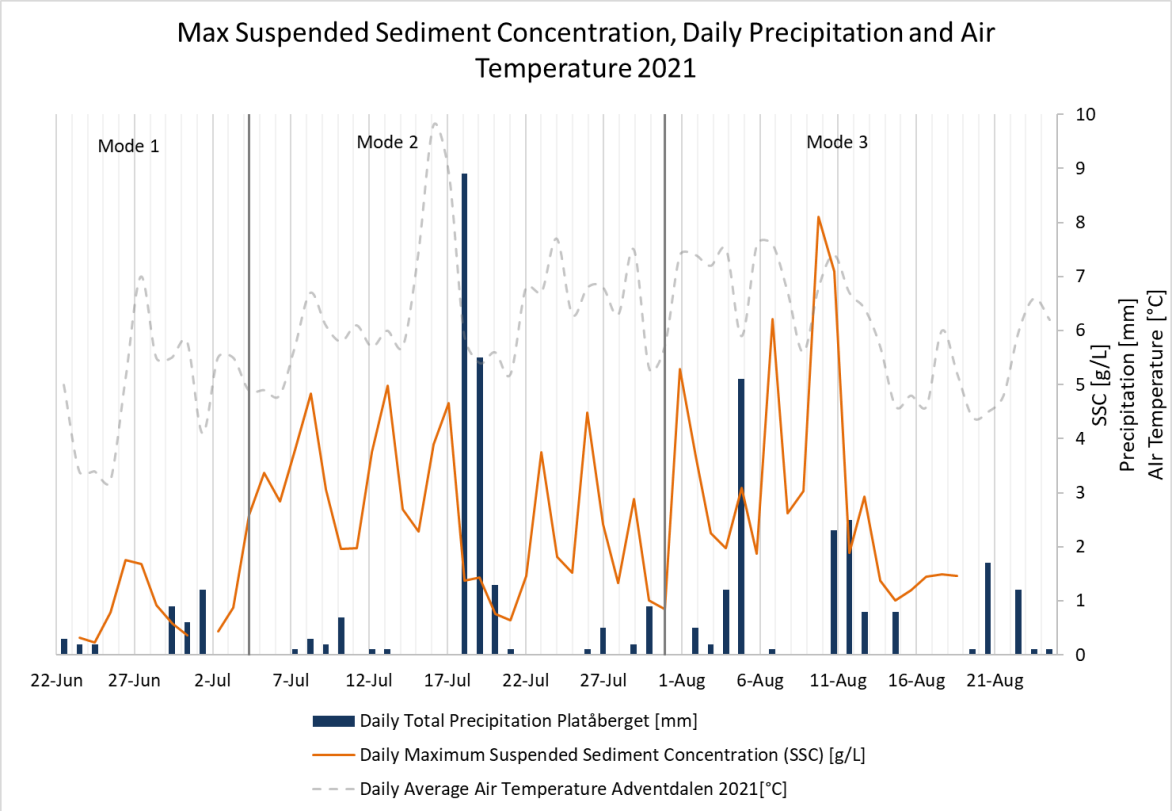

Figure 66 Maximum Suspended Sediment Concentration (SSC) [g/L], Daily Total Precipitation at Platåberget [mm], and Daily Average Air Temperature in Adventdalen [°C]. High precipitation does not have a clear correlation with high SSC throughout the melting season. Some increase in SSC occurred after rainfall in early August. Air temperature has some correlation with SSC in modes 1 & 2, but not in mode 3.

In Mode 3, the late-season, a large increase in SSC coincided with a small peak in discharge (Figure 65). This suggests that discharge is a contributing factor but may not be the main control on sediment transport in the late season. Air temperature was stable during this increased SSC, and precipitation in late-season was on average higher than earlier in the season (Figure 66). The excursion in SSC is suspected to be due to seasonal active layer thaw which makes more sediment available towards the late-season, regardless of daily temperature fluctuations. Air temperature correlation with SSC is found somewhat in modes 1 & 2, which is likely related to glacier melting and/or active layer thaw. Secondary influences on sediment transport may be more important later in the melting season, including slump events in the moraine systems.

There have been previous observations of peaks in SSC preceding peaks in discharge in Arctic catchments. This has been seen to decrease over the melting season (Gurnell et al., 1994). SSC peaks preceding discharge occurred multiple times in Longyearelva in 2021, including 7th July, 23rd July, and 10th August (Figure 65). This indicates that as discharge is rising, available sediment in the river bottom and banks is immediately eroded and transported. There is no discernible pattern of decreasing preceding of SSC peaks over the season. In glacial catchments it is also common that sediment transport occurs in larger, discontinuous events (French, 2007; Overeem & Syvitski, 2008). This is supported by irregular, large increases in SSC over modes 2 & 3, particularly in the late-season.

The possibility of correlation in discharge and SSC was further investigated. Daily average discharge was plotted against daily maximum SSC over the full period and the three modes (Figure 67). This approach also aimed to test the choice of modes. The maximum SSC was used rather than the average as not all days had night samples, thus the results may have been skewed. There was no discernible correlation in discharge over the full period of June to August. This supports the application of modes and the idea of changing sediment source and transport control over the season. There is some correlation in discharge and SSC in modes 1 and 2. This supports the choice of modes and suggests that discharge has some control on SSC in these periods. Mode 3 has low correlation, supporting the interpretation that discharge has some influence but is not a main control on SSC in the late season.

Outliers are most apparent in modes 1 and 3 (Figure 67B&D). In mode 1 this is associated with the latest date in the mode, suggesting that this represents a transition from mode 1 to 2 (Figure 68). This shows how sediment concentration can suddenly increase with a slight increase in discharge as sediment becomes available for erosion through thawing. Multiple high SSC outliers were observed in mode 3. These are associated with days of very high diurnal variation. It could be argued that one additional mode could be added from around 14th August due to the decrease in diurnal variability, low discharge, and SSC towards the end of the monitoring period.

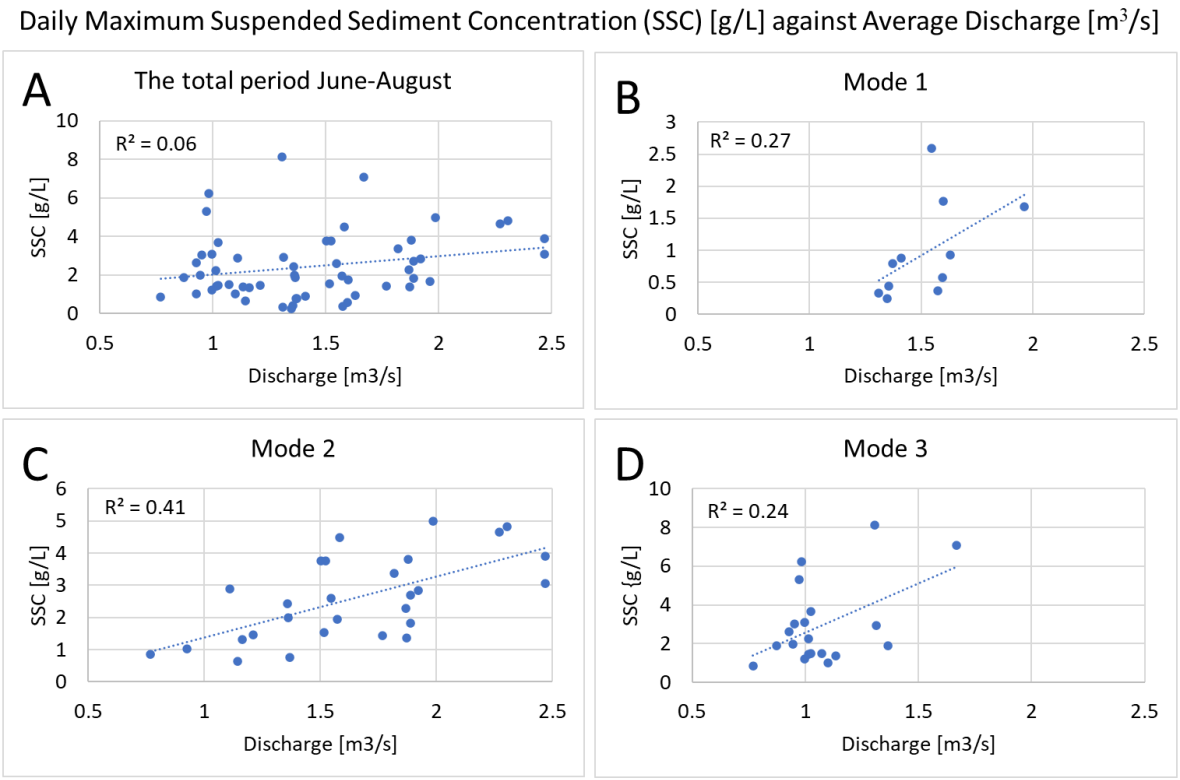

Figure 67 Daily Maximum Suspended Sediment Concentration (SSC) [g/L] against Average Discharge [m^3/s] during different periods. A) the total period June-August; no correlation, B) Mode 1; correlation with outliers related to end of mode, C) Mode 2; correlation, and D) Mode 3; a little correlation with outliers related to peak event.

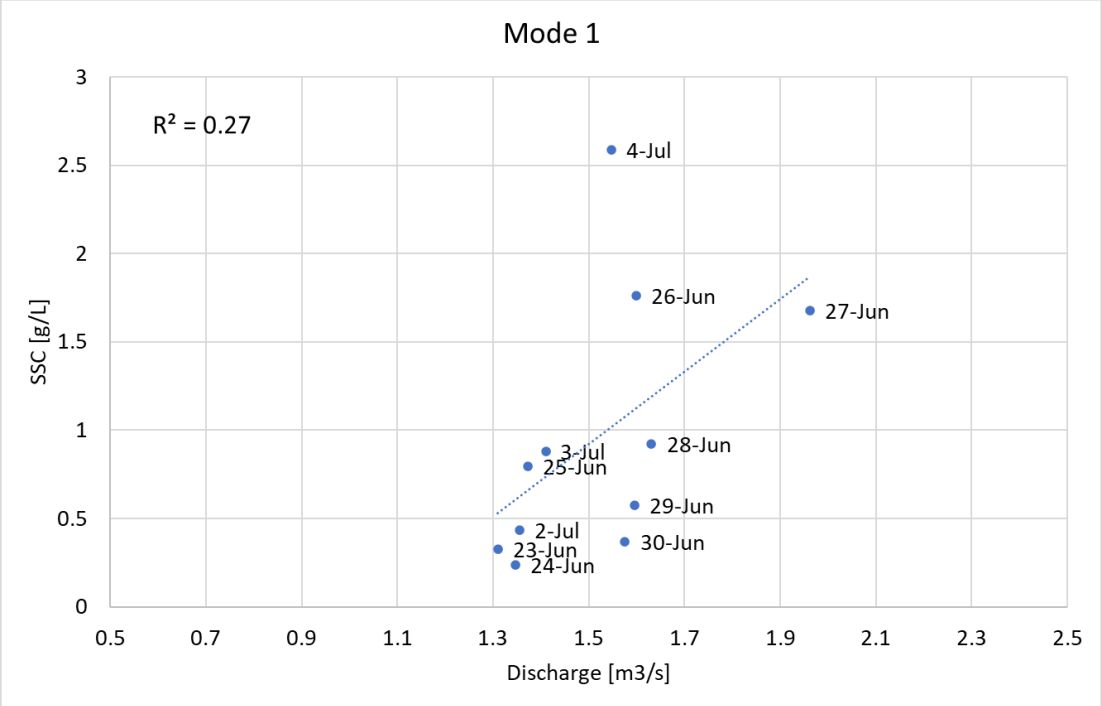

Figure 68 Daily Maximum Suspended Sediment Concentration (SSC) [g/L] against Average Discharge [m^3/s] during mode 1 from 23rd June to 4th July 2021. The most significant outlier was on 4th July with maximum SSC >2.5g/L and average discharge <1.7m^3/s. The relationship between discharge and SSC started to change towards the end of mode 1.

5.3.2 Transport of bedload sediments

Transport of coarse grains up to small boulders was observed in Longyearelva in 2021. Rocks of size >300mm in diameter were transported 10s of meters. This indicates a high potential for river bottom and bank erosion. This is supported by field observations of tall river banks and the steep river-formed valley through Larsbreen moraine. High bedload transport is expected to increase roundness with transportation distance, which is supported by the roundness analysis. Transportation of boulders is considered a normal occurrence in Longyearelva. This is explained through comparison of weather and sediment transport in 2021 and previous years, where 2020 is an example of a more extreme summer season (Løvaas, 2021). The summer 2021 can be considered a base-line year due to the relatively low air temperatures, and no extreme discharge or sediment transport events. As such, the bedload transport in 2021 is thought to represent a minimum for recent and coming years in Longyearelva.

The anthropogenic confinement of Longyearelva may promote further bedload transport due to typical increase in discharge with a decrease in number of channels. The transportation of rocks >300mm was observed in a part of the river with at least two braided streams (Hu-PT). Thus, even larger rocks are thought to be transported in the single channel parts.

5.3.3 Sediment source inferred from high sediment transport events

Events of high sediment transport are expected to be related to specific sediment source inputs. The Late-July Flooding in 2020 is an example of a very high air temperature event. A temperature record of 21.7°C was followed by very high discharge and suspended sediment concentration of up to 24.1g/L (Løvaas, 2021). The main source of sediment that resulted in this sediment transport event has not been determined. However, the high temperature promoted thawing of ground ice which would have made more sediment available for erosion, gravitational movement, and transportation. One theory is that this event caused melting in the ice/till boundary in the moraine systems, triggered slumping of sediment into active channels, and further increasing river bank erosion during this event. This would decrease the stability of the moraines and river banks, which could continue to release sediment during a time period after the event.

If a similar flooding event had occurred in June or early July, a lower sediment concentration would be expected due to sediment locked in frozen ground. This suggests that sediment sources and transport would have different responses to weather events over the season. The long-term consequences of this event may be an increase of sediment transport over following seasons. This is argued based on to the formation of tall erosion banks, retrogressive development of slumps exposing ice-core, and the seeming acceleration of moraine degradation over recent years.

5.4 Sediment sources and transportation over time

This study aims to understand how sediment input and transport in Longyearelva changes on a daily, seasonal, and long-term scale. This is key to understanding the consequences of a warming Arctic on the source-to-sink system.

5.4.1 Daily fluctuations

Daily cycles of increasing and decreasing discharge and suspended sediment concentration (SSC) were recorded in Longyearelva over the melting season in 2021. Daily fluctuations were small in the early season, large and inconsistent in the mid-season, and large in the late season. The most common occurrence was that discharge and SSC was low in the morning and increased in the afternoon and evening. This cycle follows the increase and decrease in air temperature. Increasing temperature in the day promotes thawing of the ground and melting of glacier ice. A larger meltwater input is therefore concurrent with the release and exposure of sediments for erosion. This supports the importance of the glaciers as a primary sediment source (Hanssen-Bauer et al., 2019).

The observed daily fluctuations in SSC in Longyearelva are typical of Arctic rivers (Bennett & Glasser, 2011; Hodgkins et al., 2003). It was expected that this trend would be most clear in the mid-late season coinciding with peak glacier melting. The daily fluctuations were the largest during this period, confirming this idea. However, the sediment transport peak occurred earlier in the afternoon compared to in the evening in the early- and mid-season (Figure 69). This indicates that seasonal peak melting may already have passed by the end of July. As such, other runoff contributors such as precipitation may be more important in the late season. Some increase in SSC was observed following rainfall in the beginning of August 2021 (Figure 66). A future increase in rainfall frequency and intensity has been predicted (Hanssen-Bauer et al., 2019). This has the potential to increase sediment transport in the late melting season in the coming years.

The earlier daily peaks in SSC in the late season could be because sediment is more easily eroded due to active layer thaw. This supports the idea that ground thaw is an important control on sediment input and transportation in Longyeardalen.

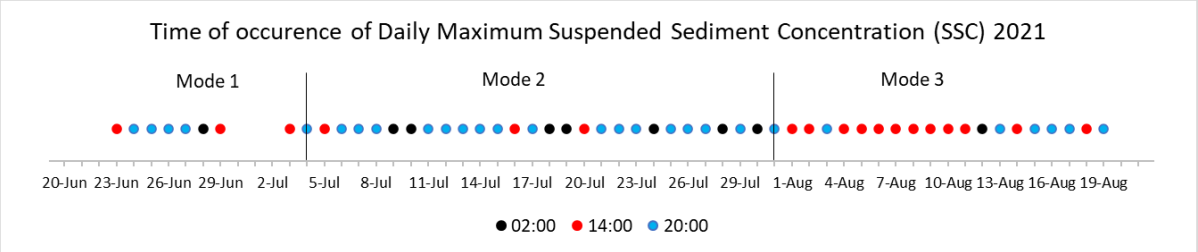

Figure 69 The time of occurrence of daily maximum suspended sediment concentration (SSC) in Longyearelva 2021. Times of occurrence are night (02:00), afternoon (14:00), and evening (20:00). Evening maximum was most common in modes 1 & 2, and afternoon maximum was most common in mode 3. Extracted segment from Figure 56.

5.4.2 Variation over the season

Sediment transport in Longyearelva varies with discharge over the melting season. Variation over the season involves the change in controls of sediment input and transportation in the river. Seasonal variability is influenced by the frozen ground typical of Arctic environments.

More sediments become available for erosion over the season as the active layer thaws. This follows the expectation that SSC will increase over the summer up to a certain point. In 2021, SSC was measured lowest in the early season despite a similar or higher discharge compared to later parts of the season with higher SSC. These observations fit with the expectation of seasonal ground thaw and sediment availability.

The distribution of fine and coarse sediment may change over the season. When a large amount of sediment is frozen in the ground in the early season, it is expected that mostly fine sediment would be transported during that time. Assuming that more coarse sediment becomes available with increasing discharge, more coarse sediment would be transported in the mid-late-season. Coarse sediment transportation promotes erosion as rocks interact with the river bottom or sides. This creates positive feedback of increased erosion with higher discharge and thawing ground. Erosion also exposes rocks below to the surface and within river banks, promoting further thaw. This positive feedback provides conditions for an acceleration in sediment erosion and transport from the start of thawing to the late-season.

The correlation in discharge and sediment concentration seen in June and July (Figure 65) fits with the assumption of a glacier-melt controlled river discharge and sediment input. A concurrent increase in discharge and sediment concentration could be a result of:

- Increased primary input of sediment from the glacier due to melting
- Increased river bank/bed erosion due to higher discharge able to transport more and coarser sediment, assuming sufficient availability in thawing ground

In August, the correlation between discharge and SSC was lowest. Some days of high precipitation were observed on days with high SSC (Figure 66). High SSC at this time may be a result of other sediment source inputs compared to earlier in the season. This relies on a thawed active layer throughout the melting season, which may cause:

- Increased secondary input from slumps in moraines related to high temperature over the summer or a high precipitation event increasing pore pressure
- Increased river erosion despite consistent discharge due to low stability in river banks

The real impact and magnitude of the shift in sediment control relies on active layer thaw. Hence, a future increase in active layer thickness or an earlier yearly start to thaw with a longer melting season would have consequences for sediment transport. This could increase the total yearly sediment load and shift the seasonal variation of sediment transportation in Longyearelva.

The relative importance of different sources of sediments is expected to vary over the melting season. River erosion and the frequency and intensity of slumps in the moraine systems is thought to increase over the season. However, other sediment sources may show a reversed trend. For example, snow avalanche sediments may be added to active channels early in the season during snowmelt. Yearly new avalanche deposits are not frozen in the ground, and therefore immediately available following snowmelt. Aeolian sediment is another example, where this fine-grained material is available early in the melting season following transportation and deposition over the winter. Transportation of fine sediments requires low discharge. Thus, this may occur in the early-season, possibly depleting the aeolian sediment source over the season.

5.4.3 Variation between the seasons

Interannual variability is important to consider for the interpretation of seasonal and long-term monitoring data. This can aid the understanding of weather event impact on glaciofluvial source-to-sink systems. This could be used alongside climate projections to suggest what can be expected of sediment transportation in Longyeardalen in the future. Variation between seasons includes shifting active channels, which may change the hydrological connectivity of sediment sources each year. Some years may have a larger amount of sediment input from snow avalanches if channels flow close to active slopes. The frequently shifting active channels in Longyeardalen suggest that temporary storage of source material is likely, possibly increasing interannual variation in sediment sources.

Variation between seasons includes irregular years with deviations from average weather conditions. Occasional years with very high temperature and/or rainfall are expected to have consequences such as increased thickening of the active layer and increased erosion (Hanssen-Bauer et al., 2019). The question of the longevity of these effects is to be seen, but it can be assumed that the effects do not simply reset after a year of more stable temperature. It would be expected that extreme temperature or precipitation years could enhance climate effects on land, glaciers, and hydrological systems for several years.

In 2020 a new temperature high record was set in Longyearbyen. This resulted in unusually high discharge and suspended sediment concentration in Longyearelva (Løvaas, 2021). In 2021 the temperature was lower and more stable, giving very different conditions for sediment input and erosion in the river. Thus, the season in 2021 is considered a good baseline of data to address if consistent increase in air temperature is needed for increased sediment load or if the rare "extreme" year will have significant long-term effects.

Suspended Sediment Load (SSL) is an important indication of the total suspended sediment transport in the system. Significant variability between years has been recorded. This seems to be related to different temperature and discharge. Daily Average Discharge and SSL from 2021 is compared to 2020 (Figure 70 & Figure 71). The melting season in 2020 was a lot more intense and variable than in 2021. A five times increase of SSL was reached during the Late-July Flooding in 2020 (Løvaas, 2021). The aim of comparison is to consider possible yearly trends in discharge and sediment load in relation to sediment sources. Common characteristics in discharge and SSL for each mode during both years are described:

- Mode 1: Similar discharge except for some days of very low discharge in 2020 (Figure 70). SSL <1000tonne for both years (Figure 71). Low SSL is likely related to limited available sediment as the ground is (mostly) frozen at this time of year.
- Mode 2: Similar discharge ~2m^3/s for both years, except for the Late-July Flooding in 2020 (Figure 70). SSL increases and decreases in phases through the mode in 2020 and 2021 (Figure 71). The exact timing is different for the years, but similar values were found for both discharge and SSL in the two consecutive years.
- Mode 3: In both years a decrease in overall discharge was observed, with one main peak during mid-August (Figure 70). In 2021 the SSL was higher during this peak than during equivalent discharge measurements earlier in the season (Figure 71). In 2020 the late season peak in discharge was higher than typical peaks earlier in the season, but SSL was lower or equal to peaks earlier in the season.

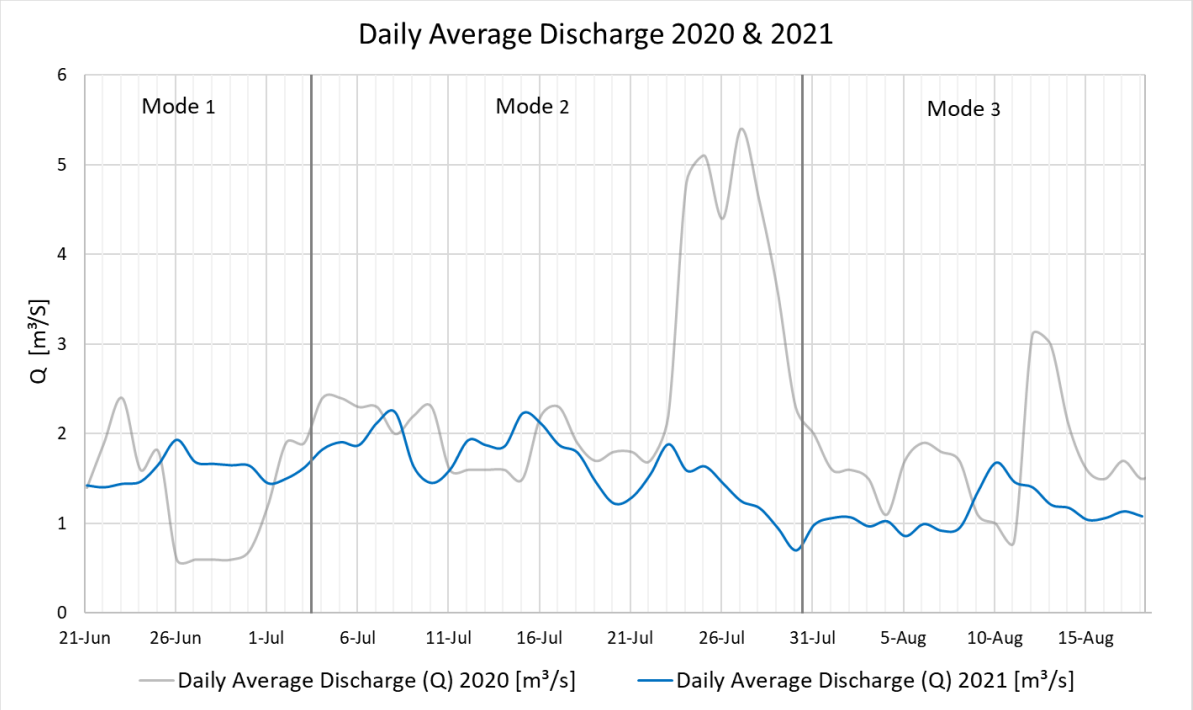

Figure 70 Daily Average Discharge [m^3/s] in 2020 & 2021, divided into modes 1-3. Mode 1: higher starting discharge in 2020, but a large dip, and in 2021 a lower starting discharge with a slight increase. Mode 2: similar discharge except for the flooding event in 2020 with peaks >5m^3/s. Mode 3: Overall lowered discharge with some peaks at different times for the two years.

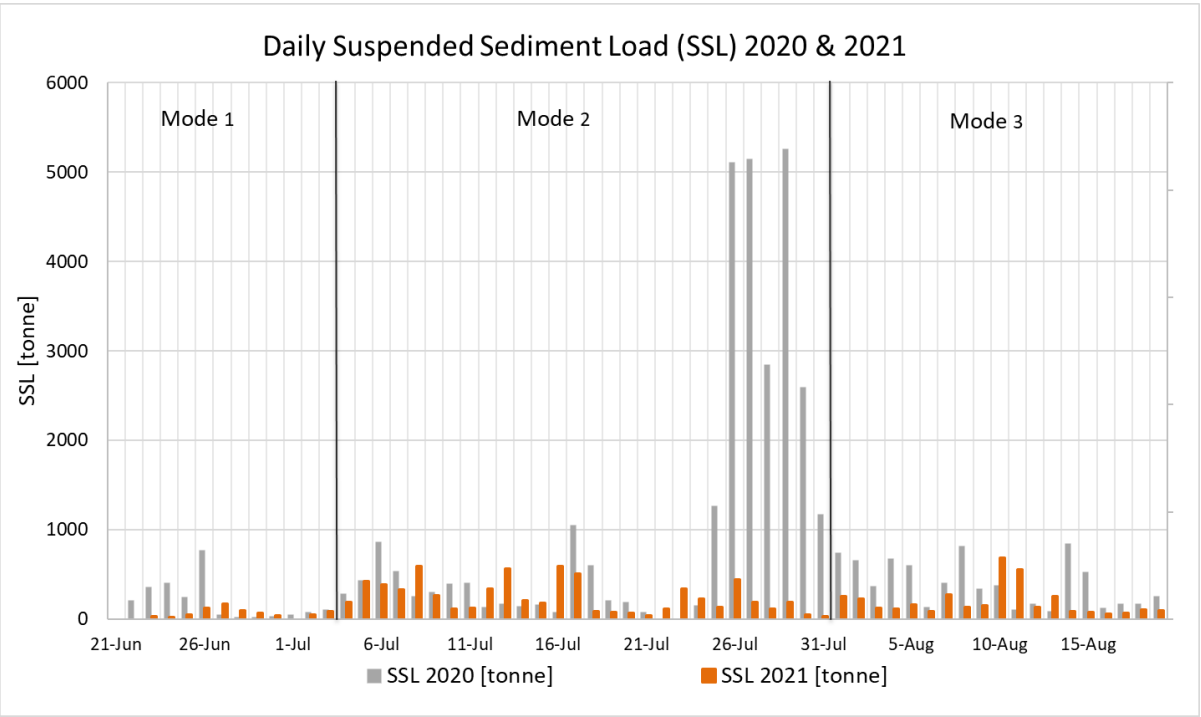

Figure 71 Daily Suspended Sediment Load (SSL) [tonne] in 2020 and 2021 divided into modes 1-3. Mode 1: higher SSL in 2020, very low in 2021. Mode 2: Similar SSL in three phases for both years, except for the extreme SSL increase >5000tonne during the Late-July Flooding in 2020. Mode 3: Mostly higher SSL in 2020 than in 2021 following flood event with a decrease in both years from the middle of August.

The observations from mode 3 in 2020 and 2021 show that the relationship between discharge and suspended sediment concentration (SSC) during the late-season was very different between the two years. This supports the interpretation that discharge is not the main control on sediment transportation in Longyearelva during the late-season. It is important to note that the flooding in 2020 seems to have caused an increase in sediment transportation also in the late-season after the event. The two significantly different consecutive years give an indication of how air temperature has an influence on glacial melt and discharge, which controls sediment transport particularly in the middle of the season.

5.4.4 Long-term development of sediment sources and transport

The morphology and deposits in Upper Longyeardalen are mixed and complex. This has resulted in a variability of sediment sources input to Longyearelva. Seasonal and long-term changes have occurred in the glaciers, moraine systems, and glaciofluvial system over the past ten years. This includes glacier retreat, degradation in moraines, and shifting of active channels. The past and current development can be used to suggest possible future changes in the source-to-sink system in a warming Arctic.

Degradation of the moraine systems has accelerated over the past years and this is expected to continue. This will impact the total contribution of sediment from the moraine systems, and the relative contribution between the two systems. The total volume of material that has been removed through slumping before 2021 was 1.7 $x10^6$ m^3 in the Larsbreen moraine system and 1.1 $x10^6$ m^3 in the Longyearbreen moraine system. This compares to a volume of <0.5 $x10^6$ m^3 in each moraine system in 2009. The increase in slump activity was most prominent from 2009-2019 in Larsbreen moraine system, and 2019-2021 in Longyearbreen moraine system. This indicates that the acceleration of slumping has occurred at different times and speeds in the two systems. This shows that the relative contribution of sediment from the two moraines may be shifting over time. A greater volume of sediment has the potential to be transported from the Larsbreen moraine system. This system has a larger area of degraded moraine material with hydrological connectivity. Downstream of the moraine systems, the sediment input from river erosion is expected to be larger on the Larsbreen side. This is due to the large glaciofluvial fan with frequently shifting channels and tall erosion banks. As such, it is thought that the long-term development of primary and secondary moraine and river erosion sediment sources will continue to be greatest from Larsbreen.

It is possible that the Longyearbreen moraine system will develop into a more prominent temporary storage system. Some glaciofluvial deposition was found in the glacial forefield. This has a lower topography than the original moraine morphology, suggesting some vertical glaciofluvial erosion of till. The moraine system may change in different ways through the continued deposition of glacial sediment combined with vertical glaciofluvial erosion and collapse. One possibility is the continued deposition of glacial sediment and the formation of a glacial lake. Another possibility is the formation of a v-valley through the moraine system similarly (but on a slightly smaller scale) to the Larsbreen moraine system. This could increase the input of sediment to Longyearelva from the Longyearbreen moraine system in the future. Increased vertical erosion through till would promote a larger relative sediment input from moraine sources compared to e.g. glacial or snow avalanche sources.

An important question remains whether the total sediment transportation in Longyearelva is expected to increase or decrease in the future. The glaciers in Longyeardalen are central to

runoff and sediment input. The glaciers are both small and retreating. Several small glaciers on Svalbard show signs of decreasing runoff contribution, i.e. they have passed “peak water” (Nowak et al., 2020). If this is the case for the Longyearbreen and Larsbreen glaciers, it can be expected that an eventual decrease in glacial meltwater runoff would decrease sediment load in the long-term (Overeem & Syvitski, 2008). A decrease in the transportation of coarse grains and larger rocks could further decrease river erosion.

On the other hand, warming of the Arctic may also result in a long-term increase in sediment transport (Orwin et al., 2010). In Longyeardalen, this theory is supported by projected increases in average annual temperatures, increased rainfall, increased active layer thickness, and observations of accelerating retrogressive development of thaw-slumps. The contribution of secondary and transportation sediment sources in Longyeardalen was most important in the late-season 2021 despite lower discharge. This suggests that sediment transport would increase at least for the short-term, and for longer than would be initially expected solely based on glacier melting and retreat.

Increased rainfall frequency and intensity could shift the runoff contribution towards a less glacier controlled catchment in the future. This could change the daily and seasonal pattern in discharge and suspended sediment transportation. Pattern changes relies on the temporal distribution of rainfall, which could occur as daily trends, e.g. evening rain, or as events of intense rain. Evening rainfall may lead to high amplitude daily fluctuations in sediment transport. Irregular rainfall events could result in more uneven seasonal sediment transportation. Event-based sediment transport is thought to be further encouraged by the degradation of moraine systems. Slumps and collapses in the moraine systems could increase the magnitude of high sediment transport events. Infiltration of rainfall may increase the ice content in permafrost, temporarily stabilizing ground but increasing the potential magnitude of slope failures (Hanssen-Bauer et al., 2019). It is therefore expected that warming in the Arctic will result in more high, irregular peaks in sediment transport. A consequence of this could be higher river erosion around the Longyearbyen settlement.

Rainfall events or very high temperatures in the late-season is expected to have a larger consequence compared to an equal event in the early season. This is due to increased instability in the ground in the late-season. The thickness of thawed ground is greater, which could cause deeper and larger slumps. This is supported by the very high sediment transportation associated with the Late-July Flooding in 2020.

In the long-term, longer melting seasons may shift sediment transport peaks to earlier in the season. This could be expected to result in seasonal depletion in sediment sources towards the late-season, similar to in Alpine catchments (Gurnell et al., 1994). However, with the continued presence of permafrost and seasonal thaw, it seems unlikely that the sources would be completely depleted before the eventual freeze-up. Thus, the total sediment load is expected to initially increase with increased temperature and longer melting seasons. Years with seasonal sediment transport patterns similar to 2020 may occur again in the future, but such extreme years are not assumed to be necessary for increased sediment transportation. This is supported by high late-season sediment transportation in 2021 and the acceleration of slumping in the moraine systems over the past 10 years that could lead to more event-based peaks in sediment transport.

5.5 Uncertainty

Uncertainties in the study arise from challenges in the Arctic of limited previous knowledge, short data series, and accessibility of field sites. Efforts have been made through the study to apply a range of methods to adapt to these challenges. This includes mid- and late-season drone mapping, repeated photography, sediment sampling multiple times each day, and extensive data search. The application of multiple methods and approaches has resulted in a range of possible sources of information, which may improve reliability.

Ambiguity is an important factor of uncertainty. There are multiple primary and secondary sediment sources in Longyeardalen that may cause changes in sediment transportation. Transportation of suspended and bedload sediments in Longyearelva depends on; air temperature, precipitation, glacial meltwater, groundwater, permafrost thaw, glaciofluvial erosion, and anthropogenic influence. This results in ambiguity in the cause of change in discharge and sediment concentration on a daily, seasonal, and long-term basis.

Some specific aspects of uncertainty in the results are listed:

- Discharge measurements were done in a single channel. However, the exact flow path may have changed somewhat over the season due to river bottom/bank erosion. No significant shift was observed; thus the data is considered reliable. Yet, this may have resulted in a small systematic uncertainty in the discharge data.
- Due to limited knowledge, the flow of groundwater was not considered when drawing the borders of the catchment. The presence of permafrost influences groundwater flow differently and less predictably compared to non-permafrost catchments. The potential runoff contribution from groundwater is therefore uncertain.
- The distance from the Upper Longyeardalen sources and the suspended sediment concentration (SSC) measurement station is >3km. River erosion and temporary deposition occurs along this stretch. The significance of temporary deposition is uncertain and may delay the recording of sediment transport. Anthropogenic reworking of sediment also occurred in this stretch, increasing sediment transport. Slumping in the moraine systems may be recorded as a delayed increase in SSC at the measurement station.
- The areal coverage of drone mapping of Larsbreen moraine system from 2021 does not reach the glacier and the slopes along the moraines. This was due to accessibility and drone limitations. Some estimations of area of slumping were therefore inferred based on the 2019 orthophoto. This may lead to an underestimation of areas of slumping.
- Orthorectification of the upper drone models was challenging due to a limited number of fixed reference points. This leads to up to a few meters of uncertainty in the exact position of deposit borders and geomorphological elements in the moraine systems.
- Orthophotos from 2009 had a lower resolution, and partial cover from shadows. Thus, it was sometimes difficult to tell the exact extent of slump scars. This could mean a higher uncertainty in estimations of old areas.

5.6 Recommendations for future work

The continued monitoring of Longyeardalen and investigations of sediment sources has provided further ideas of the development of sediment transport over time. Continuation of monitoring alongside further investigations is recommended for the coming years. It would be important to monitor discharge to see whether peak water has passed, and whether the daily and seasonal pattern will change. It might be useful to measure sediment transport in the upper parts of the valley as well as the lower part. This might aid the understanding of sediment input during transportation from river erosion, and temporary deposition. It would be beneficial to monitor bedload transport in future years. The recovered passive tracers from 2021 were stored at UNIS for potential future use.

It is recommended to further investigate the active layer in Longyeardalen. This could include drone mapping of the moraine systems in future years. Overlaying digital elevation models (DEMs) from multiple years could be used to measure scarp height in more detail and indicate potential changes in active layer thickness in detachments and retrogressive slumping. Active layer thickness could also be investigated at different locations from the source to sink, with probe measurements of depth to permafrost. This could be used to test if the depth decreases with distance from the sea towards the glaciers. As recommended by (Nowak et al., 2020), boreholes and water flux measurements in the active layer could be used as an addition to long-term hydrological monitoring.

6 Conclusions

This master thesis has aimed to understand how seasonal thaw and long-term climate change is impacting the sediment sources in Longyeardalen. The study was completed as part of the long-term monitoring project "Hydrology, Sediment transport and erosion in Longyeardalen" (RiS ID 11641) alongside a twin study focusing on the Longyearelva river-to-ocean system (Ottem, 2022).

Sediment sources and transport in the Longyeardalen source-to-sink system have been defined and monitored in detail over the melting season 2021. This was done through a range of field and data methods. Quaternary and geomorphological mapping was completed using drone photography and field observations. Sediment movement was quantified in moraine systems, and particle roundness was analysed in the valley. Monitoring was done of hourly discharge, four times daily suspended sediment concentration, and bedload transport.

Key results from the study:

- Quaternary Map of Upper Longyeardalen with geomorphological elements (Figure 28, Appendix A)
- Mean Discharge from 22/06/21 - 25/08/21 was 1.3 ± 0.1 m^3/s
- Maximum Discharge on 08/07/21 of 3.2 ± 0.3 m^3/s
- Maximum Suspended Sediment Concentration (SSC) on 10/08/21 of 8.1 ± 0.8 g/L
- The competence of Longyearelva river is at least 300 - 350 mm in diameter rocks
- The area of Upper Longyeardalen moraines affected by degradational slumping was <1% in 2009 and ~5% in 2021
- The total volume of slumped sediment in the moraines by 2021 was 2.8 ± 0.6 $x10^6$ m^3
- The total volume of material that has slumped in the moraines in the past two years (2019-2021) was 0.9 ± 0.2 $x10^6$ m^3
- The backscarp height of slump scars in 2021 was up to at least 170cm and 158cm tall in the Longyearbreen and Larsbreen moraine systems, respectively
- Erosion scarps in the glaciofluvial fan in Upper Longyeardalen were up to at least 2.2m tall
- The roundness of particles increases with transportation distance in Longyearelva

The results from this study have been used to discuss whether warming-related degradation of moraines, slopes and river banks will be significant sediment sources with different seasonal patterns of sediment released compared to glacier melting. Findings that support this hypothesis are; 1) high and irregular late-season sediment transport, 2) low correlation between discharge and suspended sediment transport in the late-season, 3) acceleration of slump-activity in the moraine systems over the past 10 years, and 4) frequently shifting active channels that have formed tall erosion banks. It is concluded that degradation is an important sediment source in Longyeardalen with continued warming in the Arctic. The relative importance of the secondary sediment sources compared to glacier melting is difficult to discern due to ambiguity. It is likely that glacier and direct moraine sediment still constitute a significant portion of sediment transported in Longyeardalen. It is suggested that the most consequential result of secondary sediment input is changes in seasonal patterns of sediment transport, i.e. a higher portion of total transport in the late-season and more event-based sediment transport.

To further address the stated hypothesis, and define and quantify the sediment sources in Longeyardalen over time, the following questions were discussed:

What are the important sediment sources in the Longyeardalen source-to-sink system?

The most important sediment sources in Longyeardalen are glaciers, moraine systems, slumping and other thaw-driven gravitational movement in the moraines, and river erosion. Aeolian deposition, rock glaciers, and slope processes seem to contribute a smaller amount of sediment to the system. These sources are subject to interannual variability due to hydrological connectivity. Snow avalanche and aeolian sediment may be more important in the early season as this sediment may not be locked in frozen ground. Slumping, and anthropogenic disturbance are suggested as the most irregular, event-based sediment sources.

How does sediment input and transport in Longyearelva change on a daily, seasonal, and long-term scale?

Sediment transport fluctuates daily due to temperature-controlled glacial melt and active layer thaw, with peaks mostly in the afternoons and evenings. The most irregular daily fluctuations occurred in July. The daily SSC peak occurred earlier in the day in August, suggesting increased sediment availability due to deeper extent of thaw and increased river erosion. Over the melting season, sediment transport occurred in weekly cycles with an overall increase from July to August. This is interpreted to be due to variable air temperature, seasonal increase in sediment availability through active layer thaw, and positive feedback of increased river erosion. The long-term development of sediment transport in Longyeardalen could include; 1) longer melting seasons shifting the peak to earlier in the season, 2) a shift of sediment sources to more secondary sources, 3) more event-based sediment transport with higher peaks, and 4) increased control of rainfall on discharge and sediment transport.

How does warming and active layer thaw influence sediment sources and transport in Longyeardalen?

Warming may increase instability of the ground, increase glacier meltwater in channels, and therefore result in higher sediment transport from secondary and transportation sources. Increased rainfall is expected following warming, which may lead to more event-based sediment transport in Longyeardalen. The depth extent of active layer thaw is important for how much sediment is available for transport. Slumps and river erosion were especially subject to seasonal increase due to active layer thaw. These secondary sources are also considered most sensitive to warming and increased rainfall intensity and frequency.

How much slumping has occurred in the Larsbreen and Longyearbreen moraine systems in recent years? Is this an important sediment source?

The total volume of sediment that has been removed by slumping in the moraines is at least 2.8×10^6 m^3. Most slump scars were mapped along or on slopes above active channels, indicating that a lot of sediment moved by slumping may be transported downstream. The average yearly volume of slumped material has doubled from 2009 to the past three years. The acceleration of slumping in the past years suggest retrogressive development. It is expected that degradation of the moraines will continue to accelerate with warming climate. This may increase the importance of slumping as a sediment source.

It is recommended that long-term monitoring is continued in Longyeardalen and supplied by repeated drone modelling. It would be useful to investigate active layer thickness from source-to-sink in the valley and in thaw-slump scars to test if the thickness changes over time due to warming. Further work would continue to build this important dataset of climate influence in Longyeardalen. It is hoped that the efforts of this study, together with the twin study of river-ocean interactions and continued long-term monitoring, may aid the understanding of source-to-sink systems in the Arctic and the potential consequences for the Longyearbyen settlement.

References

AMAP. (2017). Snow, Water, Ice and Permafrost in the Arctic (SWIPA). *Arctic Monitoring and Assessment Program (AMAP)*, xiv + 269.

Ashmore, P., Bertoldi, W., & Tobias Gardner, J. (2011). Active width of gravel-bed braided rivers. *Earth Surface Processes and Landforms*, *36*(11), 1510-1521. https://doi.org/10.1002/esp.2182

Ashworth, P. J., Best, J. L., & Jones, M. (2004). Relationship between sediment supply and avulsion frequency in braided rivers. *Geology*, *32*(1), 21. https://doi.org/10.1130/g19919.1

Awang Ali, A. N., Ariffin, J., Mohd. Razi, M. A., & Jazuri, A. (2017). Environmental Degradation: A Review on the Potential Impact of River Morphology. *MATEC Web of Conferences*, *103*, 04001. https://doi.org/10.1051/matecconf/201710304001

Barchyn, T. E., & Hugenholtz, C. H. (2012). Winter variability of aeolian sediment transport threshold on a cold-climate dune. *Geomorphology*, *177-178*, 38-50. https://doi.org/10.1016/j.geomorph.2012.07.012

Bennett, M. M., & Glasser, N. F. (2011). *Glacial geology: ice sheets and landforms*. John Wiley & Sons.

Bogen, J. (1996). Erosion rates and sediment yields of glaciers. *Annals of Glaciology*, *22*, 48-52. https://doi.org/10.3189/1996aog22-1-48-52

Bogen, J., & Bønsnes, T. E. (2003). Erosion and sediment transport in High Arctic rivers, Svalbard. *Polar Research*, *22*(2), 175-189. https://doi.org/10.3402/polar.v22i2.6454

Brattli, B. (2019). *Ingeniørgeologi løsmasser*. Akademika.

Burki, V., Hansen, L., Fredin, O., Andersen, T. A., Beylich, A. A., Jaboyedoff, M., Larsen, E., & Tønnesen, J.-F. (2010). Little Ice Age advance and retreat sediment budgets for an outlet glacier in western Norway. *Boreas*. https://doi.org/10.1111/j.1502-3885.2009.00133.x

Burn, C. R., & Lewkowicz, A. (1990). Canadian landform examples-17 retrogressive thaw slumps. *Canadian Geographer/Le Géographe canadien*, *34*(3), 273-276.

Burrows, R., & McClung, D. M. (2006). Snow cornice development and failure monitoring. International Snow Science Workshop, Telluride Colorado,

Christiansen, H. H., Gilbert, G. L., Demidov, N., Guglielmin, M., Isaksen, K., Osuch, M., & Boike, J. (2020). Permafrost temperatures and active layer thickness in Svalbard during 2017/2018 (PermaSval). *SESS Report 2019*, 237-249.

Dingman, S. L. (2015). *Physical hydrology*. Waveland press.

Eckerstorfer, M., Christiansen, H. H., Rubensdotter, L., & Vogel, S. (2013). The geomorphological effect of cornice fall avalanches in the Longyeardalen valley, Svalbard. *The Cryosphere*, *7*(5), 1361-1374. https://doi.org/10.5194/tc-7-1361-2013

Etzelmüller, B., & Frauenfelder, R. (2009). Factors Controlling The Distribution of Mountain Permafrost in The Northern Hemisphere and Their Influence on Sediment Transfer. *Arctic, Antarctic, and Alpine Research*, *41*(1), 48-58. https://doi.org/10.1657/1523-0430-41.1.48

Etzelmüller, B., Hagen, J., Vatne, G., Ødegård, R., & Sollid, J. (1996). Glacier debris accumulation and sediment deformation influenced by permafrost: examples from Svalbard. *Annals of Glaciology*, *22*, 53-62.

Etzelmüller, B., Ødegård, R. S., Vatne, G., Mysterud, R. S., Tonning, T., & Sollid, J. L. (2000). Glacier characteristics and sediment transfer system of Longyearbreen and Larsbreen, western Spitsbergen. *Norsk Geografisk Tidsskrift - Norwegian Journal of Geography*, *54*(4), 157-168. https://doi.org/10.1080/002919500448530

Farnsworth, W. R., Allaart, L., Ingólfsson, Ó., Alexanderson, H., Forwick, M., Noormets, R., Retelle, M., & Schomacker, A. (2020). Holocene glacial history of Svalbard: Status, perspectives and challenges. *Earth-Science Reviews*, *208*, 103249. https://doi.org/10.1016/j.earscirev.2020.103249

Førland, E. J., Benestad, R., Hanssen-Bauer, I., Haugen, J. E., & Skaugen, T. E. (2011). Temperature and Precipitation Development at Svalbard 1900–2100. *Advances in Meteorology*, *2011*, 1-14. https://doi.org/10.1155/2011/893790

Førland, E. J., Isaksen, K., Lutz, J., Hanssen-Bauer, I., Schuler, T. V., Dobler, A., Gjelten, H. M., & Vikhamar-Schuler, D. (2020). Measured and Modeled Historical Precipitation Trends for Svalbard. *Journal of Hydrometeorology*, *21*(6), 1279-1296. https://doi.org/10.1175/jhm-d-19-0252.1

French, H. M. (2007). *The Periglacial Environment* (3rd ed.). John Wiley & Sons Ltd.

Gariano, S. L., & Guzzetti, F. (2016). Landslides in a changing climate. *Earth-Science Reviews*, *162*, 227-252. https://doi.org/10.1016/j.earscirev.2016.08.011

Gilbert, G. L., Instanes, A., Sinitsyn, A., & Aalberg, A. (2019). *Characterization of two sites for geotechnical testing in permafrost: Longyearbyen, Svalbard* (Norwegian GeoTest SIte (NGTS), Issue. N. G. Institutt. http://hdl.handle.net/11250/2632119

Grønsten, H. A. (1998). *Hydrological Studies and Simulations Of a High Arctic Catchment Longyearelva, Spitsbergen* [Master Thesis, The University of Oslo/University Centre in Svalbard].

Grove, J. M. (1988). *The Little Ice Age*. Routledge.

Gurnell, A., Hodson, A., Clark, M., Bogen, J., Hagen, J., & Tranter, M. (1994). Water and sediment discharge from glacier basins: an arctic and alpine comparison. *IAHS Publications-Series of Proceedings and Reports-Intern Assoc Hydrological Sciences*, *224*, 325-334.

Hach Company. (2003). *Sigma 900 MAX Portable Sampler: Instrument manual* (Catalog Number 8992).

Hanna, J. (2019). *Upper Longyear Valley 3D Model*. https://sketchfab.com/3d-models/upper-longyear-valley-6de211ba341b48f599a9a03db75d6575

Hanssen-Bauer, I., Førland, E. J., Hisdal, H., Mayer, S., Sandø, A. B., & Sorteberg, A. (2019). Climate in Svalbard 2100 - a knowledge base for climate adaptation. https://doi.org/10.13140/RG.2.2.10183.75687

Hasnain, S. I., Thayyen, R. J. (1999). Discharge and suspended-sediment concentration of meltwaters, draining from the Dokriani glacier, Garhwal Himalaya, India. *Journal of Hydrology*, *218*, 191-198. https://doi.org/10.1016/S0022-1694(99)00033-5

Hermanns, R. L. (2016). Landslide. In *Selective Neck Dissection for Oral Cancer* (pp. 1-3). https://doi.org/10.1007/978-3-319-12127-7_183-1

Highland, L. M., & Bobrowsky, P. (2008). *The landslide handbook - A guide to understanding landslides.* U.S. Geological Survey Circular 1325. https://pubs.usgs.gov/circ/1325/

Hjulström, F. (1935). Studies of the morphological activity of rivers as illustrated by the river fyris, bulletin. *Geological Institute Upsalsa*, *25*, 221-527.

Hodgkins, R. (1997). Glacier hydrology in Svalbard, Norwegian High Arctic. *Quaternary Science Reviews*, *16*, 957-973.

Hodgkins, R., Cooper, R., Wadham, J., & Tranter, M. (2003). Suspended sediment fluxes in a high-Arctic glacierised catchment: implications for fluvial sediment storage. *Sedimentary Geology*, *162*(1-2), 105-117. https://doi.org/10.1016/s0037-0738(03)00218-5

Hodson, A., Nowak, A., & Christiansen, H. (2016). Glacial and periglacial floodplain sediments regulate hydrologic transfer of reactive iron to a high arctic fjord. *Hydrological Processes*, *30*(8), 1219-1229. https://doi.org/10.1002/hyp.10701

Humlum, O., Christiansen, H. H., & Juliussen, H. (2007). Avalanche-derived rock glaciers in Svalbard. *Permafrost and Periglacial Processes*, *18*(1), 75-88. https://doi.org/10.1002/ppp.580

Humlum, O., Instanes, A., & Sollid, J. L. (2003). Permafrost in Svalbard: a review of research history, climatic background and engineering challenges. *Polar Research*, *22*, 191-215. https://doi.org/10.1111/j.1751-8369.2003.tb00107

Hungr, O., Leroueil, S., & Picarelli, L. (2013). The Varnes classification of landslide types, an update. *Landslides*, *11*(2), 167-194. https://doi.org/10.1007/s10346-013-0436-y

Jaboyedoff, M., Carrea, D., Derron, M.-H., Oppikofer, T., Penna, I. M., & Rudaz, B. (2020). A review of methods used to estimate initial landslide failure surface depths and volumes. *Engineering Geology*, *267*, 105478. https://doi.org/10.1016/j.enggeo.2020.105478

Keating, K., Binley, A., Bense, V., Van Dam, R. L., & Christiansen, H. H. (2018). Combined Geophysical Measurements Provide Evidence for Unfrozen Water in Permafrost in the Adventdalen Valley in Svalbard. *Geophysical Research Letters*, *45*(15), 7606-7614. https://doi.org/10.1029/2017gl076508

Killingtveit, Å., Pettersson, L. E., & Sand, K. (2003). Water balance investigations in Svalbard. *Polar Research*, *22*(2), 161-174.

Kokelj, S. V., Lantz, T. C., Tunnicliffe, J., Segal, R., & Lacelle, D. (2017). Climate-driven thaw of permafrost preserved glacial landscapes, northwestern Canada. *Geology*, *45*(4), 371-374. https://doi.org/10.1130/g38626.1

Lafrenière, M. J., & Lamoureux, S. F. (2019). Effects of changing permafrost conditions on hydrological processes and fluvial fluxes. *Earth-Science Reviews*, *191*, 212-223. https://doi.org/10.1016/j.earscirev.2019.02.018

Lamb, H. (1977). General discussion: climatic analysis. *Philosophical Transactions of the Royal Society of London. B, Biological Sciences*, *280*(972), 341-350.

Lenzi, M. A., Mao, L., & Comiti, F. (2003). Interannual variation of suspended sediment load and sediment yield in an alpine catchment. *Hydrological Sciences Journal*, *48*(6), 899-915. https://doi.org/10.1623/hysj.48.6.899.51425

Lewis, T., Lafrenière, M. J., & Lamoureux, S. F. (2012). Hydrochemical and sedimentary responses of paired High Arctic watersheds to unusual climate and permafrost disturbance, Cape Bounty, Melville Island, Canada. *Hydrological Processes*, *26*(13), 2003-2018. https://doi.org/10.1002/hyp.8335

Lewkowicz, A. G., & Way, R. G. (2019). Extremes of summer climate trigger thousands of thermokarst landslides in a High Arctic environment. *Nat Commun*, *10*(1), 1329. https://doi.org/10.1038/s41467-019-09314-7

Longyearbyen Lokalstyre. (2017). *Arealplan for Longyearbyen planområde 2016-2026*. https://www.lokalstyre.no/arealplan-2016-2026.486570.no.html

Løvaas, M. A. S. (2021). *Management of a High Arctic River* [Master Thesis, NTNU]. Trondheim. https://hdl.handle.net/11250/2781625

Major, H., & Nagy, J. (1972). Geology of the Adventdalen map area: With a geological map, Svalbard C9G 1: 100 000.

Mannerfelt, E. S. (2017a). *Larsbreen Landslides 2017 on Svalbard - 3D Model*. https://sketchfab.com/3d-models/larsbreen-landslides-2017-on-svalbard-28d7679ba15d43e08e7e9b54e27e91e9

Mannerfelt, E. S. (2017b). *Summer melt at Longyearbreen 2017 - 3D Model*. https://sketchfab.com/3d-models/summer-melt-at-longyearbreen-2017-60ad918236de494188b92dafa332532f

Matveev, A. (2019). Variable effects of climate change on carbon balance in northern ecosystems. *IOP Conference Series: Earth and Environmental Science*, *226*, 012023. https://doi.org/10.1088/1755-1315/226/1/012023

McNamara, J. P., Kane, D. L., & Hinzman, L. D. (1998). An analysis of streamflow hydrology in the Kuparuk River Basin, Arctic Alaska: a nested watershed approach. *Journal of Hydrology*, *206*(1-2), 39-57.

Mertes, J. R. (2015). *Longyearbreen 2015 - 3D model*. https://sketchfab.com/3d-models/longyearbreen-2015-574d822dd0fa4b34b8b511e143b2f9f6

Moore, R. D. (2005). Slug injection using salt in solution. *Streamline Watershed Management Bulletin*, *8*, 1-6.

Moreno-Ibáñez, M., Hagen, J. O., Hübner, C., Lihavainen, H., & Zaborska, A. (2021). *SESS report 2020*. Svalbard Integrated Arctic Earth Observing System. https://sios-svalbard.org/SESS_Issue3

Mount, J. F. (1995). *California rivers and streams: the conflict between fluvial process and land use*. Univ of California Press.
Nichols, G. (2009). *Sedimentology and Stratigraphy* (2nd ed.). Wiley-Blackwell.
Nilsson, C., Polvi, L. E., & Lind, L. (2015). Extreme events in streams and rivers in arctic and subarctic regions in an uncertain future. *Freshwater Biology*, *60*(12), 2535-2546. https://doi.org/10.1111/fwb.12477
Norges Geologiske Undersøkelse. (n.d.). *API og WMS-tjenester: Løsmasselinjer, Løsmasser*. https://www.ngu.no/emne/api-og-wms-tjenester
Norwegian Meteorological Institute. (n.d.). *Seklima: Observations and Weather Statistics*. https://seklima.met.no/
Nowak, A. (2021). *Longyearbreen 2021 - 3D Model SvalDEM*. https://sketchfab.com/3d-models/longyearbreen-2021-6fc64233f4004aab904512157d89aa6c
Nowak, A., Hodgkins, R., Nikulina, A., Osuch, M., Wawrzyniak, T., Kavan, J., Lepkowska, E., Majerska, M., Romashova, K., Vasilevich, I., Sobota, I., & Rachlewicz, G. (2020). From land to fjords: The review of Svalbard hydrology from 1970 to 2019 (SvalHydro). *SESS Report 2020*. https://doi.org/10.5281/zenodo.4294063
NPI. (n.d.). *Norwegian Polar Institute Map Data and Services*. https://geodata.npolar.no/
NVE. (2017). *Tiltaksplan: Flom- og erosionssikringstiltak in Longyearelva*.
NVE. (2020). *Sikringstiltak i Longyearelva: Forsterking av bunnsikringer og forlengelse av flom og erosjonssikringsanleggene*.
Orwin, J. F., Lamoureux, S. F., Warburton, J., & Beylich, A. (2010). A Framework for Characterizing Fluvial Sediment Fluxes from Source to Sink in Cold Environments. *Geogr. Ann.*, *92*(2), 155-176. https://doi.org/10.1111/j.1468-0459.2010.00387.x
Østrem, G. (1964). Ice-cored moraines in Scandinavia. *Geografiska Annaler*, *46*(3), 282-337.
Østrem, G. (1975). Sediment transport in glacial meltwater streams.
Ottem, M. J. D. (2022). *The Longyearelva river-to-ocean system; Monitoring an anthropogenic arctic fluvial system in changing climate over short and long timescales* [Master Thesis, NTNU]. Trondheim.
Overeem, I., & Syvitski, J. P. M. (2008). Changing sediment supply in Arctic rivers. *IAHS Publ.*, *325*. https://doi.org/10.13140/2.1.1857.1528
Paul, F., & Bolch, T. (2019). Glacier Changes Since the Little Ice Age. In T. Heckmann & D. Morch (Eds.), *Geomorphology of Proglacial Systems* (pp. 23-42). Springer. https://doi.org/10.1007/978-3-319-94184-4_2
Peirce, S., Ashmore, P., & Leduc, P. (2018). The variability in the morphological active width: Results from physical models of gravel-bed braided rivers. *Earth Surface Processes and Landforms*, *43*(11), 2371-2383. https://doi.org/10.1002/esp.4400
Priesnitz, K., & Schunke, E. (2002). The fluvial morphodynamics of two small permafrost drainage basins, Richardson Mountains, northwestern Canada. *Permafrost and Periglacial Processes*, *13*(3), 207-217.
Radulovic, M., Radojevic, D., Devic, D., & Blecic, M. (2008). Discharge calculation of the spring using salt dilution method–application site Bolje Sestre Spring (Montenegro). *25*.
Repp, K. (1988). The Hydrology of Bayelva, Spitsbergen. *Hydrology Research*, *19*(4), 259-268. https://doi.org/10.2166/nh.1988.0018
Riger-Kusk, M. (2006). *Hydrology and hydrochemistry of a High Arctic glacier: Longyearbreen, Svalbard* [Master Thesis, University of Aarhus/The University Centre in Svalbard]. http://hdl.handle.net/11250/277221
Rogger, M., Chirico, G. B., Hausmann, H., Krainer, K., Brückl, E., Stadler, P., & Blöschl, G. (2017). Impact of mountain permafrost on flow path and runoff response in a high alpine catchment. *Water Resources Research*, *53*(2), 1288-1308. https://doi.org/10.1002/2016wr019341

Rowland, J. C., Jones, C. E., Altmann, G., Bryan, R., Crosby, B. T., Hinzman, L. D., Kane, D. L., Lawrence, D. M., Mancino, A., Marsh, P., McNamara, J. P., Romanvosky, V. E., Toniolo, H., Travis, B. J., Trochim, E., Wilson, C. J., & Geernaert, G. L. (2010). Arctic Landscapes in Transition: Responses to Thawing Permafrost. *Eos, Transactions American Geophysical Union*, *91*(26), 229-230. https://doi.org/10.1029/2010eo260001

Rubensdotter, L. (2016). *Preliminary Quaternary Map of Longyeardalen*. Norges Geologiske Undersøkelse.

Rudy, A. C. A., Lamoureux, S. F., Kokelj, S. V., Smith, I. R., & England, J. H. (2017). Accelerating Thermokarst Transforms Ice-Cored Terrain Triggering a Downstream Cascade to the Ocean. *Geophysical Research Letters*, *44*(21), 11,080-011,087. https://doi.org/10.1002/2017gl074912

Schweizer, J., Bruce Jamieson, J., & Schneebeli, M. (2003). Snow avalanche formation. *Reviews of Geophysics*, *41*(4). https://doi.org/10.1029/2002rg000123

Serreze, M. C., & Barry, R. G. (2014). *The Arctic climate system* (2nd ed.). Cambridge University Press.

Stenius, S. (2016). *Flomberegning for Longyearelva, Spitsbergen, Svalbard (400)*.

Sund, M. (2008). Polar hydrology. *Norwegian water resources and Energy Directorate's work in Svalbard. NVE Report*, *2*.

Tonkin, T. N., Midgley, N. G., Cook, S. J., & Graham, D. J. (2016). Ice-cored moraine degradation mapped and quantified using an unmanned aerial vehicle: A case study from a polythermal glacier in Svalbard. *Geomorphology*, *258*, 1-10. https://doi.org/10.1016/j.geomorph.2015.12.019

Ulrich, M., Morgenstern, A., Günther, F., Reiss, D., Bauch, K. E., Hauber, E., Rössler, S., & Schirrmeister, L. (2010). Thermokarst in Siberian ice-rich permafrost: Comparison to asymmetric scalloped depressions on Mars. *Journal of Geophysical Research*, *115*(E10). https://doi.org/10.1029/2010je003640

Varnes, D. J. (1958). Landslide types and processes. *Landslides and engineering practice*, *24*, 20-47.

Vatne, G., Etzelmüller, B., Sollid, J., & Ødegård, R. S. (1995). Hydrology of a polythermal glacier, Erikbreen, northern Spitsbergen. *Hydrology Research*, *26*(3), 169-190.

Wada, T., Chikita, K. A., Kim, Y., & Kudo, I. (2018). Glacial Effects on Discharge and Sediment Load in the Subarctic Tanana River Basin, Alaska. *Arctic, Antarctic, and Alpine Research*, *43*(4), 632-648. https://doi.org/10.1657/1938-4246-43.4.632

Wadell, H. (1932). Volume, Shape, and Roundness of Rock Particles. *The Journal of Geology*, *40*(5), 443-451. https://doi.org/10.1086/623964

Wanner, H., Beer, J., Bütikofer, J., Crowley, T. J., Cubasch, U., Flückiger, J., Goosse, H., Grosjean, M., Joos, F., Kaplan, J. O., Küttel, M., Müller, S. A., Prentice, I. C., Solomina, O., Stocker, T. F., Tarasov, P., Wagner, M., & Widmann, M. (2008). Mid- to Late Holocene climate change: an overview. *Quaternary Science Reviews*, *27*(19-20), 1791-1828. https://doi.org/10.1016/j.quascirev.2008.06.013

Westoby, M. J., Brasington, J., Glasser, N. F., Hambrey, M. J., & Reynolds, J. M. (2012). 'Structure-from-Motion' photogrammetry: A low-cost, effective tool for geoscience applications. *Geomorphology*, *179*, 300-314. https://doi.org/10.1016/j.geomorph.2012.08.021

Woo, M.-k. (2012). *Permafrost Hydrology* (1 ed.). Springer. https://doi.org/10.1007/978-3-642-23462-0

Yde, J. C., Riger-Kusk, M., Christiansen, H. H., Tvis Knudsen, N., & Humlum, O. (2008). Hydrochemical characteristics of bulk meltwater from an entire ablation season, Longyearbreen, Svalbard. *Journal of Glaciology*, *54*(185), 259-272. https://doi.org/10.3189/002214308784886234

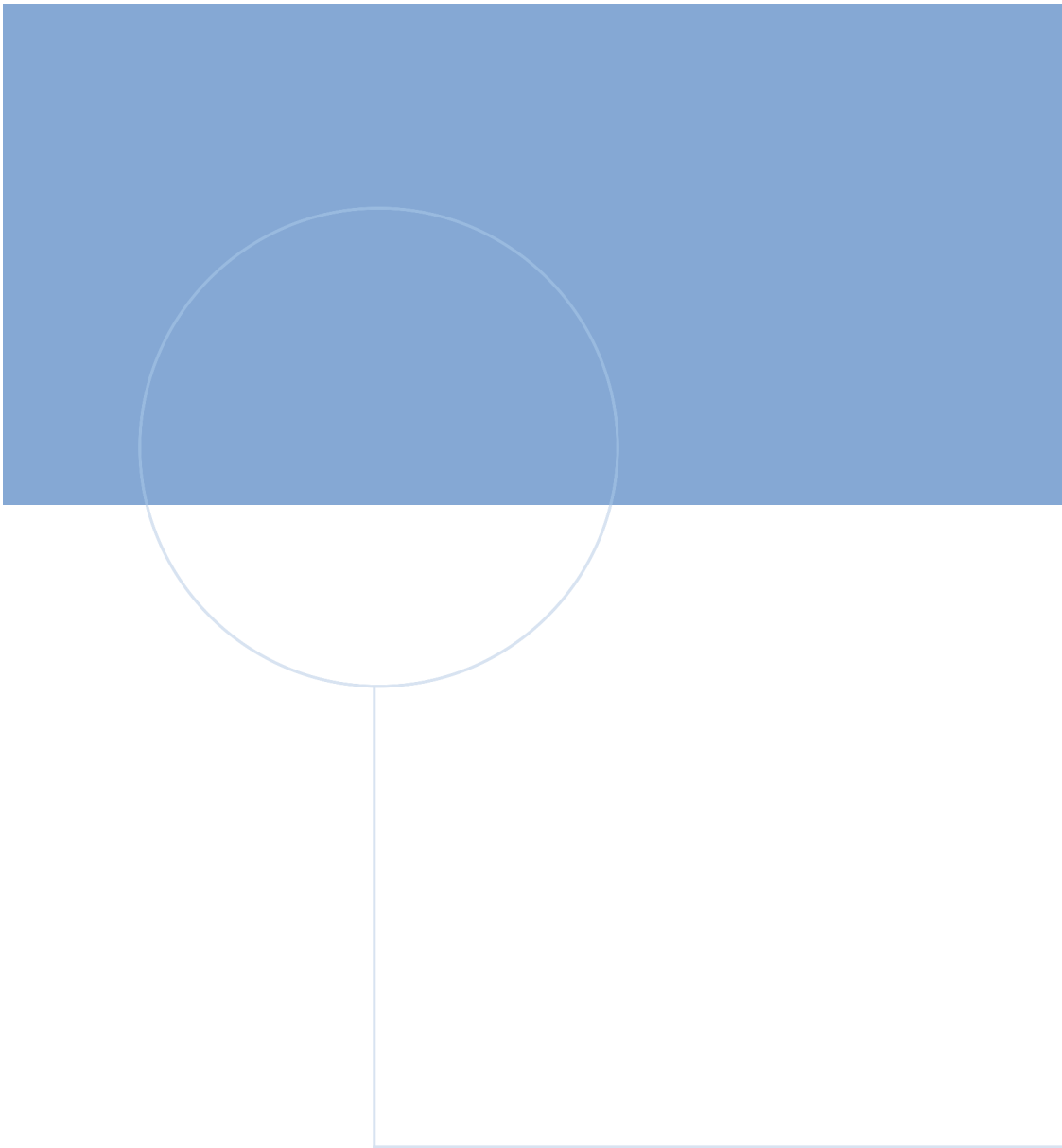

NTNU

Norwegian University of
Science and Technology